Rezanova V.G., Rezanova N.M.

SOFTWARE FOR THE RESEARCH OF NANOFILLED POLYMER SYSTEMS

The first chapter of the monograph describes the theoretical basis of regulation of the structure and properties of incompatible polymer mixtures through the introduction of nanoadditives.

The second section contains programs developed by the authors for mathematical modeling and research of the properties of nanofilled polymer mixtures

Monograph is intended for a wide range of teachers, scientists, post-graduate students, masters and students majoring in computer science and chemical technologies of specialized higher educational institutions, engineering and technical workers in the computer and chemical industries.

MINISTRY OF EDUCATION AND SCIENCE OF UKRAINE
KYIV NATIONAL UNIVERSITY OF TECHNOLOGIES AND
DESIGN

Rezanova V.G., Rezanova N.M.

SOFTWARE FOR THE RESEARCH OF NANOFILLED POLYMER SYSTEMS

Recommended by the Academic Council of the Kyiv National University of
Technologies and Design (Protocol № 2 of September, 25, 2024)

Kyiv - 2024

UDK 004.42:[544+001.894]

Author:

REZANOVA V. G. – Candidate of Technical Sciences, Associate Professor of the Department of Computer Science, Kyiv National University of Technologies and Design;
REZANOVA N. M. – Laureate of the State Prize of Ukraine in the field of science and technology, candidate of technical sciences, Kyiv National University of Technologies and Design.

Rezanova V.G., Rezanova N.M. Software for the research of nanofilled polymer systems. Monograph. – K.: ArtEk, 2024. – 263 p.

The first chapter of the monograph describes the theoretical basis of regulation of the structure and properties of incompatible polymer mixtures through the introduction of nanoadditives**.** The second section contains programs developed by the authors for mathematical modeling and research of the properties of nanofilled polymer mixtures

Monograph is intended for a wide range of teachers, scientists, post-graduate students, masters and students majoring in computer science and chemical technologies of specialized higher educational institutions, engineering and technical workers in the computer and chemical industries.

INTRODUCTION

The creation of qualitatively new materials with improved adjustable characteristics is one of the key areas of development in the field of polymer technology. The most promising way is the combination of polymer matrices with nanofillers of different chemical nature, size and configuration. The rapid development of nanotechnology is due to the fact that any property of substances in the nanostate is associated with a characteristic (critical) length. The main physical and chemical parameters vary under conditions when the dimensions of solid bodies become equal to the critical lengths of the nanometer range. At the same time, the electronic structure, conductivity, reactivity, melting and glass transition temperatures, mechanical characteristics, etc. change. The existence of such a dependence makes it possible to design materials with different, predetermined properties from the same starting atoms.

The actuality of the problem is evidenced by the fact that in recent years, the number of publications devoted to the development of theoretical foundations and practical ways of providing new specific functions to nanocomposites has increased dramatically throughout the world [www.scopus.com]. Scientific and technological aspects of this problem are summarized in a number of fundamental monographs [1-9]. Nano additives are chosen taking into account the possibility of achieving the desired characteristics of composites, their cost, impact on recycling and biodegradability, etc. Today, layered aluminosilicates, silicas, carbon derivatives, nanoparticles (NPs) of metals, their oxides,

etc. are widely used as nanofillers. Nanocomposites filled with natural or modified clay exhibit high strength and modulus of elasticity [2,10-12], thermal and fire resistance [4,8] and significantly improved dielectric [13] and barrier [14] characteristics. Epoxy-nanoclay composites are widely used in the aerospace, defense, construction and automotive industries, as clays are an ideal reinforcing material. At the same time, they are harmless to the environment, easily processed and have a low price [15]. Carbon nanotubes (CNTs) provide the effect of reinforcement and shielding from electromagnetic and microwave radiation, improve thermal characteristics, provide dielectric, anti-corrosion, biosensor properties, etc. [16-22]. Polyvinyl alcohol fibers with a high degree of CNT orientation were obtained by the method of layer-by-layer planting, which made it possible to increase their strength by 25 times and provide electrical conductivity equal to copper [17]. Polymeric materials filled with nanoparticles of metals or metal oxides exhibit high operational characteristics in combination with antimicrobial, thermal, electromagnetic, sorption, antiallergic, photocatalytic, antistatic properties and the ability to self-clean [23-30]. More effective modifiers are combined substances that allow expanding the range of functional characteristics of new products [31-35]. Polyvinyl alcohol nanofibers containing a silver/titanium oxide nano-additive exhibit simultaneous antimicrobial, photocatalytic, and dirt-repellent effects [34]. Polyurethane nanofibrous material filled with silver/zinc oxide bimetallic nanoparticles has higher antibacterial activity against many microorganisms compared to individual components, and provides complete inhibition of some of them [35]. Combined

4

substances in which NPs of metals or metal oxides are deposited on the surface of mineral sorbents (montmorillonite, diatomite, zeolite, silica) are of considerable interest [36-43]. Due to the combination of properties of various components, and often their synergistic action, materials containing such fillers have unique characteristics. They show a complex of various properties: heat and fire resistance, high sorption and antitoxic indicators. Their high photocatalytic activity ensures the purification of air and wastewater from pharmaceuticals [39-42]. In our research [41,42], it was shown that polypropylene microfibers, which contain silver/silica or silver/alumina nanoadditives in their structure, have a bactericidal effect on a number of strains of microorganisms and fungi. At the same time, their mechanical indicators, dimensional stability, specific surface area and hygroscopicity increase.

Modification of melts of polymer mixtures with nanoadditives is more effective than their individual initial components, as it allows to additionally change the properties due to the regulation of the morphology of the systems. Nanofillers can contribute to increasing the degree of dispersion of the dispersion or its coarsening, cause the coalescence of droplets into clusters or liquid jets, and the formation of continuous structures or domains of irregular shape [4,44-48]. The introduction of clays with different degrees of hydrophobicity into the polystyrene/polypropylene (PS/PP) mixture made it possible to increase the strength of the products due to the reduction in the size of the PS droplets and the increase in the homogeneity of their distribution [47]. In

polyamide/polylactide (PA/PL) mixtures, in the presence of organomodified clay, there is a qualitative change in the type of polyamide morphology in the PL matrix - a transition from a drop-matrix to an interwoven type. As a result, the heat resistance and plasticity of the composite material increase without a negative impact on its stiffness and strength [48]. Natural aluminosilicates are used for the creation of so-called "green" (biodegradable) polymer nanocomposites and processing of secondary raw materials [49-51].

In general, the change in the morphology of nanofilled polymer mixtures is regulated by a number of main factors: the compatibilizing (emulsifying) effect of additives, their influence on the rheological properties of the components and the processes of melting and crystallization, as well as the selective localization of nanoparticles in the volume of one of the components or at the boundary of their separation (thermodynamic and/or kinetic effects) [52-58]. Thermo- and organically modified montmorillonite exhibits a compatibilizing effect in the melt of the polypropylene/polystyrene mixture and allows controlling the process of in situ formation of PP microstreams in the PS matrix [52]. The modifying effect of clays leads to a decrease in the diameters of microfibrils in the modified systems to 1.7 μm compared to 2.7 μm in the original mixture. At the same time, the homogeneity of their distribution by diameters increases, which is evidenced by a decrease in such indicators as the standard deviation, dispersion, and coefficient of variation. In this case, thermomodified clay is a more effective structural modifier. Redistribution of nanofiller in incompatible

melts of polymer mixtures occurs in such a way that the total free energy of the system is minimized. The final location of nanoparticles is determined by the conditions of mixing the ingredients (single or multi-stage, sequence of their introduction, used equipment, shear rate, temperature and time). An important role is also played by the rheological properties of polymers and the degree of interaction between the surface of NPs and the functional groups of polymer macromolecules, as well as the possibility of Brownian motion. Many studies have shown that simultaneous mixing of all components, as a rule, contributes to the uniform distribution of the filler in the system, and two-stage mixing - preferential placement in one of the phases or on the border of their separation. It was shown that upon preliminary mixing of hydrophilic silica (SiO_2) with melt PP, and then with polystyrene, nanoparticles migrated to the PS phase [53]. At the same time, hydrophobic SiO_2 NPs moved into the interfacial region and acted as a rigid layer. Using two-stage mixing, selective localization of carbon nanotubes in one of the phases of the polystyrene/polyvinylidene fluoride mixture was ensured, which made it possible to adjust the mechanical and dielectric properties of the composites [55]. Using the example of PP/polyvinyl alcohol (PVA) composites filled with srublo/silica (Ag/SiO_2) nanoparticles, it is shown that the sequence of mixing the components allows to regulate their macro- and microrheological characteristics [56]. The viscosity of the modified system decreased when a nano additive was introduced into the dispersed phase (PP) component, and when added to the PVA melt or when the ingredients were mixed

simultaneously, the viscosity of the compositions increased. The preliminary introduction of Ag/SiO$_2$ nanoparticles into the PP melt contributes to the formation of a dispersed type of structure with a uniform distribution of polypropylene particles in the PVA matrix. When a dispersion medium is added to the melt, a mutually continuous morphology (entwined structures) is formed, when it is impossible to determine which polymer is the dispersed phase and which is the matrix. By simultaneous mixing of all components, a layered structure is realized in the form of concentrically arranged rings. The second approach, which ensures the preferential arrangement of nanofillers in the melt of the polymer mixture, consists in controlling the thermodynamic interactions of nanoparticles with one or both dimensional phases. This is achieved by choosing the chemical nature, shape and size of nanoparticles, modifying their surface, as well as the simultaneous use of a nano additive and a compatibilizer [58-63]. The possibility of controlling the selective distribution of hydrophilic silicon dioxide in a mixture of polylactide/copolymer of ethylene with vinyl acetate (EVAC) by changing the number of silanol groups (silanol number) on the surface of filler nanoparticles was shown [59]. It was established that NPs with a low value of silanol number were located in the component of the dispersed phase (EVAC), with an average value - both in the EVAC melt and in the interphase space, and with a high number of silanol groups were localized only at the boundary of the phase separation. A significant increase in the tensile strength of biodegradable composites based on polylactide was achieved due to interfacial adhesion and the formation of a percolation

network in the matrix with the simultaneous use of organomodified montmorillonite and multilayered CNTs [60]. With the addition of two modifiers - polypropylene grafted with maleic anhydride (compatibilizer) and hydrophobic silica (nano additive), the size of the particles of the dispersed phase in the matrix was reduced by 25 times, against 12, which occurred when only the compatibilizer was used [61].

Among the various types of structures formed during the flow of melts of polymer mixtures, an important place is occupied by the matrix-fibrillar morphology, which is formed as a result of the phase distribution of components. This is a special type of structure consisting of an isotropic matrix filled with micro- or nanofibrils with a high ratio of their length to the diameter. The formation of such a morphology in thermodynamically incompatible polymer systems is one of the most effective methods of improving their mechanical characteristics due to the uniform distribution and orientation of fibrils in the polymer matrix [4,20-22,40-42,52,64-75]. At the same time, there is a self-reinforcing effect, the degree of which can be adjusted by changing the ratio of the length to the diameter of the fibrils of the dispersed phase component. An important factor in creating a matrix-fibrillar morphology in polymer mixtures is ensuring the necessary degree of interaction between the components in the transition layer. The introduction of a third component into the mixture, which has a compatibilizing effect, contributes to the increase of compatibility between phases and the formation of a thinner stable dispersion. By varying the content of carbon nanotubes [20-21], alumina nanoparticles [25], fumed silica [67, 68],

mixed oxide TiO_2/SiO_2 [40] and titanium dioxide [64, 65] in PP/co-polyamide (SPA) mixtures and polyethylene terephthalate (PETF)/PP respectively obtained composite threads with increased strength and dimensional stability. This was achieved by reducing the diameters of PP and PETF microfibrils and improving the homogeneity of the diameter distribution. By extracting the matrix polymer from composite threads and films, in which the matrix-fibrillar structure is formed, microfibers and thin-fiber nonwoven materials are obtained on their basis (complex threads, precision filters, medical products, sorbents, etc.). Materials made of ultra-fine fibers retain the positive properties inherent in products made of classic synthetic fibers: strength, high dimensional and wear resistance. At the same time, due to the very small diameter of individual filaments, products made of them acquire a number of specific characteristics, namely; a high specific surface, which determines hygienic properties at the level of natural fibers and better sorption and heat-insulating characteristics. The presence of combined silver/silica or silver/alumina nanoparticles in microfibers gives thin fibrous materials antimicrobial activity against test strains of microorganisms and fungi [41,42]. The introduction of nanoadditives of original and modified silica into the PP/CPA mixture reduced the diameters of individual filaments, which increased the cleaning efficiency and precision of filters based on them [42]. With the addition of zirconium oxide NPs to the specified mixture, the average diameter of microfibrils decreased to 640 nm [71]. The high homogeneity of the structure of the filter layer led to the improvement of the operational characteristics of the material -

a two-layer filter ensures the efficiency of cleaning the gas medium at the level of materials without filler, which consist of 4-6 layers. At the same time, the simultaneous use of a compatibilizer and nanoadditive is more effective than individual substances, due to the manifestation of their synergistic effect [20,21,64,74]. Polyethylene terephthalate fibrils in the PP matrix with the maximum length and minimum diameter were obtained by modifying the PETF/PP mixture with the introduction of TiO_2 nanoparticles and grafted maleic anhydride [64]. The addition of sodium oleate compatibilizer to melts of PP/CPA mixtures containing Ag/SiO_2 nanoparticles or carbon nanotubes led to a decrease in the average diameter of microfibrils by 3-4 times compared to the original mixture [20,74].

Today, despite its simplicity and effectiveness, the potential of the described method of creating polymer nanocomposites remains underutilized. One of the reasons is the lack of a fundamental theory and a unified concept regarding the influence of nanodisperse additives and compatibilizers on the formation of phase heterogeneity of incompatible polymer systems. Further research on nanofilled mixtures is relevant in terms of establishing general patterns of formation of various types of structures, including microfibrillar ones. For this, it is necessary to perform a significant number of additional experiments on the effect of nanoadditives of different chemical nature, size and shape on the micro- and macrorheological properties of melts of thermodynamically incompatible mixtures and their effect on the performance of nanocomposites. Polymeric systems are

quite complex, and for their study, a significant number of multifactorial experiments must be performed with mandatory parallel experiments and further processing of the obtained results. Sometimes the number of factors and experiments is artificially reduced by reducing the volume of the investigated factor space or the number of levels of parameter variation. The use of mathematical research methods helps to speed up experiments and increase the reliability of their results. In order to build a plan for conducting experiments, we created software (software) that allows you to automatically establish the relationship between the content of ingredients and the properties of the system using three types of models of the dependence of the initial parameters on the content of components - incomplete cubic, cubic and quadratic [76- 82]. The software was also developed to calculate the coordinates of the points of the experimental plan and process the results of the effect of nanoadditives on the rheological properties of polymer dispersions, interphase cells and structure formation processes, including the in situ formation of microfibrils of the dispersed phase in the matrix [83-85]. The application of mathematical planning of an experiment with the use of the created software makes it possible to speed up the conduct of experiments tenfold, sharply reduce their number, and quickly identify the optimal variant of the researched process. This will contribute to the development of methods for directional regulation of the dimensional characteristics of microfibrils by introducing thermodynamically incompatible mixtures of modifying additives into the melt. As a result, the properties of nanocomposites and thin fibrous materials based on them will

significantly improve and the spectrum and fields of their application will expand. This approach is one of the priority directions for creating composites with predetermined properties, and the obtained results will make a significant contribution to the theory and practice of processing nanofilled polymer systems.

CHAPTER 1
REGULATION OF THE STRUCTURE AND PROPERTIES OF INCOMPATIBLE POLYMER MIXTURES THROUGH THE INTRODUCTION OF NANOADDITIVES

1.1. Polymer compositions with a controlled structure

1.1.1. Compatibility of polymer mixtures and their phase morphology.

Mixing polymers is a more effective way of obtaining new composite materials with predictable properties compared to the synthesis of new monomers and polymers. At the same time, various types of polymer mixtures are formed - from simple binary to combinations of block copolymers and homopolymers, interpenetrating networks, reactive compatible systems, molecular composites, emulsion mixtures, etc. The peculiarity of the properties of polymer systems is related to their phase structure. At the same time, they can be fully compatible, incompatible and partially compatible. In thermodynamically compatible systems, homogeneity is observed at least on the nanometer scale, if not on the molecular level. They are characterized by only one glass transition temperature (Ts), which is between the Ts of both components. In partially compatible mixtures, a small amount of one component dissolves in the other, and both phases are homogeneous and have their own glass transition temperatures. At the same time, the values of Ts are shifted from the values for individual components to the glass transition temperature of the ingredients in the mixture. Most polymer mixtures are thermodynamically incompatible, consisting of separate phases

and a transition layer. Depending on the degree of compatibility of components and processing conditions, different types of morphology can be obtained, which provide improved characteristics of composites, namely: high mechanical indicators and impact toughness, strength in combination with stiffness, barrier characteristics. Multiphase polymer mixtures can have a discrete (drops or fibers in the matrix) or continuous (intertwined) phase structure (Fig. 1.1) [85].
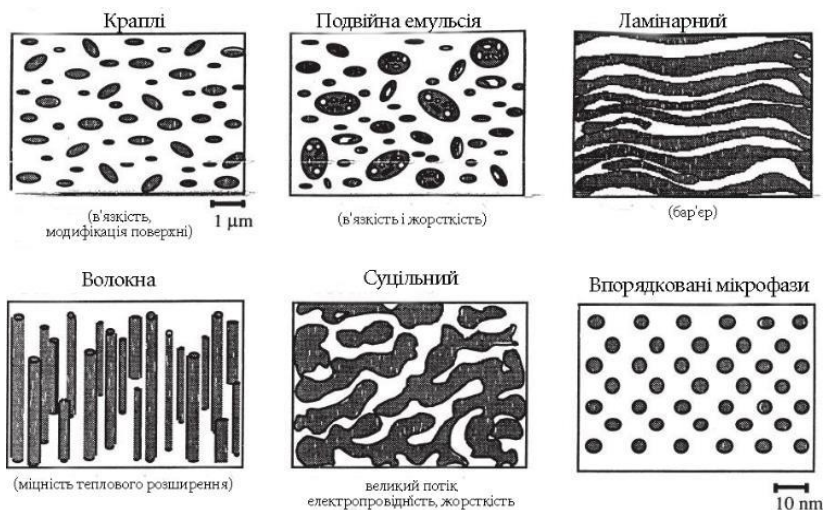

Fig. 1.1 – Types of morphologies of polymer mixtures

Weak adhesion at the boundary of phase separation in incompatible mixtures causes the instability of the morphology and the associated low mechanical properties. To create compositions with improved characteristics, it is necessary to increase its compatibility, which can be achieved by introducing appropriate block or graft copolymers (inert

15

compatibilization). Under inert compatibilization, one chain of the copolymer has an affinity with a certain component of the mixture, and the second one with another. These copolymers can be prepared beforehand and added to the polymer mixture, or synthesized in situ during the mixing process. The introduced additives, as a rule, are placed at the interface between the components, fix their segments in the corresponding polymer, reduce the interfacial tension and stabilize the dispersion, preventing coalescence [86]. With reactive compatibilization, block copolymers are obtained that act as compatibilizers in place during melt mixing. There are different types of reactive compatibility. If both components have reactive groups, they easily react with each other. Improvement of compatibility is also achieved by adding a reactive polymer to the system, which is mixed with one of the components of the mixture and reacts with the functional groups of the second component. Thus, a block or graft copolymer is formed at the interface of the phase separation. One of the most effective copolymers for reactive compatibilization are grafted polymers of maleic anhydride (MA). The anhydride group can react with terminal amino groups of polyamides (PA) and hydroxyl terminal groups of polyester [87].

The morphology of incompatible mixtures depends on many factors: the composition of the mixture, the ratio of component viscosities, interfacial tension, mixing parameters (time, extruder screw geometry, and its rotation speed) [44,88]. By changing the mixing conditions, a wide range of sizes and shapes of the dispersed phase component is obtained - from

submicron to hundreds of micrometers. At the same time, they can have spherical, ellipsoidal, cylindrical and ribbon-like shapes with solid or multiplet morphology. The final structure is a balance between the processes of droplet disintegration and their coalescence. The ratio of the viscosities of the dispersed phase and the matrix (viscosity coefficient K) is one of the most important parameters for controlling the structure of the mixture. As a rule, high values of K result in a coarser morphology, while a low viscosity coefficient results in a finer morphology. It is generally accepted that under the condition K=1, structures with the minimum diameter of the droplets of the dispersed phase and uniform in size are formed [4,88]. In polymer mixtures, the component with a lower content usually forms the dispersed phase, and the continuous phase is the component with a higher content. Provided that the concentration of the two polymers is close, the more viscous component tends to form a dispersed phase, and the less viscous component is the dispersion medium [88]. Interphase modification of polymer mixtures helps to reduce the size of the droplets of the dispersed phase and narrow their size distribution.

Mixing of incompatible polymers in the extruder at high screw speed leads to a finer morphology, as it creates an intense shear stress field, which contributes to effective dispersion of droplets. An increase in mixing time also results in a finer morphology. In fig. 1.2 shows the scheme of formation of the structure of the composition during the mixing of melts of incompatible polymers [88]. At the entrance to the extruder, the granules or powder of the dispersion medium are

melted, and the droplets of the dispersed phase are peeled off and separated into a separate phase. Next, they stretch into layers that break up into jets and then droplets.
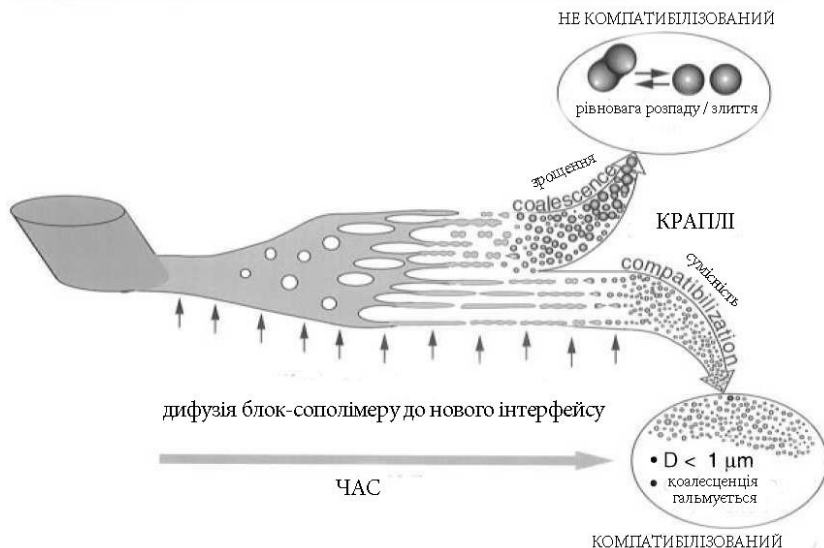

Fig. 1.2 – Scheme of the formation of the morphology of the mixture when mixing melts of incompatible polymers

1.1.2. Nano-filled composites

The use of nanofilled polymer mixtures and compositions is one of the cost-effective methods of creating materials with unique properties due to synergistic effects and features of the heterogeneous structure [1-9,89-91]. This provides the possibility of controlled regulation of their indicators without the synthesis of new polymers, as well as the ability to stable processing of primary and secondary raw materials. One of the modern trends in the development of industry is the solution of environmental and social issues,

18

which, along with economic ones, play an important role in the development and implementation of new technologies. The so-called "green" technologies can be considered as the production of materials with reduced pressure on the environment due to the use of low-toxic environmentally safe polymers and modifiers [92,93]. Today, natural mineral compounds of various origins (metals and their oxides, carbon derivatives, clays) or specially synthesized substances are widely used as modifiers, which are effective nanofillers for polymers and provide an ecological aspect of production.

One of the important issues in the creation of nano-filled polymer materials is the achievement of a certain structural organization of the components of a heterogeneous system and the determination of ways of regulating the morphology of incompatible polymer mixtures. From the point of view of thermodynamics, the spherical form of droplets is the most stable, and their formation in the composition is conditioned by the minimization of the separation surface and depends on the ratio of viscosities of the components of the mixture and the amount of interfacial tension [4,88]. Nanoparticles affect both of these parameters, which opens up a wide range of possibilities for regulating the morphology of the polymer dispersion. The addition of NPs in a small amount makes it possible to obtain stable non-spherical particles, microstreams, coalescent clusters, chains, and a network structure. Traditional approaches to control the morphology of polymer dispersions consist in changing the amount of ingredients and their rheological properties, controlling the kinetics of mixing and dispersion processes, as well as using

interphase modifiers that improve the affinity between polymers [1-9,44-48]. In recent years, considerable attention has been paid to regulating the morphology of polymer mixtures due to their preferential localization in the system and the possibility of the formation of spatial structures in the polymer dispersion [53-60]. At the same time, the most studied is the influence of nanoparticles on the degree of dispersion of components in incompatible polymer mixtures. Most researchers believe that the reduction of the geometric dimensions of the particles of the dispersed phase and the formation of a finer morphology of the mixture when adding a nanofiller is related to their influence on the rheological characteristics of the components. A change in the ratio of viscosities and elasticity of polymers can shift the balance in the processes of decay and coalescence. An increase in the viscosity of any of the phases counteracts the coalescence of the droplets. In addition, the filler particles themselves can form a three-dimensional network, which contributes to the inhibition of droplet coalescence and prevents their coalescence. The effectiveness of the action of the filler is determined by its predominant localization in the volume of one of the phases, or on the border of their separation, which is most characteristic of anisometric nanoparticles, for example, such as carbon nanotubes. An increase in the local concentration of CNTs in the interfacial zone contributes to the formation of a percolation type of structure [55,94]. An effective method of regulating the phase morphology of dispersed systems is the simultaneous introduction into the polymer mixture of nanoparticles of different chemical nature

(hydrophilic and hydrophobic) [95-97]. Placement of NPs related to it in the matrix polymer leads to an increase in melt viscosity, while another type accumulates in the interphase zone, forming a kind of "shell", and reduces the probability of droplet coalescence and ensures the formation of a finer morphology of the mixture [97] . Thus, along with other factors, control and regulation of the localization of solid nanoadditives in polymer mixtures is a key parameter that ensures the achievement of the desired characteristics of nanocomposites. Migration and localization of nanoparticles depends on thermodynamic and kinetic factors. The distribution of fillers in incompatible polymer mixtures occurs in such a way as to minimize the total free energy of the system. The uneven distribution of nanoparticles provides a reduction in the free energy, which depends on the surface tension, or the free surface energy of the components. The final distribution of nanofillers depends on the mixing conditions, the rheological properties of the components, and the degree of interaction between the filler and the components [52-60,98-102]. A significant amount of research is devoted to the study of the influence of silica additives on the structure of polymer mixtures [46,47,60-65]. So, when introducing 3.0 wt. % of hydrophilic or hydrophobic silica in the polypropylene/polystyrene (PP/PS) mixture, the average particle size of the dispersed phase (PS) decreased from 3.7 to 0.85 μm (for hydrophilic SiO_2 particles) and to 1.25 μm (for the hydrophobic additive) . This effect is due to the predominant localization of nanoparticles in one of the phases or on the border of their separation. With the preliminary

introduction of hydrophilic SiO_2 into the PP melt, the nanoparticles migrated to the PS phase. At the same time, hydrophobic SiO_2 NPs move into the interphase region and act as a rigid layer that prevents coalescence and stabilizes the PP/PS mixture [53]. An important parameter that affects the transfer and the phenomenon of selective localization of a nanofiller in a mixture of polymers is the geometric shape of nanoparticles [101,102]. The authors [47] studied the influence of layered clays with different hydrophobicity on the rheological properties and morphology of PP/PS mixtures and showed that melt viscosity and droplet size decreased as the hydrophobicity of NP clays decreased. In a mixture of polyamide/copolymer of acrylonitrile, butadiene, and styrene (PA/ABS), hydrophilic particles of silicon dioxide are concentrated in the polyamide phase, while hydrophobic particles are usually localized at the boundary of the phase separation, which leads to a decrease in the size of the copolymer particles [103]. The influence of thermodynamic and kinetic parameters on the migration and localization of silica micro- and nanoparticles in a polylactide/polyethylene PL/PE mixture with high interfacial tension was studied in the article [104]. Thermodynamically, the equilibrium placement of unmodified and modified (grafted with succinic anhydride) silicon dioxide particles in the polylactide phase and at the phase interface, respectively, is predicted using the equation given in [105]. The introduction of unmodified microbial nanosilica into the melt of PL and highly viscous PE leads to the localization of particles in the polylactide phase, while the particles of modified SiO_2 are concentrated in the melt of

polyethylene. When studying the influence of kinetic parameters, silica additives were pre-mixed with polyethylene melt, and then the resulting granules were mixed with polylactide. It was shown that NPs of original and modified silica remain localized in the PE phase. A decrease in the viscosity of polyethylene leads to the migration of silicon dioxide to the phase calculated according to the equation of thermodynamic equilibrium localization [105]. Electron microscopy confirmed that 35% of hydrophilic silica NPs moved from the PE phase into the polylactide melt. At the same time, most of the filler particles (65%) remained in the volume of polyethylene in the form of aggregates. Selective placement at the boundary of phase separation is characteristic of nanoadditives with high compatibility to one of the components, if they are previously introduced into a polymer with low affinity. A three-stage mechanism of NP migration into a thermodynamically favorable phase is proposed, namely: diffusion from the bulk phase to the separation boundary, drainage (rupture) of the film between the particle and the transition layer, and migration in the volume of the interphase region. On the other hand, it was shown that TiO_2 nanoparticles are preferentially located at the boundary of the phase separation, regardless of the sequence of their introduction [65]. As a rule, simultaneous mixing of all ingredients contributes to the uniform distribution of NPs in the mixture, and two-stage mixing promotes selective localization in one of the phases or on the border of their separation [47].

The study of the relationship between the microstructure and the rheological characteristics of the

interface showed that the mechanism of stabilization of Newtonian emulsions by surfactants can also be applied to polymer mixtures with interfacially adsorbed nanoparticles [106,107]. For the polylactide/polyurethane mixture, it was found that in the presence of interphase-adsorbed nanosilica, the adhesion between the polymer phases and the reinforcement effect of the mixture are enhanced [107]. An increase in the strength and modulus of elasticity of the products is associated with qualitative morphological changes, namely, the transition from a droplet to a network structure of the composition. The so-called Janus-like fillers (Janus particles), which due to their amphiphilic nature, act as effective compatibilizers, attract more and more attention of researchers. At the same time, they are mainly concentrated at the phase separation boundary and have a synergistic effect on the morphology of polymer mixtures [108-110].

The shape of the particles of the dispersed phase can be controlled most effectively if the nanoadditive is preferentially localized at the boundary of the polymer/polymer separation. At the same time, the intensity of interaction between drops changes, which can either merge into liquid jets or partially merge with the formation of irregularly shaped domains. Study of the effect of interphase-active silica nanoparticles on the morphology and rheology of polybutadiene / polydimethylsiloxane mixtures with a composition of 10/90 wt. % showed that they significantly change the morphology of polymer mixtures [111]. A mechanism of coalescence of dispersed phase polymer droplets covered with a monolayer of nanoparticles was proposed (Fig. 1.3). Chains (liquid jets) (Fig.

1.3a) or clusters (Fig. 1.3b) may form depending on the polymerophilicity of the components of the mixture in relation to NPs and the equilibrium wetting angle.
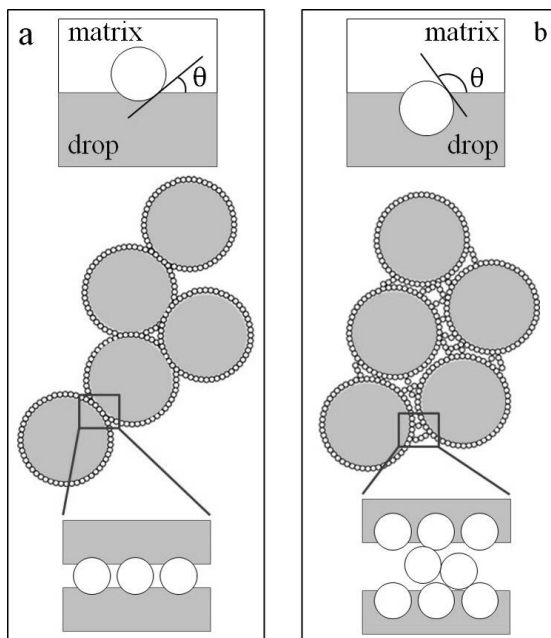

Fig. 1.3 – Scheme of clustering mechanisms with preferential wetting of nanoparticles by polymer: a) matrix, b) dispersed phase

Similar results were also obtained by other researchers [112], who showed that the predominant location of flat clay nanoparticles at the separation boundary in the PS/polymethyl methacrylate mixture with droplet-matrix morphology contributes to its thinning under the action of shear deformations during mixing. The clustering mechanism is shown in Fig. 1.4.
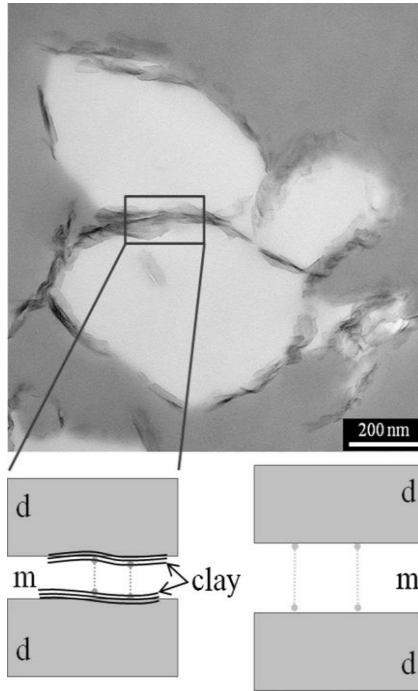
Fig. 1.4 – Scheme of thinning of polymethyl methacrylate jets covered with nanoparticles of clay in a polystyrene matrix

This mechanism is supported by the fact that the calculated force of interaction between droplets covered with a layer of nanoparticles is two orders of magnitude higher than without such a layer [112].

An important parameter that affects the movement and the phenomenon of selective localization of a nanoadditive in a mixture of polymers is also the geometric shape of nanoparticles [101,102]. Layered clay nanofillers serve as effective modifiers and make it possible to change the morphology of the mixture regardless of the saturation of the

interface with nanoparticles. One possible explanation for this is that the flat shape of the clay particles allows them to better adapt to the two-dimensional structure of the interfacial layer. The introduction of organomodified clay into polylactide-based biocomposites during the mixing process leads to a qualitative change in the morphology of the mixture: a transition from a drop-matrix to an interwoven type of structure takes place [48]. The result of such changes is a significant increase in heat resistance of compositions containing 70 wt. % of polylactide. Thermo- and organically modified montmorillonite have a compatibilizing effect in the melt of the polypropylene/polystyrene mixture and contribute to the reduction of microfibril diameters in the modified systems to 1.7 μm compared to 2.7 μm in the original mixture. At the same time, the homogeneity of their distribution by diameters increases, which is evidenced by a decrease in such indicators as standard deviation (~ 3 times), dispersion (by 8 times), coefficient of variation (~ 2 times) [52]. In this case, thermomodified clay is a more effective structural modifier. At the same time, other types of anisotropic nanoparticles (in particular, CNTs) are able to influence the shape of the droplets of the dispersed phase only under the condition of complete saturation of the interfacial layer [113]. The introduction of modified nanotubes into the polylactide/polyamide mixture, their migration and selective localization in the polymer of the dispersed phase ensured the formation of PA microstreams in the PL matrix [114]. Preferential placement of silica NPs in the matrix component (PP) in the polyolefin elastomer/polypropylene mixture contributes to changing the

morphology of the system from a co-continuous to an "island in the ocean" structure, in which elongated elastomer particles are dispersed in the matrix [66].

Thus, the modifying effect of nanoparticles manifests itself in a decrease in surface tension (a compatibilizing effect), an increase in interfacial adhesion (improvement of compatibility), and inhibition of droplet coalescence due to the physical shielding of droplets. This helps to reduce the dimensional characteristics of the dispersed phase structures in the matrix. At the same time, the predominant localization of nanoparticles in one of the phases or at the boundary of the polymer/polymer separation is one of the most effective factors in controlling the microstructure of nanocomposites. The mechanism of this process has not yet been definitively established. The influence of nano-additives on the ratio of visco-elastic properties of the components of the mixture and on interphase phenomena is experimentally confirmed. Due to their modifying effect on melts of polymer mixtures, nanofillers are an effective alternative to traditional co-polymer compatibilizers.

1.2. The effect of nanofillers on the formation of microfibrillar morphology in melts of incompatible polymer mixtures

The formation of matrix-fibrillar morphology is a special type of structure formation, during which deformation and merging of droplets of the dispersed phase occurs with the formation of liquid cylinders (microfibrils) in the polymer-matrix melt. These jets must maintain their stability in the

channel of the forming hole and at the exit from it. The final morphology is the result of a balance between the processes of deformation and decay, on the one hand, and coalescence, on the other. Deformation, capillary instability, coalescence and properties of the interfacial layer are effective factors in creating the desired structure of the polymer dispersion. In matrix-fibrillar composites, the diameter and number of filaments do not depend on the number of holes in the die, but are determined by the chemical nature and rheological properties of the components of the mixture and phenomena at the boundary of phase separation.

1.2.1. *Polyethylene terephthalate / polyolefin microfibrillar composites / nanofiller*

To date, microfibrillar composites have been obtained for many pairs of incompatible polymers, and polyethylene terephthalate/polyolefin (PETF/PO) compositions are the most studied [75,115-121]. Polyester fibers are characterized by high resistance to deformation, which makes them an ideal reinforcing element for strong, but less elastic polyolefin. Systematic studies of the processes of formation of morphology, crystallization, rheological and mechanical properties of compositions based on PET/PP mixtures were carried out in [115]. It is shown that the morphometric characteristics of the fibrillized phase of PET, namely their diameter and size distribution, depend on the coefficient of stretching of the melt during molding. At a fixed amount of longitudinal deformation, the diameters of microfibrils increased with an increase in the concentration of PET in the mixture.

The introduction of compatibilizers or nanofillers into the melt of the polymer mixture affects the rheological properties of the components and the length of the transition layer. As a result, the flow of macro- and micro-rheological processes during their flow changes, namely: deformation of drops, merging of liquid jets, their disintegration into drops, migration of the dispersed phase along the radius of the forming hole. By adding nanosized carbon to the PET/PE mixture, a new electrically conductive composite was obtained, in which carbon particles were located on the surface of polyester microfibrils [85]. The conductive network was built due to the contact and overlapping of additive particles on PET microfibrils, which led to a decrease in the percolation threshold and an increase in conductivity. In order to improve the interfacial adhesion between the polyester microfibrils and the polyolefin matrix, polypropylene grafted with maleic anhydride (PP-g-MA) was introduced into the melt of the mixture during extrusion. Studies of compatibilized blends have shown that shorter fibrils are formed in them, as the additives form a thin shell around the polyester droplets, and this counteracts their coalescence.

Detailed studies on the formation of a matrix-fibrillar structure in a polyethylene terephthalate/polypropylene mixture filled with titanium dioxide nanoparticles were performed by the authors [64, 65, 123]. It was shown that the morphology of the system is determined by the content and size of the nanoparticles of the filler, the sequence of mixing with the ingredients (pre-dispersion in the dispersed phase or matrix component or simultaneous mixing) and process parameters. It

was established that TiO$_2$ nanoparticles have a modifying effect regardless of their location in the melt mixture. However, the preferential localization of NPs at the boundary of the phase separation provides a higher compatibilization effect than if they were placed in the polypropylene matrix. This is due to the uneven distribution of the filler and the significant interaction between the functional groups of the polymer chains with solid particles of titanium dioxide. The listed factors contribute to the improvement of matrix-fibrillar morphology of composites (Fig. 1.5, Table 1.1).
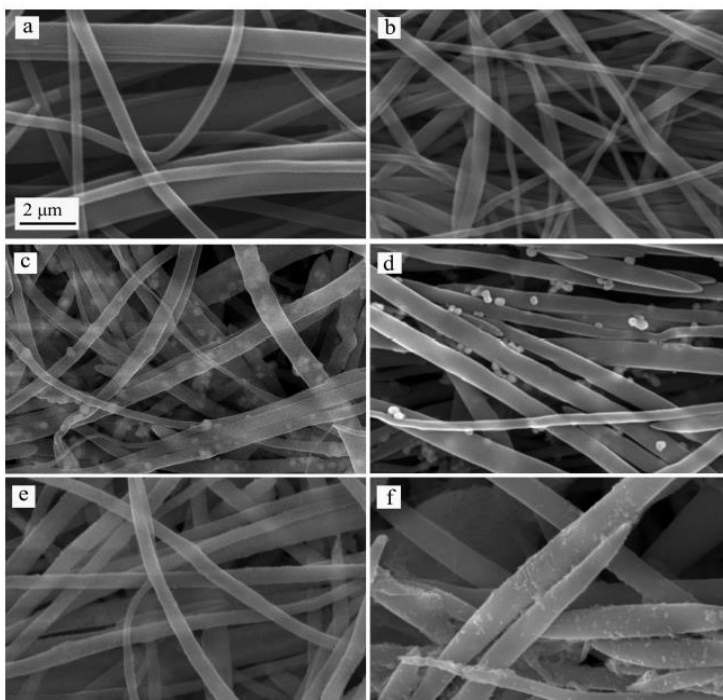

Fig. 1.5. SEM images of the PET fibrils in drawn strands, note: PP was removed by hot xylene: (a) PET/PP, (b) PET/PP/MA, (c) PET/PP/2T300, (d),PET/PP/MA/2T300, (e) PET/PP/2T15, (f) PET/PP/MA/2T15.

Table 1.1 shows data on the influence of the concentration of titanium dioxide nanoparticles with diameters of 300 nm on the dimensional characteristics of polyester fibrils in a polypropylene matrix.

Table 1.1. Effect of titanium dioxide content on diameters of PET microfibrils

Composition of the mixture PET/PP/ TiO$_2$, vol. %	Microfibrils	
	average diameter, μm	range of diameters, μm
30/70/0	5,4	2,0÷9,2
24,5/73,5/2,0	1,4	1,6÷5,6
24,0/72,0/4,0	1,1	0,6÷4,5

As can be seen from the table. 1.1, an increase in the content of nano additives in the mixture contributes to a decrease in the average diameter of the fibrils and an increase in the homogeneity of their distribution. According to the authors, the mechanism of the stabilizing effect of titanium dioxide nanoparticles on the morphology consists in reducing the free energy of mixing and the amount of interfacial tension; in addition, they act as physical barriers and prevent coalescence of polyester droplets. Additional introduction of a compatibilizer (polypropylene with grafted maleic anhydride) into the nano-filled system leads to a further decrease in surface tension, inhibition of coalescence and changes in the rheological characteristics of the components. As a result, the diameters of PET fibrils in the PP matrix decrease from (0.5-2.0) μm in the three-component system to (0.4-1.0) μm in the nano-infused compatibilized one. The simultaneous use of

TiO$_2$ nanoparticles and the PPgMA compatibilizer in PP/PET mixtures ensures the maximum improvement of the mechanical properties of composite threads due to the adjustment of the diameters and length of the polyester fibrils in the polypropylene matrix.

1.2.2. Effect of carbon nanotube additives on micro- and macrorheological properties of melts of polypropylene/coproiamide mixtures

The discovery of carbon nanotubes in 1991 caused significant progress in the field of nanotechnology and marked a new era in the material world, especially in the field of polymer nanocomposites. A complex of unique mechanical, electrical, thermal and chemical properties is inherent in single- and multilayered CNTs, as well as a high ability to transport electrons. The modulus of elasticity of carbon nanotubes approaches the values of this indicator for diamond (1.0 and 1.2 TPa, respectively), their strength is 100 times higher than the best steel samples. They are also characterized by high electrical conductivity (~ 103 S/cm), thermal stability (up to 2800 0C in a vacuum), thermal conductivity (approximately two times higher than that of diamond) [125]. It is quite difficult to obtain materials filled with carbon nanotubes using known technologies, as excess surface energy leads to their sticking and aggregation. In addition, CNTs are chemically active and when interacting with other substances they often lose their unique properties. Today, the main tasks in the formation of nano-filled fibers and composites are ensuring the uniform distribution of the additive in the polymer and the transfer of stresses from the matrix to the filler. To solve the

first task, it is necessary to destroy the CNT aggregates and distribute them evenly in the polymer melt. The second task is to ensure sufficient surface interaction at the "matrix-filler" interface, otherwise the physical and mechanical properties will not be sufficiently realized. Special methods are used to prepare homogeneous nanofilled polymer compositions: preliminary ultrasonic treatment of CNTs, high-speed mixing that creates large shear deformations, chemical and physical modification of the surface of carbon nanotubes, or a combination of the above methods [1,4,5,125]. Today, there are various methods of introducing CNTs into polymer matrices, which made it possible to create new promising materials with multifunctional properties. At the same time, the modifying effect is manifested even after adding a small amount of filler. Due to the fact that the ratio of the length of the nanotubes to the diameter is from hundreds to thousands, high conductivity was achieved already at an additive concentration of 0.0025 wt. % [126]. CNT/polymer composites are used in a wide variety of fields: as reinforced and anti-corrosion materials, solar cells, chemical sensors, adsorbents, shielding products from electromagnetic and microwave radiation, etc. [125]. KNUTD carried out fundamental studies on the effect of carbon nanotubes on the formation of a maric-fibrillar structure during the flow of melts of thermodynamically incompatible mixtures of polypropylene/co-polyamide [20,21,127-133]. The obtained results indicate that the use of solid nano-additives allows to regulate the micro- and macro-rheological properties of nano-filled polymer dispersions.

1.2.2.1. Rheological properties of melts of polypropylene/copolyamide/carbon nanotube mixtures. This section summarizes experimental data on the effect of multilayer CNT additives on the viscosity (η) of the original polypropylene melts and the PP/SPA mixture, their flow regime (n), swelling of extrudates (B) and the ability to longitudinal deformation (Fmax). Filled polymers are often considered as concentrated suspensions. For such systems, it is necessary to take into account the possibility of individual particles interacting with each other, as well as additives with the dispersion medium, which will affect the nature of the flow. Listed in the table. 1.2, the results of the study of the rheological properties of the PP melt filled with carbon nanotubes indicate an increase in the viscosity of the suspension (ηexp.) with an increase in the content of the additive from 0.05 to 5.0 wt. %.

Table 1.2. Effect of CNT additives on the rheological properties of the polypropylene melt

CNT content, wt %	η, Pa·s*		n*	B*	$F_{max},$ %*
	$\eta_{\text{эксп.}}$	η_E			
0	300	-	1,8	2,1	18000
0,05	305	300	1,8	1,6	22000
0,10	315	301	1,8	1,6	27000
0,50	350	302	1,9	1,6	29000
1,00	450	305	1,9	1,5	21000
5,00	480	323	1,9	1,4	15000

* at a temperature of 190 ^{0}C and a shear stress (τ) $5.7 \cdot 10^4$ Pa

This is consistent with the conclusion that nanoadditives cause a thickening thixotropic effect, which leads to an increase in the viscosity of polymer melts [1,4,88]. For compositions with a small concentration of CNTs ($0.05 \div 0.10$ wt. %), η increases insignificantly and coincides within the margin of error with the effective viscosity (η_E) calculated by Einstein's formula for dilute suspensions:

$$\eta_E = \eta_0 (1+2,5\Phi) \qquad (1.1)$$

where: η_0 – viscosity of the medium; Φ – volume concentration of suspended particles

The flow pattern of modified polypropylene melts almost does not change depending on the content of CNTs and obeys the power law. As expected, the elasticity of melt compositions decreases with an increase in filler concentration, as evidenced by a decrease in the swelling of extrudates (Table 1.2). This is natural for filled polymers and is associated with a decrease in the flexibility of macromolecule chains. An important scientific and practical result of the performed research is the improvement of the ability of the melt of modified PP to longitudinal deformation: the maximum possible spinneret extraction increases with the introduction of an additive up to 1.0 wt. %, which is due to the strengthening of the melt jet due to the increase in viscosity (Table 1.2). A drop in F_{max} with an increase in the concentration of CNTs to 5.0 wt. % is associated with the deterioration of the elastic properties of the melt mixture.

In the table 1.3 shows the results of the influence of carbon nanotube additives on the rheological properties of the

PP/SPA melt. The analysis of the data shows that the introduction of CNTs does not change the general pattern of a sharp drop in the viscosity of binary mixtures compared to η of the melts of the original components.

Table 1.3. Effect of CNT additives on the rheological properties of the melt of the PP/SPA mixture

The composition of the mixture PP/SPA/VNT, wt. %	η, Pa·S*		n^*	B^*	F_{max}, %*
	$\eta_{exp.}$	$\eta_{ad.}$			
100/0/0	300	-	1,8	2,1	18000
0/100/0	1230	-	1,2	1,4	95600
30/70/0	150	951	1,8	5,7	10500
30/70/0,05	160	954	1,7	6,8	7800
30/70/0,10	170	961	1,7	7,2	7600
30/70/0,50	190	966	1,7	7,0	7300
30/70/1,00	210	996	1,6	6,7	6900

*at $T=190^0C$, $\tau =5.7 \cdot 10^4$ Pa

Experimental values of the effective viscosity of melts of binary and ternary compositions are 4.7÷6.3 times lower than the additive values (η_{ad}.). The established regularity is explained by the change in microrheological processes that take place during the flow of the melts of the mixtures, namely: the deformation of the droplets of the dispersed phase in the jet and the orientation of the latter in the direction of the flow. When introducing (0.05÷1.00) wt. % of carbon nanotubes in the PP/SPA melt, the effective viscosity of the composition increases. This may be due to the fact that the melt viscosity of

the mixture is the result of the action of several opposing factors. CNT solid additives structure the melt and increase its viscosity; on the other hand, η decreases due to the formation of liquid jets of dispersed phase polymer (PP) in the SPA matrix. In this case, the formation of microfibrils has a dominant effect, which is confirmed by a sharp drop in the viscosity of nanofilled mixtures compared to η of its original components. Modified compositions, like the original mixture, are non-Newtonian fluids. At the same time, the degree of deviation from the Newtonian regime, judging by the value of n, practically does not depend on the amount of additive (Table 1.3). The influence of the filler on the elastic properties of melts of PP/SPA/BNT compositions can be seen from the change in the swelling values of extrudates *B*, which are an indirect characteristic of elasticity. For extrudates of ternary mixtures, the B value increases by 1.2÷1.3 times for all studied concentrations of CNTs. The reason for the increase in swelling is that both components of the mixture are characterized by high elasticity and acquire elastic energy during the flow in the inlet zone. In the process of melt extrusion, when moving from a wide tank to a narrow drop, the component of the dispersed phase is deformed, elongated and merged in a jet. Such anisotropic structures are new relaxing elements and determine the increase in elasticity of extrudates of mixtures. Since the amount of swelling of extrudates correlates with the dimensional characteristics of microfibrils [72], the increase in *B* indirectly indicates a change in the processes of structure formation of the dispersed phase polymer in the matrix.

An important technological characteristic of polymer melts and their mixtures is the ability to be processed into fibers and films, which is determined by the value of the maximum spinneret extraction (F_{max}). As can be seen from the table. 1.3, melts of two- and three-component mixtures have a lower ability to longitudinal deformation, compared to the original components. The drop in straightness of the mixtures is the result of several factors - incompatibility of components and weak interaction between polypropylene and co-polyamide at the boundary of phase separation, a sharp drop in shear viscosity and an increase in the heterogeneity of the three-component mixture. At the same time, it should be emphasized that the values of the maximum spinneret extraction lie in the range that allows processing of nano-filled systems into fibers and films with the existing technological equipment.

To determine the mechanism of influence of CNTs on flow patterns of PP/SPA melts, the temperature dependence of viscosity under different shear stresses was investigated and the activation energy of viscous flow (E) was calculated according to the Frenkel-Eyring formula:

$$\eta = A_0 \cdot e^{E/RT} \qquad (1.2)$$

where: A_0 – coefficient that depends on the molecular nature of the liquid;

R – gas constant (8.3 kJ/mol);

T – absolute temperature, ^0K

It was established that the dependence of viscosity on temperature in the coordinates lg $\eta = f(1/T)$ at different shear stresses is expressed by straight lines, the slope of which

remains practically unchanged for melts of mixtures with different filler content. From those listed in the table. 1.4 of the data show an increase in the activation energy of the viscous flow of the composition in the presence of carbon nanotubes, which indicates a change in the kinetic element of the flow under the influence of the additive. At the same time, the activation energy of the viscous flow naturally increases as the shear stress decreases.

Table 1.4 – Effect of CNT additives on the activation energy of viscous flow of PP/SPA melts

Concentration of CNTs, wt. %	$\check{E}$, kJ/mol at $\tau \cdot 10^4$ Pa		
	$\tau = 5{,}69$	$\tau = 3{,}47$	$\tau = 1{,}61$
0	48,3	52,1	52,4
0,05	50,4	53,0	55,0
0,10	50,4	53,0	56,0
0,50	50,0	52,0	53,1
1,00	50,0	52,0	53,1

Thus, the conducted studies showed a significant effect of carbon nanotube additives in the amount of (0.05÷5.0) wt. % on the regularity of the flow of melts of the original polypropylene and mixtures of polypropylene/co-polyamide with a composition of 30/70 wt. %.

Taking into account that the formation of microfibrillar morphology is significantly influenced by the content of the dispersed phase component, the influence of carbon nanotube additives on the viscoelastic properties and the processes of

40

structure formation of melts of PP/SPA mixtures with different polypropylene content was studied. The results of studies of the rheological characteristics of the original and modified compositions performed on a capillary microviscometer are shown in Tables 1.5, 1.6.

Table 1.5. Influence of the composition of PP/SPA mixtures on the rheological properties of melts

Composition of the PP/SPA mixture, wt. %	Viscosity, Pa·s *		n	Swelling		F_{max}, %
	$\eta_{exp.}$	$\eta_{ad.}$		B_b	B_{in}	
100/0	300	-	1,9	2,1	1,6	18000
0/100	1230	-	1,2	1,4	1,1	93000
20/80	160	1044	1,5	7,6	2,3	9200
30/70	150	951	1,7	8,6	2,4	10500
40/60	130	858	1,6	7,4	2,4	10300
50/50	100	765	1,7	7,9	2,5	8000

* at shear stress $\tau = 5{,}7 \cdot 10^4$ Pa

As can be seen from the table. 1.5, the melt viscosity of polypropylene is 4 times lower than η of co-polyamide. Naturally, an increase in the PP content in the mixture is accompanied by a drop in the viscosity of the binary composition. However, $\eta_{exp.}$ of the mixture is 6.3÷7.6 times lower than the additive values ($\eta_{ad.}$). This indicates the predominant influence of the processes of structure formation in melts of polymer mixtures on their rheological properties. The formation of anisotropic structures, which are PP microfibrils in the matrix component, causes a sharp decrease

in the viscosity of melts of PP/SPA mixtures [88]. The introduction of carbon nanotube additives leads to an increase in the viscosity of melts of PP/SPA mixtures, which is consistent with the data on the thickening effect of solid nanofillers. However, as for binary compositions, experimental viscosities ($\eta_{exp.}$) are much lower than additive ones ($\eta_{ad.}$).) (Table 1.6). The nature of the flow of modified mixtures, like the initial ones, is described by a power law. At the same time, the degree of deviation from the Newtonian flow of nanofilled compositions increases, judging by the values of the flow regime indicator (n) (Table 1.6).

Table 1.6. Effect of CNT additive on rheological properties of melts of PP/SPA mixtures

Composition of the PP/SPA/VNT mixture, wt. %	Viscosity, Pa·s *		n	Swelling		F_{max}, %
	$\eta_{exp.}$	$\eta_{ad.}$		B_b	B_{in}	
100/0/0,5	350	-	2,1	1,6	1,5	29000
20/80/0,5	210	1054	1,7	6,4	2,1	9000
30/70/0,5	190	966	1,8	6,6	2,2	7900
40/60/0,5	150	878	1,7	7,3	2,2	7000
50/50/0,5	110	790	1,8	6,2	2,4	4100

* at shear stress $\tau = 5{,}7 \cdot 10^4$ Pa

A typical feature that occurs during the outflow of polymer melts and their mixtures from a molding hole (nozzle) with any profile is an increase in the cross-section of the extrudate (swelling) in comparison with the dimensions of the nozzle. The main reason for this is the relaxation of highly

elastic deformations accumulated in the jet melt during flow through the channel, and especially in the entrance zone. The elasticity of the melt significantly affects its ability to process and preserve the shape of products. Table data. 1.6 show that the swelling values of the jets after exiting the viscometer capillary (B_{in}) for binary and ternary mixtures are (1.5÷2.3) times higher than those of the original components, but this does not prevent their stable processing. It is known that highly elastic deformations do not relax instantly. Indirectly, they can be estimated by the amount of swelling of extrudates (B_b), annealed in a free state according to a special technique [134]. From the table 1.6 it can be seen that for the investigated original and nanofilled compositions, the equilibrium swelling values of extrudates (B_b) of binary and ternary compositions are (4.4÷6.1) times higher than their corresponding values for the original polymers. This is explained by the fact that along with the high elasticity of the matrix polymer, significant amounts of elasticity accumulate in the liquid jets of the dispersed phase component. Such thermodynamically unstable structures are new relaxing elements and determine the further increase in the elasticity of the melts of the mixtures. The introduction of a solid nano-additive reduces the elasticity of the melt, which is manifested in a decrease in the value (B_b).

The ability of the melts to be processed, determined by the value of the maximum spinneret extraction, is better in the melts of the original components compared to the two- and three-component mixtures. The deterioration of the straightness of the compositions is the result of a number of factors: weak interaction between PP and SPA at the boundary of phase

separation due to their incompatibility, a sharp drop in shear viscosity and an increase in the heterogeneity of the three-component mixtures. The obtained results indicate that CNT additives do not have a negative effect on the rheological properties of the studied mixtures, which allows processing of modified PP/SPA/CNT compositions into fibers and films on traditional extrusion equipment.

The method of temperature-concentration superposition (reduction) was used to generalize data on viscosity. It is based on the fact that the change in the effective viscosity of the melt is determined by the complex of relaxation properties of the system in the initial state, that is, the highest Newtonian viscosity (η_N). The method is used when the relaxation spectra of polymer systems are similar at different temperatures and concentrations [135]. It is known that for many binary mixtures of polymers there are quite wide regions where the dependence of the viscosity on the shear rate in the given coordinates is invariant with respect to the composition. At the same time, the superposition always takes place for that dispersion medium, the melt of which is characterized by a greater anomaly of viscosity and elasticity. Regarding the possibility of concentration superposition in multicomponent compositions, information is limited. The lack of invariance for PP/SPA mixtures compatibilized with sodium oleate at different salt contents was shown [136]. This is explained by the changes in the relaxation spectrum of the melts of the modified mixtures due to the surface activity and plasticizing action of the compatibilizer. At the same time, for mixtures of PP/SPA composition 30/70 wt. % invariance of viscosity with respect to

the concentration of siloxane liquid additives and binary compositions of compatibilizers was established [136].

Processing of the viscosity data of the melts of the nano-coated PP/SPA mixtures was carried out in the given coordinates:

$$\eta_{np} = \eta / \eta_N \quad \dot\gamma_{np} = \eta_N \cdot \dot\gamma \qquad (1.3)$$

where η_N – the greatest Newtonian viscosity; $\dot\gamma$ – shear rate gradient; η_{np} – reduced viscosity; $\dot\gamma_{np}$ – the reduced shear rate gradient.

In cases where the Newtonian segment of the curve was not reached in the experiment, η_N was found by the method of extrapolation of the dependence $\lg\eta - \lg\tau$ when $\lg\tau \to 0$, as described in [135]. As can be seen from Fig. 1.6, in the coordinates $\lg(\eta/\eta_N) - \lg(\eta_N\dot\gamma)$ the points for the PP/SPA/BNT mixtures are quite densely located near one common curve.
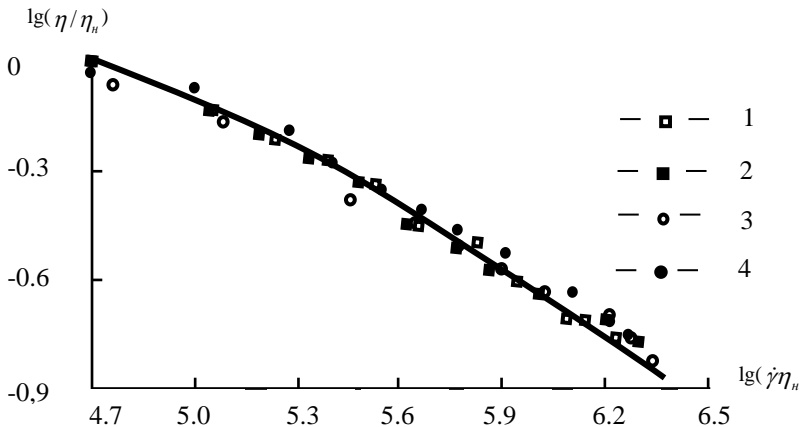

Fig. 1.6 – Dependence of the viscosity of melts on the shear rate in the given coordinates for mixtures of PP/SPA/BNT composition, wt.%: 30/70/0 (1) ; 30/70/0.1 (2); 30/70/0.5 (3); 30/70/1.0 (4)

This indicates that in the investigated nanofilled mixtures, the influence of the composition of the composition on the effective viscosity of the melt is fully manifested due to the highest Newtonian viscosity, and the possibility of concentration superposition in the melts is determined by the difference in the sensitivity of the components to the shear intensity. In practical terms, the use of the method of constructing the concentration-invariant viscosity characteristic makes it possible, knowing the concentration dependence of η_N and the dependence of the effective viscosity on the shear rate at one composition of the mixture, to determine the value of η at all shear stresses for other concentrations.

It is known that the dependence of the viscosity of the melts of the starting polymers in the given coordinates is invariant to the temperature [135]. The issue of the possibility of temperature superposition in melts of binary and modified polymer mixtures is debatable. In a number of works, it was concluded that temperature reduction for melts of polymer mixtures is, as a rule, possible. Thus, temperature-invariant curves were obtained in the given coordinates for melts of PP/SPA mixtures with additions of sodium oleate as a compatibilizer [136]. The generalization of the viscous properties of two- and three-component compositions at different temperatures performed in this work shows that temperature invariance is fulfilled for the original and modified mixtures at all studied concentrations of CNTs (Fig. 1.7).
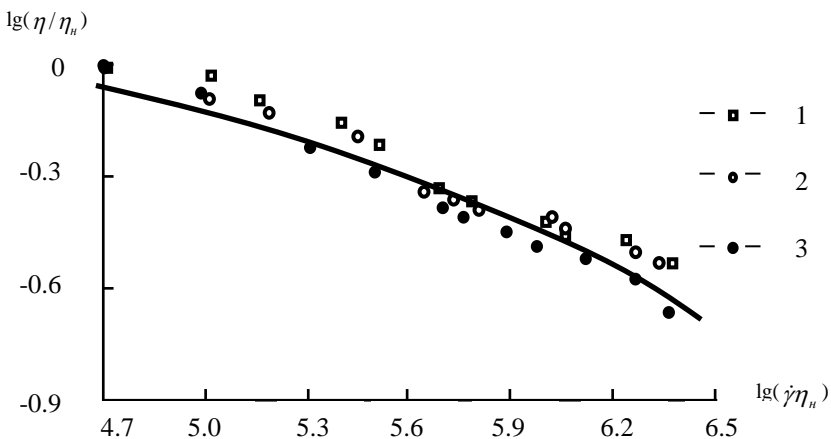
Fig. 1.7. Temperature-invariant dependence curve of the melt viscosity of the PP/SPA/BNT mixture of composition 30/70/0.5 wt. % of the shear rate in the given coordinates. Points 1-3 correspond to temperatures, ^{0}C: 190 (1); 210(2); 220(3)

Thus, it was confirmed that carbon nanotubes do not change the character of the relaxation spectrum of the melt of the original mixture, and the effect of temperature on the effective viscosity of the melts of nanofilled compositions, as for the original polymers, is manifested through η_N. The existence of a universal dependence of viscosity on the concentration of CNTs and temperature in the given coordinates proves that the relaxation spectra of melts of two- and three-component polymer mixtures are similar and are described by the same functional dependence. That is, for the melts of nanofilled compositions, the same regularities of rheological behavior take place, as for the melt of the original mixture.

Thus, it was established that the introduction of carbon nanotubes into the polypropylene/copolyamide melt allows to regulate the processes of structure formation during their flow

and does not have a negative effect on the rheological properties of melts of modified compositions. A generalization of experimental data on the viscous properties of melts of nanofilled mixtures was carried out using a method based on temperature (concentration) time or frequency superposition (adduction). This will allow, using modern devices for rheological research, to expand the change in shear rate values to 5 decimal orders and significantly increase the range of modifier concentrations.

      1.2.2.2.   Microstructure   of   extrudates   of polypropylene/copolyamide/carbon   nanotube   mixtures. Analysis of the microstructure of polypropylene extrudates with CNT additives shows that mixing the nanofiller with the melt by the extrusion method does not ensure fine and uniform dispersion. Photomicrographs of cross sections show aggreates of carbon nanotubes (1÷10) μm in size (Fig. 1.8a).

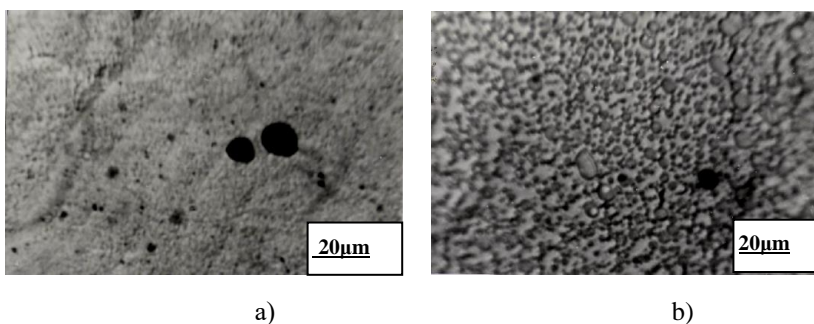a)   b)

Fig. 1.8. Microphotographs of cross-sections of extrudates of PP/SPA/VNT compositions: 100/0/0.5 (a); 30/70/0.5

Repeated extrusion of PP/BNT granules when mixed with SPA provides an increase in the degree of dispersion of carbon nanotubes, but even in the extrudates of the modified

mixtures there are inclusions of BNT aggregates (0.5÷5.0) μm in size (see Fig. 1.8b). It is known that the possibility of achieving a uniform distribution of the filler in the polymer matrix increases many times with a decrease in the size of its particles. This is due to the fact that with a decrease in size, the total specific surface area and the number of particles at the same volume content increase sharply, the distance between them in the matrix decreases and, in general, the ability to form agglomerates increases. At the same time, the high viscosity of polymer melts contributes to the growth of shear stresses, which lead to the destruction of carbon clusters; secondly, a highly viscous environment with low molecular mobility prevents the re-aggregation of carbon fillers [4]. To improve the dispersion of CNTs in the melt of the mixture, it is proposed to apply an additive to PP granules from a water-alcohol suspension and then disperse it in the polypropylene melt. The resulting modified PP/BNT granules were mixed with SPA using a worm-disc extruder.
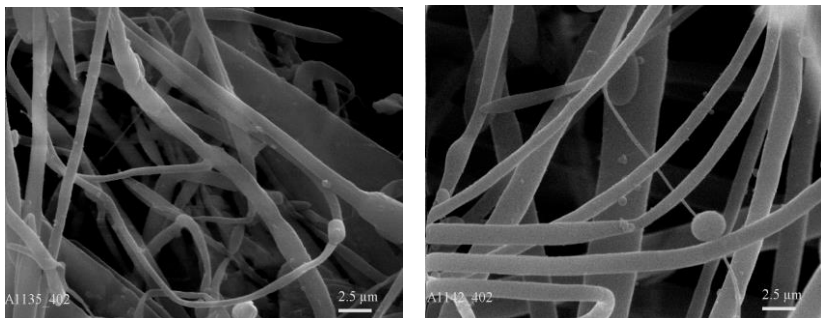
Analysis of the microstructure of extrudates of modified mixtures and PP residues washed from SPA shows that the introduction of 0.5 wt. % CNT does not prevent the deformation and fusion of polypropylene droplets with the formation of microfibrils. Microfibrillar morphology is realized when processing PP/SPA/BNT compositions containing 20; 30 and 40 wt. % component of the dispersed phase (Table 1.7). For mixtures of PP/SPA composition 50/50 wt. % there is a layered morphology, which does not change under the effect of the nanoadditive. The results of microscopic studies showed that in three-component mixtures, the average diameter ($\bar{d}$) of

microfibrils decreases, the homogeneity of their diameter distribution increases, which is evidenced by a decrease in the value of dispersion (σ^2).

Table 1.7 – Influence of CNT additives on the processes of structure formation in PP/SPA mixtures

The composition of the PP/SPA/VNT mixture, wt.%	Types of structures				
	microfibrils			particles wt.%	films wt.%
	đ, µm	wt.%	σ^2, µm^2		
20/80/0	3,6	87,4	1,7	1,4	11,2
20/80/0,5	2,7	97,1	1.1	2.4	0.3
30/70/0	3,3	72,7	1,6	4,3	23,0
30/70/0,5	3,0	96.4	0.8	2.3	1,1
40/60/0	3,8	74,1	1,5	1,9	24,0
40/60/0,5	3,5	84,4	1,7	1,7	13,9

It was also established that the nanofiller slows down migration processes, which leads to a decrease in the number of films and an increase in the proportion of polypropylene that forms microfibrils. Electron micrographs of PP microfibrils show that nanotubes have a stabilizing effect on polypropylene liquid jets. There are no varicose thickenings on the microfibrils, which are the result of their incomplete disintegration (Fig. 1.9.)

a)   b)

Fig. 1.9 – Electron microphotographs of polypropylene microfibrils from
PP/SPA/VNT mixtures of composition: 30/70/0 (a); 30/70/0.5 (b)

Conducted research on the influence of nanofiller content on the microstructure of extrudates showed that the formation of PP microfibrils in the SPA matrix occurs for all compositions in the studied range of additive concentrations (Fig. 1.10, Table 1.8).
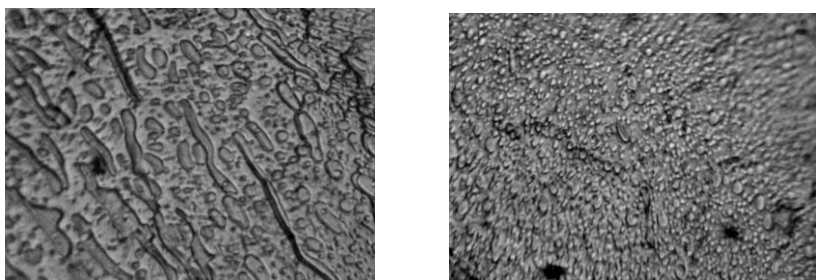
a)   b)

Fig. 1.10 – Microphotographs of cross-sections of extrudates of
PP/SPA1/VNT mixtures of composition: 30/70/0 (a); 30/70/0.1 (b).
Magnification x400 times

Addition to the mixture of only 0.1 wt. % of nanotubes sharply increases the degree of dispersion of polypropylene (Fig. 1.10). Detailed quantitative microscopic studies confirm the

51

formation of a microfibrillar structure in modified PP/SPA mixtures with additives (0.05÷1.0) wt. % CNT (Table 1.8). The predominant type of structure in extrudates with nano additives are polypropylene microfibrils, the mass fraction of which is greater than that of the original mixture. The content of nano additives significantly affects the processes of structure formation during the flow of melts of all systems. As can be seen from the table. 1.8, in extrudates of modified mixtures containing (0.05÷0.5) wt. % CNTs, the share of polypropylene used for the formation of microfibrils increases (up to 96.4 wt. %), their average diameter (đ) decreases and the homogeneity of the distribution improves.

Table. 1.8 – Influence of the content of carbon nanotubes on the processes of structure formation in the PP/SPA mixture

CNT content, wt. %	Types of structures			particles wt.%	films wt.%
	microfibrils				
	đ, µm	wt. %	σ^2, μm^2		
0	3,3	72,7	1,6	4,3	23,0
0,05	2,7	90,4	1,2	4,3	5,3
0,1	2,7	91,7	1,0	2,6	5,7
0,5	3,0	96.4	0.8	2.3	1,1
1,0	3,2	93,4	1,9	1,2	5,4

At all concentrations of the nanofiller, the number of particles and films decreases. The established improvement of microfibrillar morphology in nanofilled mixtures is explained by the stabilizing effect of carbon nanotubes on polypropylene

52

liquid jets, which prevents the breakup of thermodynamically unstable jets on drops.

1.2.2.3. The influence of binary carbon nanotube/compatibilizer additives on the rheological properties of melts of polypropylene/copolyamide blends. A decisive condition for obtaining the necessary indicators in fibers and composites filled with carbon nanotubes is the achievement of dispersion of the nanostate additive, its uniform distribution and optimal orientation in the polymer melt. It is also important to provide conditions for the transfer of stresses from the matrix to the filler. It is quite difficult to achieve this using known and developed technologies due to the high excess surface energy of CNTs, which causes them to stick together and aggregate. To solve these problems, nanotubes are pre-dispersed in solvents using ultrasound, and then introduced into the polymer melt using special equipment (planetary, disk, rotary and screw mixers). The homogeneous distribution of CNTs in the matrix is facilitated by increased adhesion at the matrix-filler interface. In order to overcome the low affinity of nanotubes to the polymer, compatibilizers and surface-active substances are introduced into the mixture, and their surface is chemically or physically modified. Functionalization of the surface of CNTs is one of the methods that prevents their aggregation, increases the affinity for polymer melts in the mixture, and ensures predictable placement in the composition [138]. Modification of carbon nanotubes with titanium stearate made it possible to reduce their content in the CNT/polyolefin mixture by an order of magnitude, compared to the original tubes, and obtain hydrophobic composites with high hardness

and wear resistance. A significant increase in the tensile strength of biodegradable composites was achieved due to interfacial adhesion and the formation of a percolation network in the matrix with the simultaneous use of organomodified montmorillonite and multilayer carbon nanotubes [139].

Among the rheological characteristics of polymer systems in the viscous flow state, the shear viscosity is the most important. It is known that the η of melts of polymer mixtures is affected by many factors: the chemical nature of the initial components and their ratio, phenomena at the boundary of phase separation, processes of structure formation during flow, content and properties of nanofillers. In Fig. 1.11 shows the results of studies of the influence of the concentration (C) of CNTs on the viscosity of melts of the original PP/SPA mixture and with the addition of a compatibilizer - ethylene vinyl acetate copolymer (EVAC) at different shear stresses (τ).
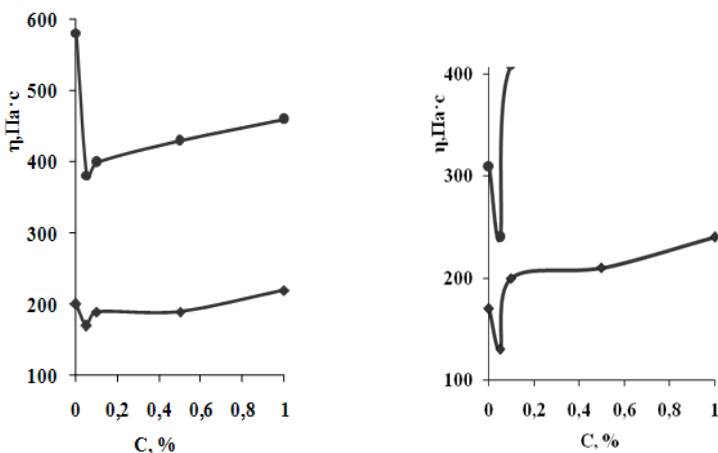

Fig. 1.11. – Dependence of viscosity of melts of PP/SPA polymer mixtures (a); PP/SPA/EVAC (b) from the concentration of CNT, points correspond to τ•10-4, Pa: 5.69(♦); 1.62(●)

The dependence of $\eta = f(C)$ for the specified compositions has a complex character - the viscosity of binary and ternary mixtures decreases when the CNT content is 0.05 wt.%. The established regularity is more evident for mixtures containing both a nanofiller and a compatibilizer. This may be related to the effect of so-called small concentrations, described in [140]. The extreme change in the rheological properties of the melts of the mixtures upon the introduction of tenths of a percent of the additive is a consequence of the change in the thermodynamic parameters of the system, primarily the thermodynamic compatibility or incompatibility of the components in the specified range of compositions. A further increase in the concentration of CNT in the mixture leads to an increase in its viscosity. At the same time, when sodium oleate is used as a compatibilizer, η increases insignificantly at all CNT concentrations.

The second important indicator is elasticity, which is indirectly characterized by the amount of swelling (B) of the extrudate upon exiting the forming hole. The cause of the swelling is the relaxation of highly elastic deformations accumulated by the components of the mixture during the flow. Along with this, liquid jets of dispersed phase polymer acquire significant elasticity values. These are thermodynamically unstable structures, which are new relaxing elements that determine the further growth of elasticity. Table 1.9 shows data on the influence of the content of carbon nanotubes and the chemical nature of compatibilizers (for their simultaneous use) on the swelling of extrudates of the PP/SPA mixture. The concentration of

compatibilizers (copolymer of ethylene with vinyl acetate and sodium oleate) in the composition was 3.0 wt. % by weight of polypropylene.

Table 1.9. Effect of CNT additives and compatibilizers on the swelling of PP/SPA mixture extrudates

CNT content, wt.%	The name of the additive		
	CNT	CNT/SEVA	CNT/sodium oleate
0	7,9	8,9	8,1
0,05	7,5	9,2	7,7
0,1	7,4	8,3	7,6
0,5	6,8	8,0	7,1
1,0	6,7	7,4	6,8

The research results indicate an increase in *B* values for four-component compositions. Additions of sodium oleate and SEVA increase the affinity between macromolecules of polypropylene and co-polyamide at the phase separation boundary, thereby contributing to the formation of thinner PP fibrils in the SPA matrix [141]. The increase in swelling of extrudates of compatibilized mixtures is an indirect indication of the formation of a more perfect morphology. At the same time, the SEVA supplement is more effective, judging by the size of the swelling. At the same time, the elasticity of the melts of the mixtures depends on the concentration of CNTs and decreases with its increase. This is due to the fact that nanotubes, falling into liquid jets of PP, prevent the release of the accumulated strain. It is known from Tomotika's classical works that stress relaxation in liquid jets proceeds by their

disintegration into drops under the action of a wave of destructive excitation. The presence of nanotubes in the jet of polypropylene melt opposes this process, since the amplitude of the wave is extinguished on the particles.

The ability of the melts of the investigated compositions to be processed into fibers and films, determined by the value of the maximum spinneret extraction (Fmax), depends significantly on the content of nanotubes and the chemical nature of the compatibilizer (Table 1.10).

Table 1.10 – Influence of the CNT content and the chemical nature of compatibilizers on the melt flowability of the PP/SPA mixture

CNT content, wt.%	The name of the additive		
	CNT	CNT/SEVA	CNT/sodium oleate
0	9300	12900	9800
0,05	10400	13200	11600
0,1	11000	16600	12500
0,5	14500	16900	13900
1,0	13600	17900	15100

Additions of compatibilizers, as expected, dramatically increase the ability of the system to longitudinal deformation. This is due to a change in the processes of structure formation of PP in the matrix under the action of two additives and an increase in the strength of the melt jet due to the formation of specific interactions at the boundary of the phase separation of the components. At the same time, the copolymer of

ethylene with vinyl acetate is more effective compared to molten salt.

1.2.2.4. The effect of binary additives carbon nanotubes/ compatibilizer on the microstructure of extrudates of polypropylene/copolyamide mixtures. The performed microscopic studies confirmed the modifying effect of the selected compatibilizers (Fig. 1.12). Microphotographs of cross-sections of extrudates of the studied compositions show that in the presence of SEVA, aggregates of nanotubes in the melt of the mixture are destroyed (Fig. 1.12a), and the degree of dispersion of PP in the matrix also increases (Fig. 1.12b).

a)   b)
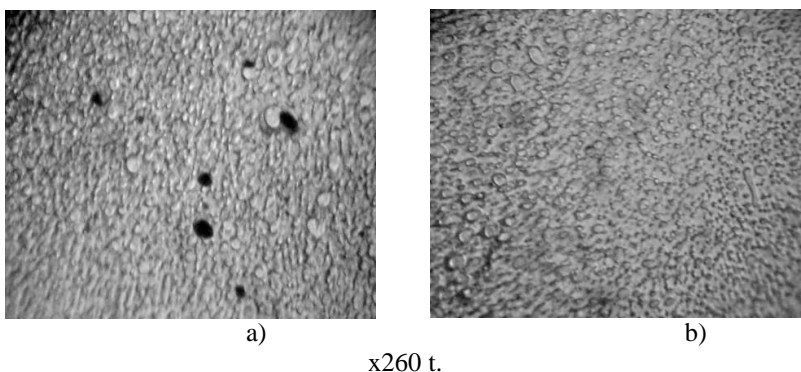
x260 t.

Fig. 1.12 – Microphotographs of cross-sections of PP/SPA/VNT extrudates (a) and PP/SPA/VNT/SEVA (b) composition 30/70/0.5 and 30/70/0.5/3.0, respectively

In four-component compositions, a more perfect morphology is formed: the average diameter of PP microfibrils ($\bar{d}$) decreases, their mass fraction increases, and a number of undesirable structures (particles, films) decrease (Table 1.11).

Table 1.11 – Influence of CNT content and chemical nature of compatibilizers on the microstructure of PP/SPA mixture extrudates

Additive		Continuous fibrils		Short fibrils	Particles	Films	Outer shell
name	quantity, wt %	$\bar{d}$, µm	wt, %	wt, %	wt, %	wt, %	wt, %
without additive		3,8	85,1	12,9	0,1	1,0	0,9
CNT	0,1	3,3	89,4	9,4	0,3	0,7	0,2
CNT /SEVA	0,1/3,0	2,8	90,8	6,8	1,2	1,2	-
CNT /sodium oleate	0,1/3,0	3,6	95,4	3,4	0,8	0,4	-

In the presence of compatibilizers, the outer thin fibrous shell is not formed.

Thus, the introduction of compatibilizers into the nanofilled composition allows you to control the morphology of the system in the direction of the formation of a more perfect microfibrillar structure.

1.2.2.5. The influence of CNT additives on the patterns of disintegration of polypropylene microfibrils in the matrix. One of the microrheological processes that determines the formation of the structure of polymer dispersions is the destruction of liquid jets (cylinders) formed *in situ* during the flow of their melt. Knowledge of the patterns of disintegration of cylinders of one polymer in the matrix of another is

important from the point of view of controlling the morphology of polymer composites.

It is known that the degree of interaction at the boundary of phase separation affects the stability of liquid jets. At the same time, the affinity of nanofilled mixtures is determined by the size of the transition layer at the polymer-nanoparticle interface. The separation surface around the nanoadditive particle has a finite thickness, within which the properties of the melt differ sharply from the similar characteristics of the original components. When the size of the particles decreases to 1.0 nm, the influence of the specific surface area increases, as large transitional layers are formed. They change the main characteristics of the melt - fluidity, crystallization, etc. At a filler concentration of 15 vol. % with nanoparticles with a diameter of 10 nm, the distance between them is 5 nm. In this case, the entire polymer matrix in the composite can behave as a transition layer. The introduction of nano-additives allows you to adjust the size and properties of the interfacial layer.

In Tomotika's classic works, it is shown that the cause of hydrodynamic instability of a liquid jet and its destruction is the occurrence of wave-like disturbances on its surface, the amplitude of which increases exponentially with time:

$$a = a_0 \exp(q t_l), \qquad\qquad (1.4)$$

where a_0 – the initial amplitude of the disturbance,

q – the coefficient of instability

The jet breaks up into drops provided that the magnitude of the perturbation amplitude is equal to its radius (R). Periodic thinning and thickening appear on the surface of the jet before

disintegration. The destruction of the jet occurs during some time, which is considered as the time of decay or life (t_l). The stability of a liquid polymer jet in the matrix of another is determined by the instability coefficient, which is a function of the wave number (X), the ratio of the viscosities of the dispersed phase and the dispersion medium ($K = \eta_1/\eta_2$) and the value of the interfacial tension between the cylinder and the matrix ($\gamma_{\alpha\beta}$) [134] :

$$q = (\frac{\gamma_{\alpha\beta}}{2\eta_1 R}) F(X, K)$$

(1.5)

It can be seen from this equation that, other conditions being equal, liquid jets will be more stable at lower values of surface tension.

To study the influence of carbon nanotubes on the processes of disintegration of PP microfibrils in the SPA matrix, the prepared longitudinal sections of the extrudates of the mixtures were placed on the heating table of the microscope, the temperature was increased and various stages of the disintegration process were photographed. At the appropriate temperature, the microfibrils become "varicose" and then break up into a chain of droplets. The initial radius of the cylinder (R), the radius of the formed droplets (r_k), and the distance between their centers were measured from the microphotographs. The obtained results were processed according to the Tomotika theory and the wavelength of the destructive disturbance (λ_m), the wave number ($2\pi R/\lambda_m$) and the tabulated function (Ω) were determined. The instability

coefficient (q) and the value of the interfacial tension ($\gamma_{\alpha\beta}$) were calculated on the basis of the microfibril decay kinetics data.

To calculate the interfacial tension, we used the dependence derived by the authors [142], based on the theory of destabilization of a liquid cylinder under the action of waves of destructive excitation in the melt of two polymers, one of which is in the form of jets in the matrix of the other:

$$\gamma_{\alpha\beta} = \frac{q \cdot \mu \cdot d_0}{\Omega(\chi, K)} \qquad (1.6)$$

where: q – the coefficient of instability;

μ – matrix polymer melt viscosity;

d_0 – the initial diameter of the jet;

χ – the wave number of the destructive disturbance;

K – the ratio of the viscosities of the dispersed phase and the matrix;

Ω – a tabulated function determined from the curve of dependence of χ on K

The experimental results regarding the effect of nanotubes on the parameters of the kinetics of PP microfibril decay and the amount of surface tension at the polypropylene/copolyamide interface are shown in Table. 1.12. The conducted studies showed that the value of γαβ reaches the highest value for the original PP/SPA mixture, which is due to the low affinity between the segments of macromolecules of non-polar polypropylene and polar co-polyamide at the boundary of phase separation (Table 1.12).

Table 1.12 – Effect of CNT content on the value of interfacial tension and parameters of PP microfibrils disintegration kinetics

Content of CNT, wt %	R, μm	λ_m, μm	Ω	q	$2\pi R/\lambda_m$	$\gamma_{\alpha\beta}$, mN/m	t_l
0	1,77	8,10	0,045	0,0348	1,3	2,60	24,6
0,10	1,73	8,53	0,048	0,0220	0,9	0,73	37,1
0,50	1,71	8,77	0,053	0,0186	0,8	0,58	42,3
1,0	1,64	9,06	0,075	0,0181	0,6	0,32	49,3

The introduction of nanotubes increases the compatibility between components in nanofilled systems, which is evidenced by a decrease in $\gamma_{\alpha\beta}$ indices for compositions of all compositions. In the presence of a nanofiller, a developed transition layer is formed at the boundary of the separation of the components of the mixture: the surface tension decreases sharply and the stability of liquid jets increases. The modification of the interphase layer is manifested in the increase in the degree of dispersal of PP particles and their deformation into liquid jets due to a decrease in energy expenditure for the formation of new surfaces of the dispersed phase. It was established that the maximum influence of additives on the processes of structure formation is manifested at concentrations at which the values of interfacial tension have minimum values.

The decay time (life time – t_l) of a liquid cylinder is directly proportional to the viscosity of the melt (η), its radius (R) and inversely proportional to the interfacial surface tension:

$$t_l = \eta \, R / \, \gamma_{\alpha\beta} \qquad\qquad (1.7)$$

A decrease in $\gamma_{\alpha\beta}$ leads to an increase in life time, which contributes to the stabilization of thinner polypropylene jets. The experimentally determined decrease in the diameter of PP microfibrils is also due to the fact that the presence of nanotubes in the polymer jet of the dispersed phase prevents the growth of the amplitude of the wave of destructive excitation. The increase in the stability of liquid PP cylinders is confirmed by a decrease in the average diameter of microfibrils (Table 1.8) and the absence of varicose microfibrils in electron micrographs (Fig. 1.6), which are the result of incomplete disintegration of jets on a drop.

The mechanism of action of nanotubes on the *in situ* formation of microfibrils of the component of the dispersed phase in the matrix consists in increasing the thermodynamic stability of thinner liquid jets. This is due to a decrease in the surface tension at the boundary of the phase separation and the amplitude of the destructive excitation wave. This is confirmed by the data obtained and processed according to the Tomotika theory regarding the disintegration of a liquid cylinder, according to which the interfacial tension drops by 5 times for the mixture with CNT additive compared to the original one, and the disintegration time increases by 1.6 times.

Thus, the experimental data confirmed the correctness and effectiveness of the choice of carbon nanotubes as

modifiers for melts of polypropylene/copolyamide mixtures. The introduction of carbon nanotube additives contributes to the *in situ* formation of microfibrils of the dispersed phase component in the polymer matrix.

1.2.3. The effect of additives of various metal oxides on the rheological properties and microstructure formation of the polypropylene/copolyamide mixture. Effective methods of modifying synthetic fibers include reducing the diameters of individual filaments, introducing nanoparticles of metal oxides into their structure, and forming them from a mixture of polymers. Polyester textile threads filled with TiO_2, Al_2O_3, ZnO, and MgO nanoparticles exhibit a wide antibacterial spectrum against pathogenic flora, photocatalytic activity, protection against UV radiation, antistatic properties, and abrasion resistance [28]. The introduction of zinc oxide NPs in the form of nanorods into polypropylene fibers provides them, in addition to antibacterial, antiallergic and improved mechanical properties. Modification of fibers with micro- and nano-sized filaments with TiO_2 and ZnO nanoparticles gives products from them the ability to self-clean like plant leaves, insect wings, etc. [7,23-30].

The formation of matrix-fibrillar morphology in thermodynamically incompatible mixtures is determined by a number of factors: the composition of the composition, the ratio of the viscosities of the components, the degree of their compatibility (the amount of surface tension at the boundary of the phase separation), processing conditions (time and speed of mixing, geometry and dimensions of the extruder screw), etc.

A necessary condition for the deformation of a drop into a jet and its preservation of a cylindrical shape is the presence of a developed transition layer, which ensures the transfer of stresses from the matrix to the dispersed phase. One of the most effective methods of influencing interphase phenomena is the introduction of a third component, which exhibits a compatibilizing (emulsifying) effect and allows to regulate the morphology of polymer dispersions. It is known that compatibilizers can be special substances or nano-sized additives. The introduction of nanoparticles into the melt of a mixture of polymers is an effective factor in regulating the process of *in situ* formation of microfibrils of one polymer in the matrix of another. This makes it possible to create qualitatively new materials with predictable characteristics due to changes in morphology and the presence of substances in the nanostate in their structure.

Studies of the effect of nanoparticles of a number of metal oxides (ZnO, Al_2O_3, TiO_2) and mixed oxide ZnO/ Al_2O_3 on the microstructure of extrudates of the PP/SPA mixture showed that they have a compatibilizing effect on the melt [142]. This is evidenced by the increase in the degree of dispersion and homogeneity of the distribution of the transverse dimensions of polypropylene droplets (particles) in the SPA matrix (Fig. 1.13, Table 1.13). The data of morphometric analysis indicate a different degree of modifying action of the investigated nanofillers (Table 1.13). Titanium oxide and mixed oxide (ZnO/ Al_2O_3) are the most effective. In their presence, coarse PP particles (with equivalent diameters $D_e \geq 10.0$ µm) disappear, the share of particles with $D_e = (1 \div 2)$

μm increases by 2.8 and 8.5 times when TiO_2 and $ZnO/Al2O_3$ nanoparticles are introduced, and the average equivalent diameter decreases from 5.1 μm (for the original mixture) to 3.0 and 2.4 μm for the modified mixtures, respectively.
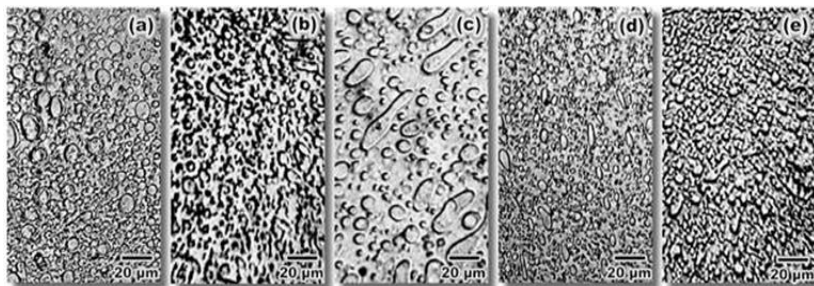

Fig. 1.13. Microphotographs of cross-sections of extrudates of the PP/SPA mixture with nanoparticles of metal oxides: a – without additives; b – TiO_2; c – ZnO; d – Al_2O_3; e – ZnO/ Al_2O_3

Таблиця 1.13 Table 1.13 – Effect of metal oxides on the degree of dispersion of PP droplets in the SPA matrix

The name of the oxide	Equivalent diameter of PP drops, μm		
	minimum	average	maximum
without additives	1,2	5,1	24,9
ZnO	0,7	4,3	24,1
Al_2O_3	1,0	3,4	18,0
TiO_2	1,0	3,0	8,9
ZnO/Al_2O_3	0,6	2,4	7,0

The homogeneity of nano-filled compositions also increases - the distribution curves of particles of the dispersed phase by equivalent diameters narrow (Fig. 1.14).
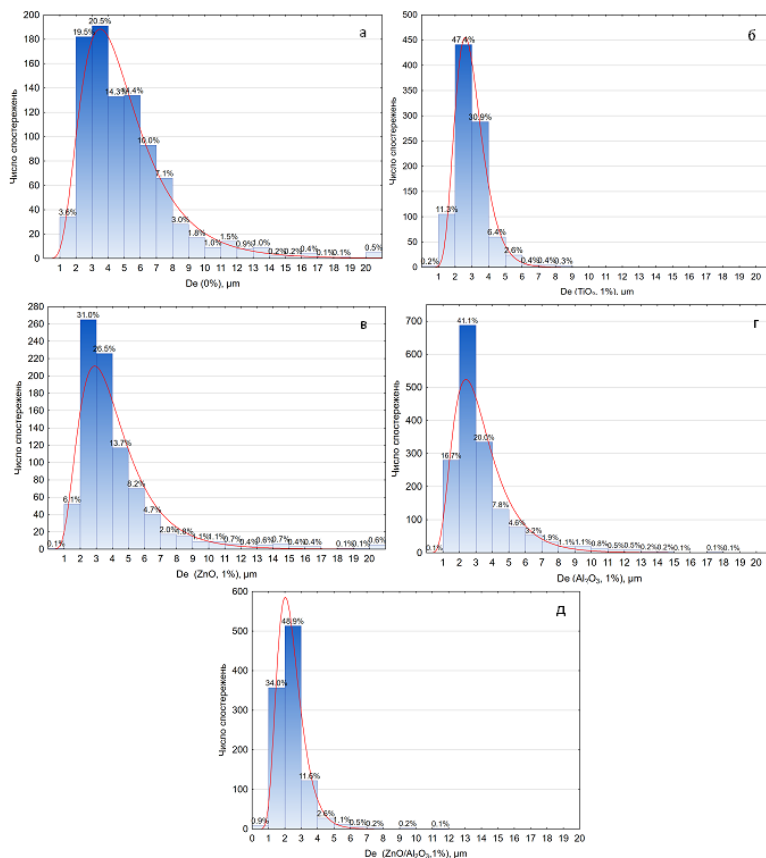
Fig. 1.14. Histograms of the distribution of PP particles by equivalent diameters in the extrudates of the PP/SPA mixture with nanoparticles of oxides of various metals: a – without additives; b – TiO_2; c – ZnO; d – Al_2O_3; e – ZnO/Al_2O_3

To determine the type of structures formed by polypropylene in the matrix, microscopic studies of PP residues after extraction of SPA from extrudates with additives of various oxides were carried out. It was established that polypropylene microfibrils are formed *in situ* during the flow

of all mixtures. At the same time, they are not the only type of structures in the extrudate: some part of polypropylene is spent on the formation of films and is in the form of highly dispersed droplets (Table 1.14).

Table 1.14 - Characteristics of the microstructure of extrudates of the original and modified mixtures

The name of the metal oxide	Microfibrils		Particles		Films, wt %
	d_m, µm	wt %	d_p, µm	wt %	
without additives	4,0	82,7	4,0	8,3	9,0
TiO_2	2,0	97,8	2,8	1,1	0,9
Al_2O_3	2,2	94,9	1,8	1,0	4,1
ZnO	3,8	92,3	4,1	2,4	5,3
ZnO/Al_2O_3	1,8	98,7	2,4	0,8	0,5

It was established that when using different oxides, the ratio between the types of morphology in the PP/SPA mixture changes, namely: the share of undesirable structures (films, particles) decreases. At the same time, the average diameter of microfibrils is minimal for compositions with mixed oxide.

The reduction of the geometric size of the particles of the dispersed phase and the formation of a finer morphology of the mixture when adding nanofillers is associated with their influence on the course of interphase phenomena and on the rheological characteristics of the starting polymers. It is known that third components, which are able to show specific interactions (hydrogen, dipole-dipole, chemical, etc.) with one or both ingredients of the mixture, improve the compatibility of polymers at the boundary of phase separation [4]. The studied

metal oxides in the nanostate have high surface energy, exhibit amphoteric properties and can form physical or chemical bonds with amino, oxide, and carboxyl groups of co-polyamide macromolecules. On the surface of titanium oxide NPs, there is always a certain amount of hydroxyl groups that can react with the end groups –COOH of co-polyamide with the formation of chemical bonds. The presence of various types of bonds in the nanofilled PP/SPA mixture contributes to an increase in the degree of compatibility, which leads to a decrease in the surface tension and the formation of thinner PP microfibrils.

The compatibilizing effect of nanoadditives is enhanced if they are preferentially localized at the boundary of the polymer/polymer interface [52-58,60,63,104]. Nanoparticles are placed in one of the phases or in the interphase region in such a way that the total free energy of the system is minimized. The competitive interaction between the polymer and NPs is a prerequisite for their migration and thermodynamically favorable location. The movement of nanosized silica from the polyethylene melt to the interphase region and to polylactide was shown and experimentally confirmed [104].

The established significant modifying effect of nanoparticles of metal oxides in the PP/SPA mixture was achieved due to the two-stage introduction of nanoadditives into the system. In the first stage, NPs of metal oxides with a polar surface were dispersed in a nonpolar polypropylene melt, and in the second stage, the obtained granules were mixed with the matrix. The affinity of nanofillers to polar co-polyamide and the poor wetting of nanoparticles by the melt of non-polar

polypropylene led to their migration from it and selective localization in the transition layer.

The second factor that determines the morphology of nanofilled mixtures is a change in the rheological characteristics of the melts of the original components in the presence of an additive. A change in the ratio of the viscosities of the melts of the dispersed phase and the matrix (η_1/η_2) and their elasticities (B_1/B_2) can shift the equilibrium in the processes of deformation and coalescence of droplets and disintegration of liquid cylinders [4,22,143]. The possibility of controlling the morphology of incompatible polymer mixtures by adjusting η_1/η_2 was shown in [143]. The processing of three-component mixtures, in which the matrix polymers were polystyrene or polyethylene oxide, and the dispersed phase was polyamide-6 and polyethylene, resulted in a thin fibrous material made of micro- and nanofibers. At the same time, the average diameter of PA-6 microfibers was ~ 9.0 μm, and PE nanofibers ~ 600 nm. The components of the mixtures were selected in such a way that the ratio of the viscosities of the fiber-forming polymers and the matrix for the first component was greater than unity, and for the second - close to 1.

Experimental data on the effect of metal oxides on the rheological properties of the original PP melt indicate an increase in its viscosity (η_1) in the presence of all additives (Table 1.15). This result is expected and can be related not only to the effect of filling with a solid substance, but also to the formation of a transition layer at the boundary of the nanofiller/polymer separation, the properties of which are

sharply different from the similar characteristics of the melt in the volume.

Table 1.15 – Effect of metal oxides on the rheological properties of polypropylene melt*

The name of the oxide	η_1, Pa·s	η_1/η_2	B_1	B_1/B_2
without additives	260	0,35	1,8	1,29
ZnO	275	0,37	1,7	1,21
Al_2O_3	300	0,40	1,6	1,14
TiO_2	350	0,47	1,5	1,07
ZnO/Al_2O_3	420	0,77	1,5	1,07

* at $\tau = 5,69 \cdot 10^4$ Pa; $\eta_2 = 740$ Pa·s; $B_2 = 1,4$

At the same time, the elasticity of the modified PP melt decreases, judging by the equilibrium swelling values ($B1$) (Table 1.15). The decrease in the values of $B1$ is due to the complication of the mobility of the segments of the PP macromolecule chains in the presence of the nanofiller. At the same time, the absolute values of the rheological characteristics depend on the nature of the metal oxide. From the table 1.15 it can be seen that the indicators of the ratio of viscosities and elasticities of PP and SPA melts change differently: the values of η_1/η_2 increase, compared to the original mixture, and B_1/B_2 - decrease to unity. Approximation of the ratios of viscoelastic properties of the components to unity is a prerequisite for better dispersion and deformation of polypropylene droplets in the co-polyamide matrix, which is confirmed by the results of the performed microscopic studies (Table 1.14).

Thus, it was established that the introduction of nanoparticles of oxides of various metals allows to regulate the microstructure of the polypropylene/copolyamide mixture melt during its flow. In nanofilled systems, a more perfect morphology is formed: the average diameter of PP microfibrils decreases, and their mass fraction increases. The modifying effect is manifested due to their influence on interphase phenomena and rheological properties of nanofilled polypropylene melt. Nanoparticles of metal oxides act as compatibilizers in the PP/SPA mixture. Additions of metal oxides also affect the rheological properties of the PP melt: its viscosity increases and elasticity decreases. The values of the ratio of the viscoelastic characteristics of the dispersed phase and the matrix in nanofilled systems depend on the oxide used and are indirectly correlated with the microstructure of the extrudates. If these ratios approach unity, the diameter of PP microfibrils decreases, and their fate increases. The most effective modifiers of the polypropylene/copolyamide mixture are titanium oxide and mixed oxide (ZnO/Al_2O_3) - the average diameter of the microfibrils is 2.0 and 1.8 μm, respectively.

1.2.4. Microfibrillar composites polypropylene /polyvinyl alcohol/nanofiller. In contrast to traditional methods of forming chemical fibers, a bundle of tens and hundreds of thousands of filaments is obtained after the extraction of a polymer dispersion medium from a composite thread with a microfibrillar structure. At the same time, an important stage of the technological process is the removal of the matrix component from the composite thread with a solvent that is

inert in relation to the polymer of the dispersed phase. It is important to use a cheap, available, non-toxic substance that does not require special safety measures when working with it. Given that water-soluble polymers are produced by industry in large volumes, it was appropriate to use polyvinyl alcohol (PVA) as a matrix component. To process PVA mixed with polypropylene into fibers and films, it was plasticized with glycerin, which was injected in the amount of 5; 10; 15 wt. %. The obtained experimental results showed that when glycerol is introduced, PVA melts without thermal destruction and goes into a viscous state at 190 oC. The concentration of the plasticizer significantly affects the rheological properties of PVA (Table 1.16).

Table 1.16 – Effect of glycerol concentration on the rheological properties of polyvinyl alcohol

Glycerin content, wt %	η, Pa·s at $\tau \cdot 10^{-4}$ Pa			n*	$F_{макс}$, * %	B*
	5,69	4,17	1,62			
5,0	430	500	600	1,4	23500	1,2
10,0	270	320	400	1,3	10000	1,2
15,0	140	170	200	1,2	6200	1,2

* at $\tau = 5,69 \cdot 10^{-4}$ Pa

When the glycerol content increases, η of the melt drops by ~3 times for all shear stresses. Melts of plasticized polyvinyl alcohol are typical non-Newtonian fluids. At the same time, the influence of the rate of deformation on the effective viscosity decreases with the increase in the concentration of the plasticizer, which is evidenced by the decrease in the value of

the index (n), which characterizes the degree of deviation from the Newtonian flow mechanism. On the curves of dependence $\eta = f$ (lg τ), the "structural" section becomes more inclined with increasing glycerol content (Fig. 1.15).
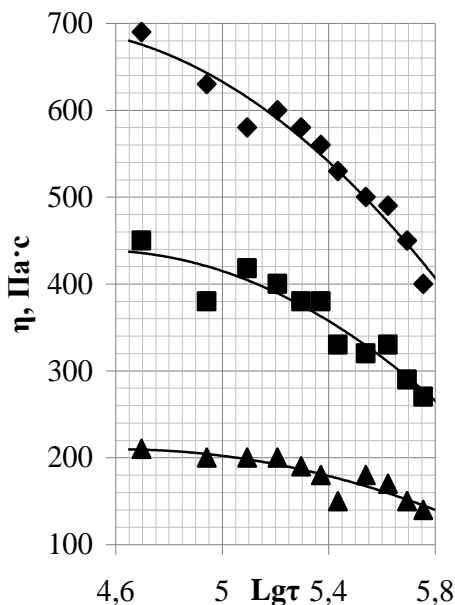

Fig. 1.15. Curves of dependence of melt viscosity on shear stress for plasticized PVA. Glycerin content, wt.%: 5.0 (♦); 10.0 (■); 15.0 (▲)

This is natural, since it is known that the plasticization of PVA occurs according to the intra-pack mechanism, that is, there is a destruction of the supramolecular structure of the polymer, which brings its flow regime closer to a Newtonian fluid.

An important feature of polymer melts is high elasticity, which is due to the accumulation of elastic deformations, which is a consequence of changes in the mutual location of macromolecule segments during their flow. Elasticity

significantly affects the ability of the melt to process and preserve the shape of the products. Upon exiting the melt from the forming hole, highly elastic deformations relax, which leads to an increase in the cross-section of the extrudate compared to the dimensions of the nozzle. The conducted studies showed that the concentration of glycerol practically does not affect the swelling of the extrudate (B) of plasticized PVA (Table 1.16). The ability of melts to undergo longitudinal deformation, determined by the value of the maximum spinneret extraction, drops sharply when the glycerol content increases to 15.0 wt. % (Table 1.16). Deterioration of directivity is caused by a decrease in the strength of the melt jet due to a drop in shear viscosity. The obtained results indicate that the plasticized polymer can be processed through the melt on traditional extrusion equipment. Conducted studies have shown that plasticized PVA does not lose solubility in cold and hot water.

1.2.4.1. Influence of the ratio of components on the rheological properties and morphology of polypropylene/polyvinyl alcohol mixtures. The viscosity of melts of polymer mixtures is largely determined by the chemical nature of the initial components, which determines their thermodynamic compatibility at the boundary of phase separation. Table 1.17 shows the rheological properties of the starting polymers and PP/PVA mixtures. From the table 1.17 shows that the obtained experimental values of the effective viscosity (η) are lower than the viscosity of the initial components and additive values (η_{ad}).

Table 1.17. Rheological properties of PP, PVA melts and their mixtures

The composition of the PP/PVA mixture, wt %.	Viscosity, Pa·c*		n	$B*$	$F_{max}*$
	η	$\eta_{ад}$			
0/100	270	-	1,3	1,4	8400
100/0	290	-	2,0	1,6	26900
20/80	100	248	1,7	2,7	5500
30/70	90	242	1,8	2,3	6200
40/60	80	236	1,7	2,1	5200

* at $\tau = 5{,}69 \cdot 10^4$ Pa

In case of introduction into PVA of 20 wt. % of polypropylene, the viscosity of the mixture is reduced by two times. An increase in its concentration is accompanied by a further decrease in η of the melt. This is a characteristic pattern for melts of mixtures of thermodynamically incompatible polymers. Weak intermolecular bonds in the interfacial layer cause low adhesion at the phase separation boundary. The value of interfacial viscosity can be 100 times smaller than η of the melt of the mixture as a whole [88]. That is why the "property - composition" dependences for thermodynamically incompatible mixtures have a negative deviation from additivity. A sharp decrease in viscosity can also be associated with the deformation and orientation of the polymer droplets of the dispersed phase (PP) in the direction of the flow. It has been proved theoretically and experimentally that to ensure the

melt flow of a mixture with deformable droplets, a smaller pressure drop (corresponding to a lower viscosity) is required than during the flow of individual polymers [135].

Melts of PP, PVA and their mixtures are typical non-Newtonian liquids, judging by the values of the index (n), which characterizes the degree of deviation from the Newtonian flow mechanism (Table 1.17). At the same time, the influence of the deformation rate on the effective viscosity for mixtures is much higher than for the matrix polymer (Fig. 1.16). This may be due to an increase in the structural heterogeneity of the melts of the mixtures.
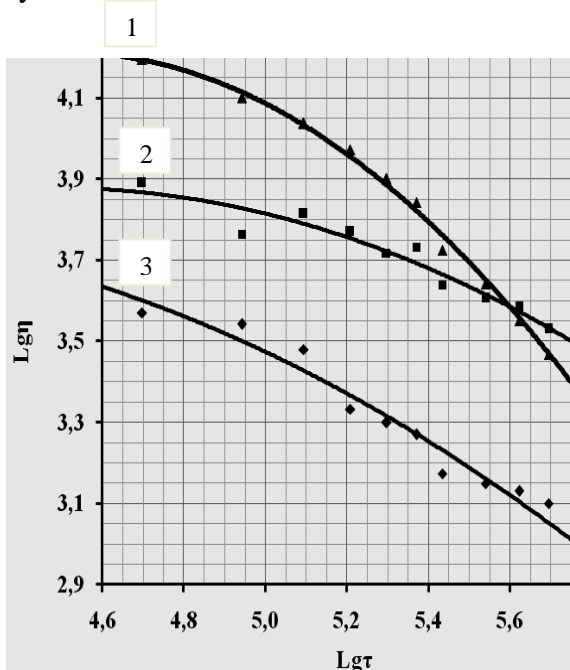

Fig. 1.16. Melt flow curves: 1 – PP; 2 – PVA; 3 – a mixture of PP/PVA with a composition of 20/80 wt. %

A characteristic feature of polymer melts and their mixtures is high elasticity, which is the result of the accumulation of deformations in the jet melt during flow through the channel. Upon exiting the melt from the forming hole, highly elastic deformations relax, which leads to an increase in the cross-section of the extrudate compared to the dimensions of the nozzle. For polymer mixtures in which a microfibrillar structure is formed, the swelling values of extrudates are several times higher than this indicator for individual polymers [72]. The values of equilibrium swelling indirectly characterize the process of formation of fibrils of the dispersed phase in the matrix: the maximum values of B are reached when microfibrils are the only type of structure in the extrudate, and their diameters are minimal. Small swelling values for PP/PVA mixtures in the studied concentration range, compared to PP/SPA mixtures [72], indicate the formation of a significant number of other types of structures (particles, films) (Table 1.17).

Microscopic studies of the processes of structure formation in the melts of PP/PVA mixtures showed that the formation of polypropylene microfibrils in the polyvinyl alcohol matrix occurs for all the studied mixture compositions (Table 1.18). The process is most clearly implemented in the case of a PP/PVA component ratio of 20/80 by weight. %: the average diameter of microfibrils is the minimum, and the mass fraction of polypropylene used for their formation is the maximum. In the case of an increase in the PP content, the degree of its dispersion worsens, which leads to an increase in

the average diameter of microfibrils and the formation of a larger number of films.

Table 1.18 - Microstructure characteristics of extrudates of PP/PVA polymer mixtures

The composition of the PP/PVA mixture, wt. %	Continuous fibrils		Short fibrils		Particles		Films
	d, μm	wt. %	d, μm	wt. %	d, μm	мас. %	wt. %
20/80	3,0	72,4	2,3	17,1	3,5	3,2	7,3
30/70	3,5	64,0	2,1	19,5	3,6	8,0	4,2
40/60	4,0	66,7	2,0	17,3	2,5	3,7	12,3

The process is most clearly implemented in the case of a PP/PVA component ratio of 20/80 by weight. %: the average diameter of microfibrils is the minimum, and the mass fraction of polypropylene used for their formation is the maximum. In the case of an increase in the PP content, the degree of its dispersion worsens, which leads to an increase in the average diameter of microfibrils and the formation of a larger number of films.

Processing and generalization of experimental data on the viscoelastic properties of polymer melts was carried out using a method based on temperature (concentration) time or frequency superposition. This makes it possible to significantly expand the range of investigated shear rate values. Modern devices for rheological research cover an interval of change in

shear rate with a width of 2-3 decimal orders. The processing of the results by the method of concentration-time superposition expands the change in the shear rate to 5 decimal orders. The essence of the superposition regarding the results of rheological studies is that the experimental data of the dependence of the logarithm of the shear stress on the logarithm of the shear rate obtained at different concentrations (temperatures) can be combined. This is achieved by moving along the axis of the shear rate by the amount of $\lg a_T$ (a_T is the gear ratio). Such a generalization is possible only when the relaxation spectra of polymer systems are similar at different temperatures and concentrations. For many binary mixtures of polymers, there are quite wide regions where the dependence of the viscosity on the shear rate in the reduced coordinates is invariant with respect to the composition [135]. For PP/PVA mixtures, the Newtonian section of the curve was not reached in the experiment, so the maximum Newtonian viscosity was found by extrapolating the dependence $lg\eta$ - $lg\tau$ при $\tau \rightarrow 0$. The results of summarizing the data for the indicated mixtures with different PP content showed the invariance of the viscosity dependence on the shear rate in the given coordinates in relation to the concentration of polypropylene (Fig. 1.17). As can be seen from fig. 1.17, in the coordinates $\lg(\eta/\eta_N)$ – $\lg(\eta_N \cdot \dot{\gamma})$ for all mixtures, the points are quite densely located near one common curve. This indicates that the influence of the composition of the mixture on the effective viscosity is manifested through the greatest Newtonian viscosity.
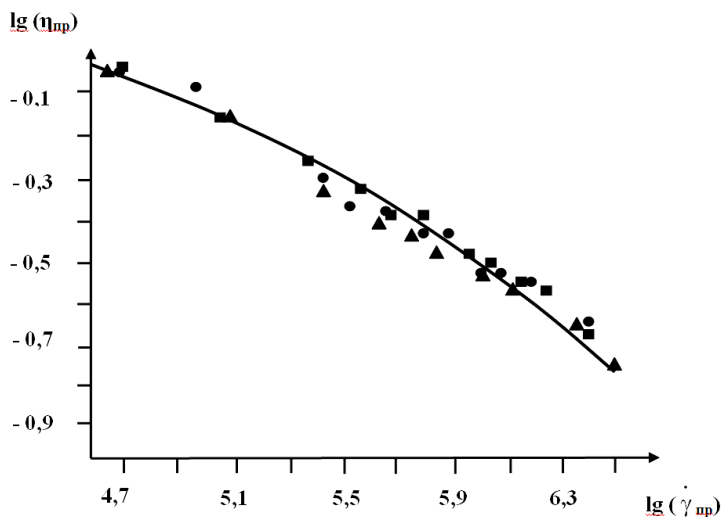
Fig. 1.17. Dependence of viscosity on shear rate in the given coordinates for melts of PP/PVA mixtures, mass %: ■ – 20/80; ▲ – 30/70; ● – 40/60

The existence of a universal dependence of η in the given coordinates proves that the relaxation spectra of the melts of the studied mixtures are similar and described by the same functional dependence. The logarithmic form of the relaxation spectrum is the same for the melts of the mixture in the entire range of concentrations. In practical terms, using the method of constructing the concentration-invariant viscosity characteristic makes it possible to determine the value of η at all shear stresses for other concentrations. For this, we use the concentration dependence η and the effect of the shear rate on the effective viscosity (assuming the same composition of the mixture).

1.2.4.2. Patterns of flow and structure formation in melts of polypropylene/polyvinyl alcohol/silica mixtures. Polymer mixtures are special colloidal systems characterized by the formation of an interphase layer. The developed transitional layer significantly affects the microrheological processes in melts of polymer mixtures, namely: deformation of droplets, merging of liquid jets in the direction of flow, their disintegration into droplets, migration of the dispersed phase along the radius of the forming hole. The introduction of nano-additives allows you to adjust the length and properties of the interfacial layer. The degree of influence of fillers on the melt properties of polymer mixtures is determined not only by the chemical nature of the components, but also by the sequence of their mixing [52-58]. Pyrogenic silica with methyl groups grafted to the surface of its particles (MSi) was chosen as a nano additive. In order to evaluate the influence of nano-sized additives on the processes of deformation of polymer droplets of the dispersed phase in the jet, studies of the microstructure of extrudates of PP/PVA/MK mixtures with a composition of 30/70/1 by weight were carried out. % obtained by three methods [69]. In the first case, methylsilica was pre-dispersed in the melt of the dispersed phase component (PP), and then the resulting PP/MC granules were mixed with matrix polymer (PVA); in the second, the nano-additive was introduced into the plasticized PVA melt, and the obtained PVA/MK granules were mixed with PP; in the third - all three components were mixed in the melt at the same time. For the research, PVA was used, which contained 7.0 wt. % glycerin.

From the fundamental Taylor relations, which describe the thermodynamic equilibrium in dispersed systems, it follows that the most effective factor that allows regulating the parameters of the phase structure is the affinity of the components. The dispersion medium during the flow acts on the droplet dispersed in it with a force T_η, which can be transferred to the droplet and deform it, provided that there is sufficient interaction between the two polymers of the mixture in the transition layer. The force T_η is proportional to the gradient of the shear rate (dV_x/dy), the viscosity of the medium (μ) and is a function of the ratio of the viscosities of the components:

$$T_\eta = C\,(dV_x/dy)\,\mu f\,(\mu/\eta) \qquad (1.8)$$

where η – viscosity of the dispersed phase polymer;

C – a constant value

A drop of dispersed phase polymer resists deformation with force:

$$T_\gamma = 2\,\gamma_{\alpha\beta}/r \qquad (1.9)$$

where $\gamma_{\alpha\beta}$ – interphase tension;

r – drop radius

Under the condition of equilibrium, when $T_\eta = T_\gamma$, the radius of the drop, and therefore of the jet, is determined by the dependence:

$$r = [C\,\gamma_{\alpha\beta}]\,/\,[\,(dV_x/dy)\,\mu f\,(\mu/\eta)] \qquad (1.10)$$

It follows from equation (1.10) that the higher the viscosity of the matrix polymer, the greater the shear rate gradient, and the lower the viscosity of the dispersed phase and the surface tension, the thinner the jets will be.

It is known that a liquid jet (cylinder) is thermodynamically unstable due to an unfavorable surface-to-volume ratio and breaks up into a chain of droplets over time. Therefore, one of the important microrheological processes that forms the microfibrillar structure in polymer dispersions is the destruction of liquid jets formed during the flow of their melts. The cause of the disintegration of the cylinder is the occurrence of wave-like disturbances on its surface, the amplitude of which increases exponentially with time.

Experimental results regarding the effect of methylsilica on the disintegration of liquid polypropylene cylinders in the PVA matrix indicate a decrease in the value of the interfacial tension in the entire range of investigated additive concentrations (Table 1.19).

Table 1.19. Characteristics of the kinetics of the disintegration of PP microfibrils in the PVA matrix

Method of mixing	Content of MSi, wt. %	$\gamma_{\alpha\beta}$, mN/m	q	t_l, s	t_l/R s/µm	r/R
PP + PVA	0	0,73	0,0375	317	259	1,4
PP / MSi + PVA	0,1	0,57	0,0225	394	374	1,4
PP / MSi + PVA	0,5	0,36	0,0189	446	415	1,4
PP / MSi + PVA	1,0	0,47	0,0198	390	378	1,4
PVA / MSi + PP	1,0	0,50	0,0205	363	301	1,5
PP + PVA + MSi	1,0	0,17	0,0156	468	452	1,5

The compatibilizing effect of silica additives in mixtures of linear polymers formed *in situ* was shown in earlier studies [140]. The authors associate the change in the length of the interfacial layer with the adsorption of macromolecules of the mixture components on the nanoparticles of the filler and with the formation of a new phase. Table 1.19 shows that the values of surface tension also depend on the method of introducing nanoparticles into the melt mixture. The maximum decrease in $\gamma_{\alpha\beta}$ occurs when the components of the mixture are mixed simultaneously. This is due to the homogeneity of the dispersion and distribution of nanoparticles in the volume of the composition and the increase in the fraction of MSi encapsulated at the boundary of phase separation. Strengthening the interaction in the transition layer due to the affinity between methyl groups on the surface of silica nanoparticles and polypropylene macromolecules can significantly increase its density and length and reduce the surface tension.

The mechanism of disintegration of liquid polypropylene microfibrils in the PVA matrix is the same for the original and nanofilled mixtures. This follows from the fact that the values of the ratio of the radii of the droplets formed and the output cylinder (r/R) are practically constant values and are (1.4÷1.5). Additions of methylsilica increase the stability of the liquid jet, which is evidenced by an increase in the lifetime (t_l), reduced lifetime (t_l/R) and a decrease in the instability coefficient (q). At the same time, the stability of polypropylene microfibrils depends on the concentration of the nanoadditive: the given time is maximum when the silica content is

0.5 wt. %. As follows from equation (1.7), the decay time (lifetime) of a liquid jet is directly proportional to the viscosity of the melt (η), its radius (R) and inversely proportional to the value of the interfacial tension [134]. Thus, other things being equal, a decrease in surface tension contributes to a decrease in the radius of polypropylene microfibrils in a polyvinyl alcohol matrix and an increase in its stability.

Microscopic studies of the remains of the dispersed phase after the extraction of the matrix polymer from the extrudates of the original and modified mixtures indicate the formation of different types of polypropylene structures: microfibrils, particles, films (Table 1.20).

Table 1.20. Microstructure characteristics of extrudates of PP/PVA/silica mixtures*

Method of mixing	Silica content, wt. %.	Continuous microfibrils			Other types of structures, wt. %		
		d, µm	σ^2, μm^2	wt. %	short fibrils, wt. %	particles, wt. %	films, wt%
PP + PVA	0	3,5	1,5	66,0	20,5	3,8	9,7
PP /MSi + PVA	0,1	1,5	1,0	66,5	27,7	0,3	5,5
PP /MSi+ PVA	0,5	1,3	0,9	70,0	27,9	1,0	1,1
PP /MSi + PVA	1,0	1,7	1,3	46,5	45,5	0,7	2,7
PVA /MSi + PP	1,0	2,3	1,6	66,8	30,2	0,1	2,9
PP + PVA + MSi	1,0	1,3	1,1	73,5	24,0	0,8	3,1

* at a shear stress of $5.69 \cdot 10^4$ Pa

Changing the concentration of the nanoadditive and the method of its introduction into the melt of the mixture allows you to adjust the microstructure of PP/PVA extrudates. An important

factor of the effect of methylsilica is a (2.0÷2.7) times decrease in the average diameter of microfibrils, an increase in the homogeneity of the distribution, judging by the value of (σ^2), and an increase in their total number. As expected, the method of introduction of MK also affects the processes of structure formation during the flow of melts of PP/PVA mixtures. At the same time, under the condition of simultaneous mixing of the components, the average diameter and dispersion of the distribution of microfibrils are minimal, and the mass fraction of polypropylene spent on their formation is maximal. This is due to the achievement of the most uniform distribution of nanoparticles in the volume of melts of the dispersed phase component and matrix polymer, as well as a decrease in the share of silica shielded by the PP melt in the jets. At the same time, the probability of finding the additive at the boundary between the PP and PVA phases is much higher than with other methods of introducing methylsilica. Improvement of the microfibrillar structure formation process is primarily associated with a decrease in the interfacial tension in nanofilled compositions.

From the point of view of thermodynamics, surface tension is the work required to form a unit area of a new surface by stretching an old one. Thus, the reduction of $\gamma_{\alpha\beta}$ at the polypropylene/polyvinyl alcohol phase separation boundary makes it possible to reduce energy costs for the formation of new surfaces of the dispersed phase, i.e. to facilitate the dispersion of PP in the PVA matrix. At the same time, there is a possibility of a large number of different types of physical connections between filler particles and

macromolecule chains due to the formation of a transition layer at the nanoparticle/polymer interface. Ten such bonds are equal in strength to one primary chemical bond. From the point of view of statistics, the probability of breaking all ten bonds at the same time is very small, therefore relatively weak physical forces ensure strong adhesion between macromolecules of the polymer and the filler [4,88]. The increase in the degree of interaction at the PP/PVA interface contributes to the transfer of stresses from the matrix polymer to the droplets of the dispersed phase, increases the amount of their longitudinal deformation and ensures the formation of polypropylene microfibrils of smaller diameters. At the same time, the increase in the number of short fibrils in the extrudates of nanofilled mixtures may be the result of the disintegration of thin jets of PP as thermodynamically more unstable (Table 1.20).

Data on the influence of the concentration and method of introducing methylsilica on the macrorheological properties of PP/PVA melts are shown in Fig. 1.15 and in table. 1.21. The effective viscosity of the melts of the modified mixtures (as well as the original) decreases by (2.1÷2.5) times compared to η of PP and PVA melts. The method of introduction of the nanoadditive does not change the general pattern of a sharp drop in the viscosity of three-component systems. At the same time, the values of the effective viscosity of nanofilled compositions are usually lower than the similar values for the binary mixture. This is due to the change in microrheological processes in the melts of nanofilled systems under the influence of methylsilica nanoparticles.

Table 1.21. Influence of the concentration and method of introducing methylsilica additives on the rheological properties of melts of original PP and PVA and their mixtures*

Name of polymers, method of mixing	MSi content, wt. %	η, Pa·s	n	B	F_{max}, %
PP	-	290	2,0	1,8	38800
PVA	-	350	1,4	1,6	23500
PP + PVA	0	140	2,1	2,0	7200
PP /MSi + PVA	0,1	130	1,8	2,0	8200
PP /MSi + PVA	0,5	130	1,9	2,1	8300
PP /MSi + PVA	1,0	120	2,0	2,1	8300
PVA /MSi+ PP	1,0	170	1,8	2,1	8100
PP + PVA + MSi	1,0	130	1,7	2,0	8300

* at shear stress $5,69 \cdot 10^4$ Pa

A significant drop in viscosity is characteristic of the melts of the mixtures, during the flow of which the polymer of the dispersed phase is deformed in the jet in the matrix component. This is due to the fact that a smaller pressure drop (which corresponds to a lower viscosity) is required to ensure the flow of the melt mixture with deformable drops than for the flow of individual polymers [135]. The melts of the studied nano-filled compositions are abnormally narrow liquids, just like the original mixture (Table 1.21, Fig. 1.18). The degree of

deviation from the Newtonian nature of the flow in two- and three-component compositions is higher than in polypropylene and polyvigil alcohol.
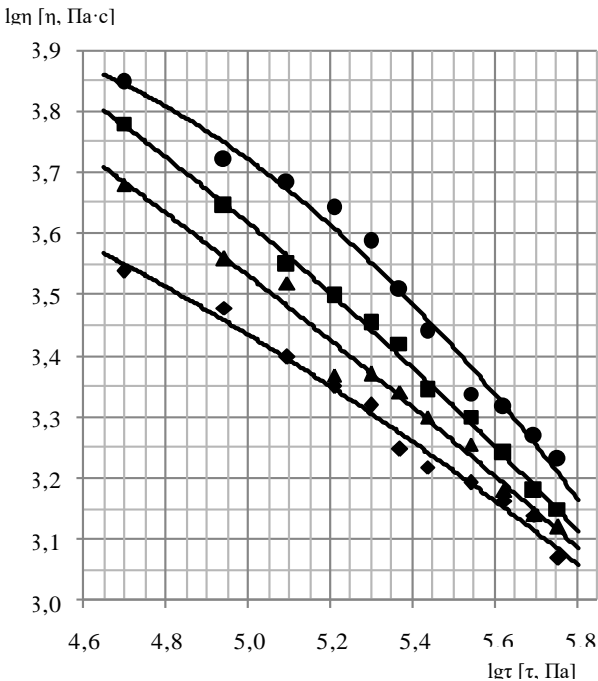

Fig. 1.18. Dependence of melt viscosity on shear stress of PP/PVA mixture (♦) and PP/PVA/silica mixtures obtained by different methods: method 1 (■); method 2 (●); method 3 (▲)

The elasticity of PP/PVA and PP/PVA/silica melts, estimated by the value of equilibrium swelling of extrudates (B), is significantly lower compared to this indicator for many mixtures with a microfibrillar structure (Table 1.21). Liquid jets of dispersed phase polymer accumulate significant deformations and make the main contribution to the overall elasticity of their melts. The equilibrium B values of extrudates

for them are several times higher than for individual polymers [72]. Low values of equilibrium swelling for the studied compositions, despite the formation of PP microfibrils in the PVA matrix, may be the result of the formation of a dense network of physical (hydrogen) bonds between the functional groups of the components of the mixture.

An important characteristic of melts is the ability to longitudinal deformation (F_{Max}) during processing into fibers and films. The melt conductivity of the PP/PVA mixture drops sharply compared to the original components, judging by the value of the maximum spinneret extraction (Table 1.21). This is due to a significant decrease in the viscosity of the melt mixture, an increase in its structural heterogeneity, as well as the formation of a dense network of intermolecular bonds. The introduction of a nano-additive facilitates the deformation of melt jets in the tensile field. The increase in the value of F_{Max} of the melts of nanofilled mixtures is the result of a change in the processes of structure formation of polypropylene in the matrix of polyvinyl alcohol under the action of methylsilica nanoparticles. It is known that the formation of anisotropic structures increases the ability of the melt to undergo longitudinal deformation [88]. The content of methyl silica and the method of mixing the components have almost no effect on the ability of the compositions to be recycled. Nano-filled PP/PVA mixtures are stably processed into fibers and films on traditional extrusion equipment. Methylsilica additives and repeated extrusions do not impair the solubility of polyvinyl alcohol in cold and hot water. This makes it possible to use plasticized PVA as a matrix polymer in the formation of

threads and films with a microfibrillar structure and to carry out the process of extraction with water.

The conducted studies showed the possibility of regulating the melt properties of polypropylene/plasticized polyvinyl alcohol mixtures by changing the concentration of methylsilica and the method of its introduction into the melt. It was established that the nanoadditive increases the thermodynamic stability of polypropylene liquid jets of a smaller diameter by reducing the surface tension at the phase separation boundary, the instability coefficient, and increasing the lifetime of the jets. Thanks to this, the average diameter of microfibrils decreases by $(2.0 \div 2.7)$ times, the number of films decreases by almost an order of magnitude, and the homogeneity of the distribution of microfibrils by diameters increases. The method of simultaneous mixing of all three components in the melt on the existing extrusion equipment proved to be the most effective. Additives of methylsilica have a positive effect on the rheological properties and the ability to deform melts of modified PP/PVA compositions, which allows them to be processed into products using traditional technological equipment. Polyvinyl alcohol does not lose its solubility in water during repeated extrusions and can be used in the production of microfibrillar thin fibrous materials.

1.2.4.3. Morphology and rheological properties of the polypropylene/polyvinyl alcohol/combined nanoadditive melt. The addition of nano-additives of different chemical nature and geometric shape to melts of polymer mixtures provides composites based on them with improved properties. At the same time, the mechanical characteristics are increased due to

self-reinforcement, their conductivity and barrier indicators are increased. Products acquire bactericidal properties, the ability to shield from electromagnetic waves, dispersion of electrostatic charge, their flammability decreases, etc. The morphology and properties of nanofilled composites depend on the concentration of the additive and the chemical nature of the functional groups on the surface of its particles. To a large extent, they are also determined by the thermodynamic compatibility of the components and the predominant localization of nanoparticles in the volume of one of the aba polymers at the phase separation boundary. Polymers, as a rule, are incompatible with each other, so they are characterized by a structure consisting of separate phases. Their properties are determined by the degree of dispersion of the particles of the dispersed phase component and the nature of the nanoadditive distribution. The optimal placement of nanoparticles determines new important qualities of the polymer composition without losing its main characteristics.

The migration and localization of nanoparticles in polymer mixtures has been experimentally confirmed and depends on thermodynamic and kinetic factors. The distribution of the filler in incompatible mixtures occurs in such a way as to minimize the total free energy of the system. In other words, the uneven distribution of nanoparticles in the composition ensures a decrease in free energy, which depends on the surface tension or free surface energy of the components. Thermodynamically equilibrium localization of solid particles in a multiphase mixture of polymers can be predicted using the equation [105]:

$$\omega = \gamma_{1s} - \gamma_{2s} \, / \, \gamma_{12} \qquad (1.11)$$

where: γ_{1s}, γ_{2s} − interfacial tension between polymers 1 and 2 and the solid substance; γ_{12} − the interfacial tension between polymers 1 and 2

From the point of view of thermodynamics, it is advantageous to place solid nanoparticles in phase 2, when $\omega >$ 1, and in phase 1, if $\omega < -1$; provided that $-1 < \omega < 1$, solid particles are localized at the boundary of the phase separation. The distribution of nanoparticles in polymer mixtures obtained by traditional methods often differs from that achieved at thermodynamic equilibrium. However, it is also possible to redistribute NPs due to a change in the method of mixing components and Brownian motion. This significantly distinguishes nanocomposites from composite materials that contain fillers with a particle size greater than 1.0 μm. The final distribution of nano-additives depends on the mixing conditions (sequence of introduction of ingredients, used equipment, temperature and time) and rheological properties of polymers. On the other hand, as is known, the localization of fillers in mixtures is determined by the degree of interaction between NPs and components. At the same time, selective localization of modifying additives determines the final morphology and properties of filled polymer composites.

The influence of the method of introducing silver/silica nanoadditive (Ag/SiO_2) on the microstructure of the extrudates and the rheological properties of the polypropylene/plasticized polyvinyl alcohol melt was studied in [56]. For the preparation of mixtures, PVA plasticizer with glycerin was used, which was introduced in the amount of 10.0 wt. %. The ratio of

components in the PP/PVA mixture was 30/70 by weight. %. As a nano additive, the bifunctional substance silver/silica was chosen, which was added in the amount of 5.0 wt. % by weight of polypropylene. Nanofilled mixtures were prepared in three ways: preliminary dispersion of nanoadditives in molten polypropylene (1) or polyvinyl alcohol (2) with subsequent mixing of granules with a polymer of the dispersed phase or matrix; in the third - all components were mixed simultaneously. The quality of dispersion of the additive in the starting polymers was evaluated by the value of the standard deviation reduced to the total concentration of the structures in the samples (Lastovtsev coefficient of heterogeneity).

The results of rheological studies indicate that the introduction of a nano-additive leads to an increase in the effective viscosity of the melts of the original components of the mixture (PP and PVA) by 1.1 and 1.7 times, respectively (Table 1.22).

Table 1.22. Effect of silver/silica nanoadditive on the rheological properties of the starting polymers

Назва зразка	η, Па·с	n	B	F_{max}, %
ПП	290	2,1	1,5	20840
ПП+Ag/SiO$_2$	330	2,2	1,3	13280
ПВС	270	1,5	1,7	16340
ПВС+Ag/SiO$_2$	450	1,7	1,4	9580

This can be the result of filling the polymer melt with a solid substance, and for PVA also its structuring due to the formation of hydrogen bonds between the silane and silanol groups of silicon dioxide and the polymer macromolecules.

The nature of the flow of modified melts does not change, they remain typical non-Newtonian fluids. At the same time, the degree of deviation from the Newtonian flow regime increases slightly, which is evidenced by the increase in the value of the indicator *n*. In the presence of an additive, the elasticity of nanofilled melts decreases due to the restriction of the mobility of macromolecule chains. The ability to longitudinal deformation also deteriorates, judging by the values of F_{max}, which is due to an increase in the heterogeneity of the system.

The effective melt viscosity of the PP/PVA binary mixture drops sharply, compared to η of the starting polymers (Table 1.22, 1.23).

Table 1.23. Influence of the Ag/SiO2 nanoadditive introduction method on the rheological properties of the PP/PVA mixture melt

The name of the sample	η, Pa·s	n	B	F_{max}, %
PP/PVA	110	2,1	2,4	8680
(PP + Ag/SiO$_2$) + PVA	140	1,8	3,2	8100
(PVA + Ag/SiO$_2$)+ PP	440	2,0	2,1	7130
PP + PVA + Ag/SiO$_2$	410	1,9	2,5	7580

This is due to the thermodynamic incompatibility between PP and PVA macromolecules at the boundary of phase separation and the formation of anisotropic structures of the dispersed phase in the matrix.

As can be seen from the Table. 1.23, the sequence of mixing components with a nano-additive significantly changes the macrorheological characteristics of the melts of the filled compositions. If a nano additive is added to the component of

the dispersed phase, the viscosity of the modified composition decreases, as well as that of the original mixture. The simultaneous mixing of the ingredients or the introduction of Ag/SiO_2 nanoparticles into the melt of the matrix polymer (PVA) leads to an increase in the viscosity of nanofilled systems (Table 1.23). The obtained results can be explained by the competing influence of a number of factors on the viscosity of melts of nanofilled systems. The main ones are the following: changes in the processes of structure formation of the component of the dispersed phase in the presence of solid nanoparticles and the interaction between the functional groups of the additive and chains of polymer macromolecules. The predominant influence of one of the processes is related to the possibility of localization of NP additive in the volume of the dispersed phase, dispersion medium or at the boundary of phase separation.

Microscopic studies have shown that silver/silica particles are dispersed differently in the melts of the original components, as evidenced by the values of the Lastovtsev heterogeneity coefficient, which is 27.8 and 11.2 for PP and PVA melts, respectively. A more uniform distribution of particles in the PVA melt is natural and due to its high polymerophilicity (wetting ability) to the surface of polar silica particles. If the ingredients are mixed in the first way, nanoparticles are preferably placed in the phase of non-polar polypropylene and at the boundary of the phase separation. This is due to the fact that when an additive is introduced into a component with poorer polymerophilicity, nanoparticles migrate to the interphase region. The concentration of NPs in it

helps to change the processes of PP structure formation in the PVA matrix and causes a drop in the melt viscosity of the mixture obtained by the first method. The increase in the viscosity of the compositions with the preliminary introduction of Ag/SiO$_2$ into the PVA melt and the simultaneous mixing of the components is due to the preferential localization of polar nanoparticles of the additive in the volume of the matrix polymer and the formation of a network of hydrogen bonds that structure the melt. The nature of the flow of nanofilled mixtures, like the original one, is subject to the power law and is almost independent of the sequence of mixing the components.

The elasticity of melts of three-component mixtures, estimated by the amount of swelling of extrudates, is also determined by the sequence of introduction of ingredients (Table 1.23). This indirectly indicates a change in the processes of PP structure formation in the PVA matrix in the presence of a nano additive. The ability to longitudinally deform the melts of all studied compositions decreases, compared to the initial one, due to the increase in the heterogeneity of the systems (Table 1.23). The directivity of compositions obtained by the first method is higher compared to others, due to the predominant localization of nanoparticles in the interfacial layer. At the same time, it is sufficient for the processing of nano-filled melts on the existing technological equipment into fibers and films.

In heterophase mixtures of polymers, the sizes of the dispersed phase formations range from submicron to tens of micrometers, and their shape can be spherical, ellipsoidal,

cylindrical, ribbon-like, etc. Analysis of micrographs of cross-sections of extrudates (Fig. 1.19) shows that changing the sequence of mixing the ingredients allows you to adjust the morphology of the PP/PVA composition. From Fig. 1.19 it can be seen that in the initial mixture polypropylene is coarsely dispersed in the PVA matrix, there is a significant amount of film structures, which is due to the thermodynamic incompatibility of the components. With the preliminary introduction of silver/silica nanodoping into the PP melt, a dispersed type of structure is formed with a uniform distribution of polypropylene particles in the matrix (Fig. 1.19 b).
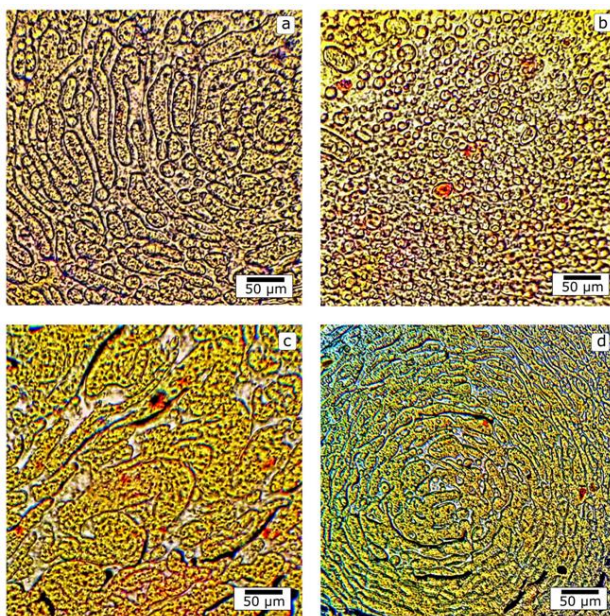
Fig. 1.19. Photomicrographs of cross-sections of extrudates: initial mixture (a) and nanofilled PP/PVA/Ag/SiO2 compositions obtained by different methods: method 1(b), method 2(c), method 3(d)

The increase in the degree of dispersion is due to the fact that the melt of non-polar PP does not wet the hydrophilic additive well, and Ag/SiO$_2$ particles with nanosizes are pushed to the boundary of the phase separation and reduce the value of the interfacial tension. The possibility of nanoparticle migration is shown on the example of a polyethylene /polylactide mixture [104]. Electron microscopy confirmed that 35% of hydrophilic silica nanoparticles moved from the polyethylene phase into the polylactide melt. At the same time, most of the filler particles (65%) remained in the volume of polyethylene in the form of aggregates.

The addition of a nanofiller to the polymer melt of the dispersion medium leads to a sharp change in the morphology of the system. Mutually continuous (entwined) structures are formed when it is impossible to determine which polymer is the dispersed phase and which is the matrix (Fig. 1.19 c). With the simultaneous mixing of all components, a layered morphology is realized in the form of concentrically arranged rings (Fig. 1.19d). The formation of these types of structures is facilitated by the formation of a dense network of hydrogen bonds between hydroxyl groups of silica and chains of polyvinyl alcohol macromolecules.

Quantitative characteristics of the microstructure of extrudates of mixtures with a dispersed type of morphology were determined by the method of morphometric image analysis. Histograms of the distribution of polypropylene particles by equivalent diameter and shape index show that in the initial mixture PP forms large shapeless agglomerates in the PVA matrix. The equivalent diameter (d_e) of almost half of the

particles is (16÷32) μm, the share of particles close to round is 41% (Fig. 1.20).
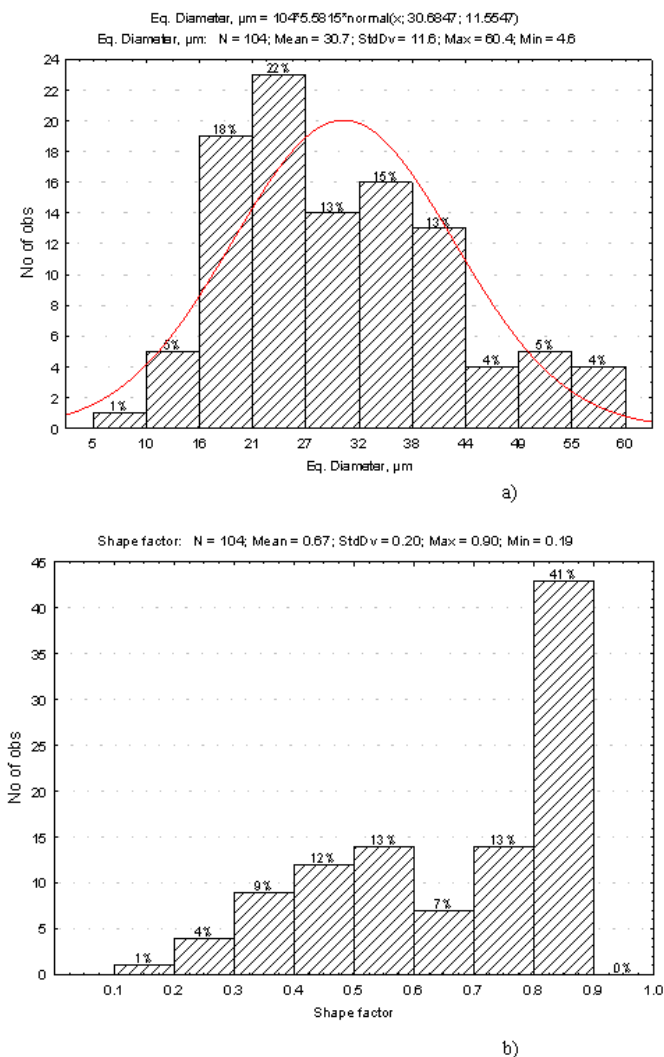

a)

b)

Fig. 1.20 – Histograms of the distribution of dimensional characteristics of PP particles in the PVA matrix in the original mixture: equivalent diameter (a), shape index (b)

Under the condition of prior introduction of Ag/ SiO_2 into the polypropylene melt, d_e of particles decreases by approximately 3.5 times, and the homogeneity of their distribution increases. Their equivalent diameter is within (4÷11) μm for 86%, and the shape becomes almost round - for 64% of the particles, the shape index (f) is 0.9÷1.0 (Fig. 1.21).
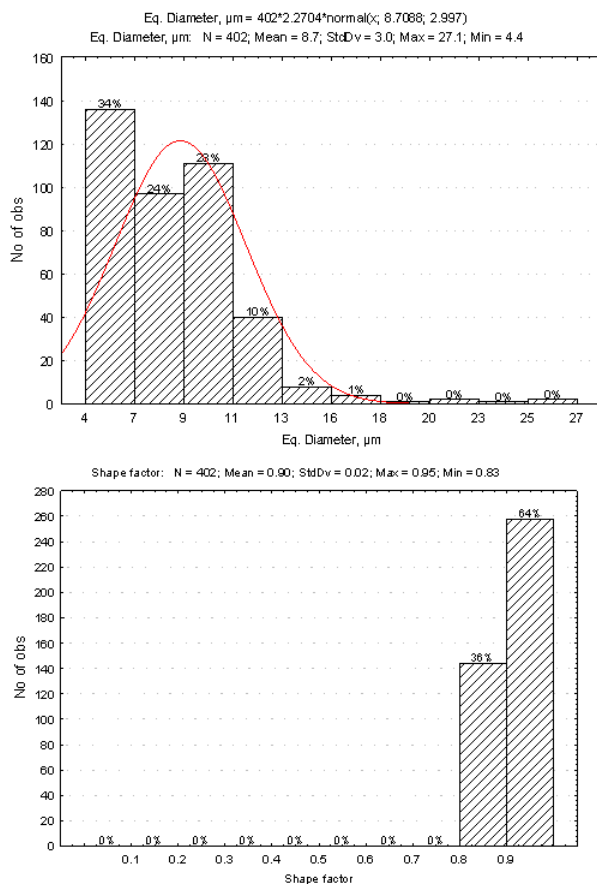

Eq. Diameter, μm = 402*2.2704*normal(x; 8.7088; 2.997)
Eq. Diameter, μm: N = 402; Mean = 8.7; StdDv = 3.0; Max = 27.1; Min = 4.4

Shape factor: N = 402; Mean = 0.90; StdDv = 0.02; Max = 0.95; Min = 0.83

Fig. 1.21. Histograms of the distribution of dimensional characteristics of PP particles in the PVA matrix for the PP/PVA/Ag/SiO2 mixture obtained by the first method: equivalent diameter (a), shape index (b)

A sharp increase in the degree of dispersion of particles of the dispersed phase and their approximation to the correct (round) shape in the presence of a hydrophilic additive is the result of a number of factors. Firstly, it is an improvement of the compatibility between polypropylene and plasticized PVA at the boundary of phase separation, and secondly, a decrease in the amount of surface tension and costs for the formation of a new surface. A similar effect also occurred in the presence of silica nanoadditives, carbon black, metal oxides, and nanoclays [10,20-25,40-43,47,52-55].

When introducing 3.0 wt. % of hydrophilic or hydrophobic silica in the polypropylene/polystyrene (PP/PS) mixture, the average particle size of the dispersed phase (PS) decreased from 3.7 to 0.85 μm (for hydrophilic SiO_2 particles) and to 1.25 μm (for the hydrophobic additive) [47]. This effect can be due to the predominant localization of nanoparticles in one of the phases or at the boundary of their separation. Hydrophilic silicon dioxide nanoparticles introduced into the polypropylene melt migrate from the polypropylene volume to the polystyrene phase. At the same time, hydrophobic silica particles move into the interfacial region and act as a rigid layer that prevents coalescence of dispersed phase droplets and stabilizes the PP/PS mixture. Our earlier studies on the effect of fumed silica on the structure formation processes in PP/PVA and PP/co-polyamide mixtures showed that their use allows to regulate the microstructure of composite threads and films and to obtain nano-filled microfibrillar materials with a smaller average diameter of individual filaments and an increased specific surface area [41, 42,67,68,72].

1.2.4.4. Structure formation in compatibilized nanofilled polypropylene/plasticized polyvinyl alcohol melts. The influence of compatibilizer/nanodisperse additive binary compositions on flow patterns and structure formation processes in melts of polypropylene/polyvinyl alcohol plasticized with glycerol was investigated in [74]. Four-component mixtures were obtained by preliminary introduction of a compatibilizer (sodium oleate) and a nanofiller (silver/silica) into the polypropylene melt and subsequent mixing of the modified granules with polyvinyl alcohol. As already mentioned, polymer mixtures are special dispersed systems characterized by the formation of a transition layer at the polymer–polymer interface. Its properties differ sharply from similar indicators of melts of components in the volume. During their flow, tensions arise in the dispersion medium, which contribute to the deformation and orientation of the droplets of the dispersed phase. At the same time, they can acquire the shape of an ellipsoid of rotation (at small velocity gradients) or turn into a liquid cylinder at higher shear stress values.

Studies of the microstructure of extrudates of four-component mixtures have shown that the simultaneous use of Ag/SiO2 and sodium oleate contributes to the further growth of the degree of dispersion and homogeneity of the distribution of PP particles in the PVA matrix (Fig. 1.22, 1.23). From the histogram shown in fig. 1.20 shows that the equivalent diameter of 88% of polypropylene particles lies within (1÷4) μm, there are no large particles (with de > 6.0 μm), and their distribution curve is almost symmetrical.
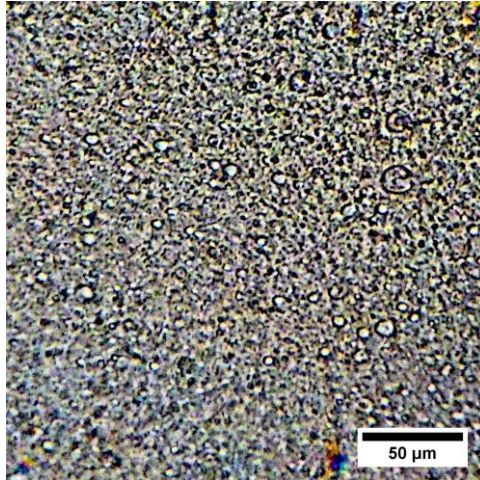
Fig. 1.22 – Photomicrograph of the cross-section of the extrudate of the four-component composition PP/PVA/Ag/SiO2/sodium oleate
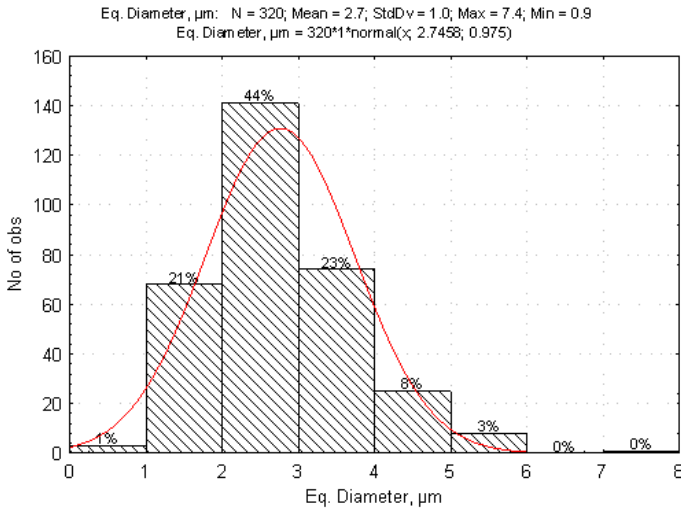

Fig. 1.23 – Histograms of the distribution of PP particles by equivalent diameters in the PVA matrix for the mixture of PP/PVA/Ag/SiO2/sodium oleate

The maximum effect of the combined action of the nanoadditive and the compatibilizer on the processes of structure formation is mainly due to a decrease in the surface tension at the polymer-polymer and nanoparticle-polymer interfaces. This is also facilitated by increasing the affinity between the components due to the formation of specific bonds between the functional groups of PVA macromolecules, silver/silica nanoparticles, and sodium oleate molecules.

Classical studies of the deformation of a drop located in a flowing medium testify to its dependence on the ratio of the viscosities of the dispersed phase and the matrix and the value of the interfacial tension. Thus, the degree of interaction of the components in the transition layer and its length will significantly affect the formation of the final morphology of the mixture extrudates. It, in turn, is the result of a balance between the processes of deformation, destruction, coalescence and redistribution of the dispersed phase polymer.

Experimental studies of the kinetics of disintegration of liquid PP cylinders in the PVA matrix showed that the stages of destabilization (formation of thickenings and thinnings) of jets and their destruction into drops for the original and modified mixtures do not differ qualitatively from those for low-molecular systems. From the parameters of the decay process given in Table. 1.24, it can be seen that the values of the ratio of the radii of the droplets formed and the initial cylinder (r/R) are 1.2–1.4 for mixtures containing a nanodisperse additive, a compatibilizer, and their binary composition.

Table 1.24. The characteristics for disintegration's kinetics of polypropylene microfibrils, and in the poly(vinyl alcogol)'s matrix

The names for blends and those component contents, mass. % of	$r/R,$	q	t_L, s	t_L/R s/µm	$\gamma_{\alpha\beta},$ mN/m
PP/PVA, 30/70	1,4	0,0375	317	259	0,73
PP/PVA/Ag/SiO$_2$, 30/70/1	1,2	0,0211	390	330	0,38
PP/PVA/natrium oleate, 30/70/3	1,2	0,0265	390	312	0,51
PP/PVA/Ag/SiO$_2$/natrium oleate, 30/70/1/3	1,3	0,0175	440	353	0,24

This indicates that the mechanism of destruction of polypropylene microfibrils in the PVA matrix is the same for binary, three- and four-component systems. At the same time, the value of the interfacial tension is determined by the chemical nature of the modifying additives. For the initial mixture, γαβ is 0.73 mN/m, and for compositions containing 1.0 wt. % of silver/silica nanowires and 3.0 wt. % natrium oleate decreases to 0.38 and 0.51 mN/m, respectively. The binary nanodisperse filler/compatibilizer system exhibits a synergistic effect - for it, the value of the surface tension is minimal. The established regularity is associated with an increase in affinity at the phase separation boundary caused by the formation of specific bonds between the functional groups of polyvinyl alcohol macromolecules, sodium oleate molecules, and the surface of silica nanoparticles.

For the formation of microfibrils from melts of polymer mixtures, it is necessary to ensure the conditions for the deformation of the droplets of the dispersed phase in the jet and the preservation of their stability in the channel of the forming hole and at the exit from it. The reason for the destruction of the liquid cylinder is the occurrence of wave-like disturbances on its surface, the amplitude of which increases exponentially with time. The lifetime of the jet is directly proportional to its radius and the viscosity of the melt and inversely proportional to the value of the interfacial tension, i.e., the stability of cylinders increases over time with a decrease in surface tension [134]. This is confirmed by the data of table. 1.24, from which it can be seen that the introduction of all investigated additives into the PP/PVA mixture contributes to an increase in the life time and reduced life time of polypropylene microfibrils in the matrix. The coefficient of instability of a liquid cylinder located in another liquid is directly proportional to the surface tension at the boundary of the phase separation. A decrease in the value of q in modified mixtures indicates an increase in the resistance of cylinders to destruction (Table 1.24).

From the point of view of thermodynamics, the specific work of dispersion is determined by the interfacial tension. A decrease in $\gamma_{\alpha\beta}$ at the boundary of the polymer–polymer phase separation makes it possible to reduce energy costs for the formation of new surfaces of the dispersed phase, to facilitate the dispersion and deformation of droplets. Detailed quantitative microscopic studies of the influence of the nanodisperse additive silver/silica and the compatibilizer sodium oleate on the microstructure of the extrudates showed

that the original additives and their binary composition have a compatibilizing effect on the melt of the PP/PVA mixture. This makes it possible to regulate the morphology of modified compositions in the direction of decreasing the average diameter of microfibrils and increasing their mass fraction. At the same time, the number of undesirable types of structures (particles and films) decreases (Table 1.25).

Table 1.25. The influence of silver/silica , natrium oleate, and those compositions on   characteristics for structure-forming processes in blend melts of PP/PVA

The names of blends and those component contents, wt. %	The characteristics for microfibers		Other structrures contents, wt. %	
	đ, µm	contents, wt. %	parts	films
PP/PVA, 30/70	3,5	86,5	3,9	9,6
PP/PVA/Ag/SiO$_2$, 30/70/1	1,6	90,6	3,3	6,4
PP/PVA/natrium oleate, 30/70/3	1,4	92,7	3,6	3,7
PP/PVA/Ag/SiO$_2$ /natrium oleate, 30/70/1/3	1,1	97,9	1,2	0,9

The simultaneous use of Ag/SiO$_2$ nanoparticles and sodium oleate is the most effective and leads to a further decrease in microfibril diameters from 3.5 µm (for the original mixture) to 1.1 µm (for the four-component mixture). At the same time, migration processes slow down, which leads to a sharp drop in the content of films (Table 1.25). We previously

showed [40] that the improvement of the matrix-fibrillar structure of the PP/SPA mixture with the introduction of TiO_2/SiO_2 mixed oxide nanoparticles is also due to their influence on the interphase phenomena and rheological properties of the melts of the components. described by other authors [64,144]. When polypropylene/polyamide (PP/PA) was added to the mixture as a polypropylene compatibilizer with grafted maleic anhydride (PPgMA), the size of PA droplets decreased by 12 times, and with the additional introduction of hydrophobic silica nanoparticles – by 25 times. The results of electron microscopy showed that silica nanoparticles are mainly localized at the PP/PA interface and reduce the interfacial tension [144]. In polypropylene/polyethylene terephthalate mixtures, the maximum length and minimum diameter of polyester fibrils in the polypropylene matrix are achieved with the simultaneous use of a nanodispersed additive of titanium dioxide and the compatibilizer PPgMA [64].

The dependence of the macrorheological characteristics of PP/PVA melts on the composition of the mixtures is presented in Table 1.26. It can be seen from the given table that the effective viscosity of the melts of the modified compositions (as well as the original) decreases by 2.9–3.5 times, compared to η of PP and PVA melts. A significant drop in viscosity is characteristic of melts of mixtures in which the polymer of the dispersed phase forms anisotropic structures in the matrix component, since a smaller pressure drop is required to ensure the flow of the melt with deformable drops than for individual polymers [135].

Table 1.26. The rheological properties of melts of propylene, poly(vinyl alcohol), and blends of them

The names of blends and those component contents, mass. % of	η, Pa·s	n	B	Φ_{max}, %
PP	290	2,0	1,8	38800
PVA	350	1,4	1,6	25300
PP/PVA, 30/70	130	2,1	2.3	7200
PP/PVA/Ag/SiO$_2$, 30/70/1	150	2,0	2.5	8500
PP/PVA/ natrium oleate, 30/70/3	100	1,7	2.7	7000
PP/PVA/Ag/SiO$_2$/ natrium oleate, 30/70/1/3	130	1,8	3.3	8200

Solid Ag/SiO$_2$ nanoparticles structure the melt and slightly increase its η, while sodium oleate has a plasticizing effect and minimizes viscosity. The nature of the flow of three- and four-component melts is subject to a power law. The smallest degree of deviation from the Newtonian flow regime is characteristic of the mixture with the addition of a compatibilizer.

A feature of polymer melts and their mixtures is the accumulation of highly elastic deformations during flow through the channel due to polymer macromolecules and deformed particles of the dispersed phase. At the same time, their relaxation leads to an increase in the cross-section of the extrudate (swelling) compared to the size of the die. The maximum degree of anisotropy is achieved when the dispersed phase forms liquid jets of continuous length, and they make the

112

main contribution to the overall elasticity of melts. For mixtures of many polymers, it is shown that the values of equilibrium swelling (B) indirectly characterize the process of formation of microfibrils of one polymer in the matrix of another. The elasticity is maximum when the only type of structure in the extrudate is microfibrils with minimum diameters [20,21,25,40-42,67-72]. This conclusion is also confirmed for the studied systems: higher values of swelling correspond to a more perfect matrix-fibrillar structure (tables 1.25, 1.26). At the same time, the swelling values of extrudates with a polyvinyl alcohol matrix are significantly lower than for mixtures of PP with co-polyamide. This is due to the formation of a network of hydrogen bonds between the functional groups of PVA macromolecules, sodium oleate and the surface of silica particles.

Fiber formation can be considered as a process of uniaxial stretching. An important technological characteristic of the melts of the mixtures, which determines the fiber-forming properties, is the indicator of the maximum degree of extraction. The higher the F_{max} value, the better the recyclability of the material. The obtained results indicate that the directivity of the melts of the studied mixtures decreases compared to the original components (Table 1.26), which is due to a sharp decrease in the viscosity of their melts and an increase in the heterogeneity of the morphology.

Thus, it is shown that the silver/silica nanodisperse additive, the sodium oleate compatibilizer, and their binary composition significantly affect the morphology and melt flow patterns of the thermodynamically incompatible

polypropylene/polyvinyl alcohol mixture. The introduction of these additives makes it possible to control the process of *in situ* formation of PP microfibrils in the PVA matrix in the direction of increasing their mass fraction and decreasing the average diameter. The maximum improvement of the matrix-fibrillar structure is achieved with the simultaneous use of both modifiers, which is due to the strengthening of the compatibilizing effect on the interfacial layer due to the nanodisperse additive. The value of the surface tension decreases from 0.73 mN/m for the initial mixture to a minimum value of 0.24 mN/m for the four-component composition. The rheological properties and uniaxial tensile strength of the studied compositions are determined by their phase heterogeneity. The formation of anisotropic polypropylene structures in the matrix component causes a sharp drop in the effective viscosity of the melts of the modified mixtures.

1.2.5. The influence of the chemical structure of the matrix polymer on the patterns of flow and the processes of structure formation in melts of nanofilled polymer mixtures. The formation of different types of morphology of one polymer in the matrix of another is determined by the chemical nature, rheological properties and ratio of the components of the mixture, as well as the presence of modifying additives (compatibilizers, nanofillers, plasticizers). The microstructure of extrudates of polymer mixtures is formed during their flow and is determined by such microrheological processes as deformation of drops and jets, disintegration of jets into drops,

coalescence of drops and jets, and migration of polymer droplets of the dispersed phase along the radius of the forming hole. The degree of manifestation of each of them depends on the compatibility or incompatibility of the polymers, their viscoelastic characteristics, content in the mixture, mixing conditions, etc.

    1.2.5.1. The influence of the chemical structure of the matrix polymer on the processes of structure formation in PP/PVA and PP/SPA mixtures. For the preparation of mixtures, PVA was used, which contained 7.0 wt. % glycerin. The results of the study of the effect of polypropylene concentration on the microstructure of extrudates of mixtures of polypropylene /polyvinyl alcohol and polypropylene/copolyamide are shown in Tables 1.27, 1.28.

Table 1.27 – Influence of the composition of the PP/PVA mixture on the characteristics of the microstructure of the extrudates

Ratio of components, wt. %	Continuous microfibrils		Short microfibrils		Particles		Films, wt. %
	d, μm	wt. %	d, μm	wt. %	d, μm	wt. %	wt. %
20/80	3.0	72.4	2.1	17.1	3.5	3.2	7.3
30/70	3.5	66.0	2.3	20.5	3.6	3.8	9.7
40/70	4.0	66.7	2.2	17.3	2.5	3.7	12.3
50/50	3.5	71.9	2.1	10.0	2.4	4.0	13.1

Analysis of Table 1.27 data indicates the peculiarity of the process of formation of PP microfibrils in the polyvinyl alcohol matrix. Unlike many other polymer mixtures, microfibrils are formed in the entire studied range of compositions, including

the area of phase change. It is known that in any emulsion, when the concentration of the component of the dispersed phase increases or under the influence of external factors, phase inversion occurs, that is, the dispersed phase and the dispersion medium change places. In low-molecular-weight systems, the phase change occurs in leaps and bounds, with a ratio of components close to unity. Mixtures of thermodynamically incompatible polymers are special colloidal systems in which the range of phase changes covers a wide range of compositions. For polypropylene/copolyamide mixtures, phase inversion occurs in the range of 40/60, 50/50, 60/40 mass ratios. % [72]. For the specified concentrations, both phases are continuous or have a layered morphology (Table 1.28).

Table 1.28. Influence of the composition of the PP/SPA mixture on the characteristics of the microstructure of the extrudates

Ratio of components, wt. %	Types of structures			
	microfibrils		particles, wt. %	films, wt. %
	d, µm	wt. %		
20/80	3,6	86,4	6,4	7,2
30/70	4,0	82,7	8,3	9,0
40/60	7,8	45,7	1,9	52,4
50/50	the microfibrillar structure is not realized			

It is known that there is a competing influence of the rheological properties of the components and the concentration of the dispersed phase polymer on the degree of its dispersion. For PP/PVA mixtures containing 20, 30, 40 and 50 wt. % of polypropylene, microfibrils with an average diameter of

(3.0÷4.0) μm are formed. This indicates that for these mixtures the coalescence processes are less pronounced than the deformations of drops and jets. Obtained experimental data on the *in situ* formation of PP microfibrils in a mixture containing 50 wt. % of the component of the dispersed phase, are consistent with the results of mathematical modeling of the processes of mixing and homogenization of melts of mixtures given in [145]. The degree of dispersion, estimated by the thickness of the "bands" (σ) of the dispersed phase, increases with an increase in its volume concentration (V):

$$\sigma = h/\gamma_c V \qquad\qquad (1.12)$$

where: h – the initial size of the elementary cube,

γ_c – shear strain

However, in practice, such a correlation is the exception rather than the rule for many melts of polymer mixtures. In PP/SPA mixtures with increasing polypropylene concentration, the average diameter of microfibrils increases, and when the PP content is ≥ 40 wt. %, it ceases to be a dispersed phase [72]. The realization of a microfibrillar structure in PP/PVA mixtures with a polymer ratio close to the phase change region may be due to the fact that glycerol acts not only as a PVA plasticizer, but also as a compatibilizer of this mixture. This helps to improve the affinity between the components at the border of their separation. Obviously, if the interfacial tension decreases, the coalescence processes slow down, the stability of the dispersion increases, and the increase in the volume concentration of the component of the dispersed phase increases the degree of its dispersion. Improvement of affinity and adhesion at the interface of phase separation contributes to

the formation of polypropylene microfibrils in the polyvinyl alcohol matrix. The possibility of forming microfibrillar morphology in PP/PVA mixtures with a high concentration of polypropylene is of important scientific and practical importance. Increasing the polymer content of the dispersed phase to 50.0 wt. % provides an increase in the productivity of the production of microfibrillar materials and the simplification of the processes of extraction and regeneration of the matrix polymer.

1.2.5.2. The influence of methylsilica additives on flow patterns and structure formation in PP/PVA and PP/SPA mixtures. The introduction of nano-additives into melts of polymer mixtures is one of the effective methods of obtaining materials with specified adjustable characteristics. The studies carried out at KNUTD show that additives of metal oxide nanoparticles, carbon nanotubes, original and modified silica have a double effect in melts of PP/PVA [22,56,69,74] and PP/SPA [20,21,25,40-42,67,68,142]. Nanofillers provide microfibrillar materials with a set of desired indicators due to entering into their structure; on the other hand, they are an effective factor in regulating the process of PP microfibril formation in the polymer matrix. Nanoparticles of silicon dioxide provide filter materials from nano-filled PP microfibrils with a combination of high productivity and cleaning efficiency. The improvement of selectivity is due to the improvement of the structure of the filter layer due to the reduction of the average diameter of polypropylene microfibrils and the increase of their homogeneity of distribution in terms of dimensional characteristics.

118

Modification of silica by applying silver nanoparticles to its surface gives microfibrillar materials antimicrobial activity against many microorganisms and increases the retention capacity of filters [41,42].

Analysis of the remains of the dispersed phase after the extraction of the matrix polymer from the extrudates of PP/PVA and PP/SPA mixtures with a composition of 30/70 wt. % indicates that polypropylene forms microfibrils in the PVA and SPA matrix. Introduction of 1.0 wt. % of methylsilica nanoparticles (MSi) does not change the nature of structure formation in the melts of the mixtures regardless of the chemical nature of the matrix polymer. Microfibrillar morphology is formed in both compositions. Microscopic studies of microfibril bundles showed that the addition of methylsilica NPs significantly affects the dimensional characteristics of PP fibrils and the ratio between different types of structures (Table 1.29). In the investigated modified compositions, the average diameter of microfibrils decreases by 1.5÷2.0 times, the homogeneity of their distribution increases, judging by the value of dispersion (σ^2), and the mass fraction of particles and films decreases. A decrease in the dimensional characteristics of the dispersed phase and the predominant formation of polypropylene microfibrils with minimum diameters in nanofilled mixtures may be associated with an increase in the degree of compatibility between the macromolecules of the components in the interfacial layer due to the compatibilizing action of methylsilica nanoparticles. The obtained results are consistent with the previously proposed mechanism regarding the stabilizing effect of nanoparticles on

liquid jets of the component of the dispersed phase in the matrix polymer. Its essence is that nanoadditives have a compatibilizing effect (reduce the value of surface tension at the boundary of phase separation) and inhibit the growth of the amplitude of the destructive disturbance wave. Thus, it contributes to an increase in the degree of dispersion and the formation of cylinders (microfibrils) of a smaller diameter [67-69].

Table 1.29. The influence of methylsilica additives on the characteristics of the microstructure of the extrudates of the mixtures

The name of the mixture	Types of structures					
	continuous fibrils			short fibrils, wt. %	particles wt. %	films, wt. %
	d, µm	σ^2, µm^2	wt. %			
PP/PVA	3,5	1,5	66,0	20,5	3,8	9,7
PP /PVA/MSi	1,7	1,3	46,5	45,5	0,7	2,7
PP /CPA	4,0	2,4	47,6	2,8	0,1	49,5
PP /CPA/MSi	2,6	1,9	69,3	2,0	2,1	13,5

The increase in the length of the interfacial layer is explained by the adsorption of the chains of macromolecules of both polymers on the nanoparticles, which are located along the boundary of the separation of the components, and the formation of a new phase. Improvement of thermodynamic compatibility occurs more often for those pairs of polymers in which the majority of the nanoadditive is localized at the boundary of the phase separation. The compatibilizing effect of nanoadditives is described for a number of polymer mixtures obtained by mixing in the melt [21,42,46-48,52-56,64-71]. For

example, the introduction of nanosized titanium oxide into the melt of the polyethylene terephthalate/polypropylene mixture [65] and the combined titanium oxide/silica nanoadditive into the polypropylene/copolyamide mixture [69] contributes to the deformation of the droplets of the dispersed phase component into liquid jets and ensures a decrease in the average diameter of the microfibrils by 3.8 and 2.2 times, respectively.

Data on the kinetics of disintegration of PP microfibrils in the PVA and SPA matrix experimentally confirm the reduction of surface tension in nanofilled mixtures (Table 1.30).

Table 1.30 – The influence of methylsilica additives on the parameters of the disintegration of polypropylene microfibrils

The name of the mixture	$\gamma_{\alpha\beta}$, mN/m	q	t_l, s	t_l/R
PP/PVA	0,73	0,0375	317	259
PP/ PVA /MSi	0,47	0,0198	390	378
PP/CPA	2,60	0,0398	84	38,9
PP/CPA/MSi	0,75	0,0250	75	62,4

The values of the interfacial tension, determined using the theory of liquid cylinder failure, are quite small, which is typical for melts of polymer mixtures and is associated with the presence of a transition layer at the boundary of phase separation. The decrease in interfacial tension in three-component systems is due to the fact that MSi nanoparticles participate in the formation of a transition layer due to the formation of a large number of different types of physical bonds between filler particles and macromolecule chains at the

nanoparticle/polymer interface. Strengthening the interaction between components due to the affinity of methyl groups on the surface of silica nanoparticles to PP macromolecules significantly increases the density and length of the interfacial layer and decreases the value of $\gamma_{\alpha\beta}$. An increase in the stability of the PP liquid cylinder in the PVS and SPA matrix is evidenced by an increase in the reduced life time (t_l/R), as well as a decrease in the instability coefficient (q). The formation of microfibrils of one polymer in the matrix of another is realized with the appropriate degree of interaction of components at the boundary of phase separation due to the transfer of forces from the matrix to the droplets of the dispersed phase. In mixtures of incompatible polymers, chains of macromolecules of both components can be adsorbed on nanoparticles located in the interphase layer. This increases the adhesion between the components and connects the phases. The increase in the degree of interaction at the interface between the PP/PVA and PP/CPA phases contributes to the transfer of stresses from the matrix polymer to the polypropylene droplets, increases the amount of their longitudinal deformation and ensures the formation of thinner microfibrils. At the same time, an increase in the number of short microfibrils in extrudates of mixtures with a polyvinyl alcohol matrix may be the result of the breakdown of the thinnest jets of the polypropylene melt as the most thermodynamically unstable.

The chemical nature of the matrix polymer significantly affects the rheological properties of nanofilled mixtures. There is a fundamental difference in the "viscosity - methylsilica

concentration" dependence for PP/PVA and PP/SPA mixtures (Fig. 1.24).
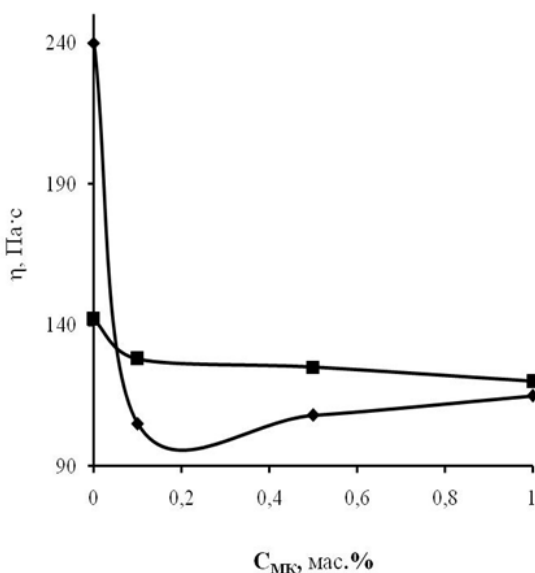

Fig. 1.24. Dependence of the viscosity of melts of PP/PVA (■)
and PP/SPA (♦) mixtures on the content of methylsilica

The effective viscosity of melts of PP/PVA mixtures containing (0.1÷1.0) wt. % MSi, decreases with increasing additive concentration. When introducing 0.1 wt. % of methylsilica in the melt of the PP/CPA mixture, the viscosity of the melt decreases by 2.4 times, and subsequently increases with an increase in the content of nanoparticles of methylsilica. At the same time, the value of the effective viscosity of the modified compositions remains lower than the melt η of the original mixture. The extreme change in the melt viscosity of the mixture upon the introduction of tenths of a percent additive can be explained by the effect of so-called small

additives, described by the authors [140]. It is associated with a change in the thermodynamic parameters of the system, primarily the compatibility or incompatibility of components. A further increase in viscosity is due to the thickening effect on the melt of the solid additive. At the same time, it should be emphasized that the general regularity of a sharp drop in the viscosity of their melts compared to η of the melts of the original components is preserved for all mixtures.

The chemical structure of the matrix polymer determines the nature of the dependence of detonation on the content of methylsilica nanoparticles for extrudates of nanofilled mixtures. The values of equilibrium swelling of PP/PVA/MK extrudates remain at the level of the original composition and do not depend on the concentration of methylsilica (Fig. 1.25).
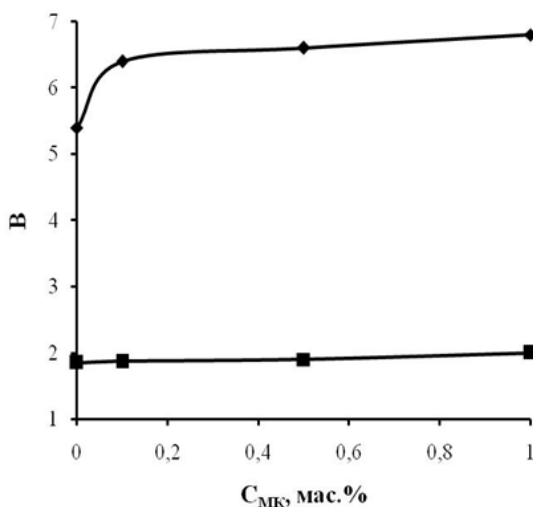
Fig. 1.25. Dependence of the amount of swelling of extrudates of PP/PVA (■) and PP/SPA (♦) mixtures on the content of methyl silica

Conducting 0.1 wt. % MSi in the PP/SPA melt leads to an increase in the swelling of the extrudate. A further increase in the nanoadditive content has little effect on the value of B, while its values are almost 3 times higher than for three-component mixtures with a polyvinyl alcohol matrix.

Additives of methylsilica improve the ability to process melts of both studied compositions, which is evidenced by an increase in the value of the maximum spinneret extraction (Fig. 1.26).
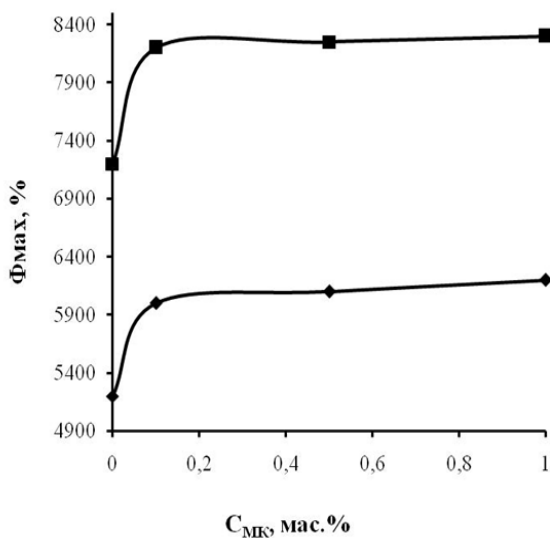

Fig. 1.26. Dependence of the maximum possible spinneret extraction of melts of PP/PVA (■) and PP/SPA (♦) mixtures on the content of methyl silica

The amount of longitudinal deformation increases significantly with the introduction of 0.1 wt. % methylsilica and remains unchanged with an increase in the content of the additive. At the same time, the chemical nature of the matrix

polymer does not affect the nature of the dependence "property - concentration of nanoadditive". The established regularity can be due, firstly, to a change in the processes of structure formation of polypropylene in the matrix of polyninyl alcohol and co-polyamide under the action of nanoadditives. Secondly, the formation of physical (hydrogen) bonds between the functional groups of the mixture components contributes to the improvement of the processing ability of the modified systems.

Studies of the process of extraction of polyvinyl alcohol from extrudates of two- and three-component compositions showed that repeated extrusions and additives of methylsilica do not affect the solubility of PVA in cold and hot water. Raw and modified PP/PVA blends can be stably processed into fibers and films on traditional extrusion equipment.

Thus, the performed experimental studies made it possible to establish the peculiarities of the micro- and macrorheological properties of melts of mixtures of polypropylene with matrix polymers of different chemical nature. An important difference in the processes of structure formation in mixtures of polypropylene/plasticized polyvinyl alcohol is that even with a ratio of components of 50/50 wt. % there is no change of phases, but the formation of polypropylene microfibrils in the matrix of polyvinyl spmrt takes place. The viscosity of melts of PP/PVA and PP/SPA mixtures decreases sharply compared to η of the original components. This is due to their insignificant interaction at the boundary of phase separation and the formation of polypropylene jets in the matrix polymer. Equilibrium swelling values of extrudates of PP/PVA mixtures are almost 2.5 times

lower than similar indicators for PP/SPA mixtures. They do not depend on the content of polypropylene and cannot be used as an indirect characteristic of improving the process of forming a microfibrillar structure in compositions with a polyvinyl alcohol matrix. The ability to longitudinal deformation of melts of PP/PVA mixtures is 1.4 times higher than that of PP/SPA melts. At the same time, it should be noted that the value of the maximum spinneret extraction of the melt jet of the original co-polyamide exceeds this indicator for polyvinyl alcohol by 2.7 times.

The introduction of methylsilica nanoparticles significantly improves the process of forming polypropylene microfibrils, regardless of the chemical nature of the matrix polymer. The mechanism of action of the nano-additive consists in reducing the value of surface tension at the boundary of phase separation and in increasing the thermodynamic stability of liquid jets of PP with a smaller diameter.

The process of extracting the matrix polymer (plasticized polyvinyl alcohol) from the composite threads or films formed from the original and modified mixtures can be carried out with a simple non-toxic cheap solvent - hot or cold water. This makes it possible to develop environmentally friendly technologies for the production of polypropylene microfibrillar products (complex threads, filter or special materials).

1.3. Conclusion

The analysis of the literature, as well as our research, showed that the creation of polymer nanocomposites, regulation and study of their properties is one of the most important areas of development in the field of polymer technology. Significant interest in such materials is due to the fact that they combine low cost with a set of unique characteristics that are not inherent in the original components. Purposeful management of the morphology of polymer mixtures during their processing is a rather complex task, which is determined by the totality of their physical and chemical properties and technological parameters. Adding a small amount of nanoparticles to polymer mixtures is a modern and promising direction for providing new predetermined properties to composite materials based on them. Today, a significant number of effective nanofillers for polymers and their mixtures have been created. There are also many technological techniques that lead to the creation of a wide range of sizes and shapes of particles of the dispersed phase in the polymer matrix. The use of nanofillers is a powerful tool for regulating the microstructure of polymer mixtures, which determines the characteristics of composites based on them. The influence of nanoparticles on the micro- and macrorheological properties of melts of thermodynamically incompatible polymer mixtures is determined by a combination of the following factors:

• the chemical nature of the ingredients, the composition of the composition and the morphometric characteristics of the nanofiller;

• rheological properties of the components and the ratio of their viscoelastic indicators;

• the value of the surface tension at the boundary of the phase separation;

• degree of compatibility of polymers of the mixture and interphase interaction;

• conditions of the process of mixing ingredients;

• type of dispersed phase structure and its dimensional characteristics;

- • predominant localization of nanoparticles in the volume of one of the components or on the border of their separation.

However, to a large extent, the established regularities are empirical, intuitive in nature and require theoretical justifications for the creation of new possible structures and their corresponding practical implementation. The main mechanisms of the influence of nanoparticles on the morphology of polymer dispersions are still debatable and require theoretical generalizations. The presented results and established regularities testify to the possibility of purposeful control of the microstructure of materials and the need for further research in this direction in order to obtain nanocomposite mixtures with a given set of properties. This approach to the development of materials with a predicted structure is promising, but requires a certain strategy and detailed knowledge of the basic parameters that affect the formation of morphology.

Further research using the developed software for planning experiments and processing the results of experiments

on the effect of nanofillers on the rheological properties of polymers and their mixtures, on interphase phenomena (the amount of surface tension, stability of liquid jets), dimensional characteristics of the structures of the dispersed phase component, will allow to determine the key factors, which will ensure the formation of the desired type of morphology. The established regularities and mechanisms of the formation of various types of structures in polymer dispersions will make a significant contribution to the general theory of the processing of nano-filled compatibilized systems. The practical result will be the possibility of purposeful control of the microstructure of melt mixtures in order to obtain polymer nanocomposites with improved predetermined characteristics for their wide use in various industries and in everyday life.

CHAPTER 2
SOFTWARE FOR PROCESSING AND SUMMARIZING EXPERIMENTAL DATA

2.1.1. Software for determination of temperature-concentration superposition by shear rate in melts of polymer mixtures. For the processing and generalization of experimental data on the viscoelastic properties of polymer melts, there is a method based on temperature (concentration) time or frequency superposition (adduction) [146]. The essence of the superposition with respect to the results of rheological studies is that the experimental data of the dependence of the logarithm of the shear stress on the logarithm of the shear rate, obtained at different concentrations (temperatures), can be combined by moving along the axis of the shear rate by the amount of lg aT (aT is the conversion factor). The use of this method makes it possible to significantly increase the range of investigated shear rate values. Modern devices for rheological research cover an interval of change in shear rate with a width of 2-3 decimal orders. The processing of the results by the method of concentration-time superposition expands the change in the shear rate to 5 decimal orders.

Generalization of viscosity data was carried out using the method proposed by authors [146], which is based on the fact that the change in effective viscosity is determined by the complex of relaxation properties of the system in the initial state, i.e., the largest Newtonian viscosity ($\eta_{\text{н}}$). For this, the following coordinates were used:

$$\eta_{np} = \eta \, / \, \eta_{\text{н}} \qquad \dot{\gamma}_{np} = \eta_{\text{н}} \cdot \dot{\gamma} \qquad (2.1)$$

where: $\eta_{_{\text{н}}}$ – maximum Newtonian viscosity; $\dot{\gamma}$ – shear rate gradient; η_{np} – reduced viscosity; $\dot{\gamma}_{np}$ – reduced shear rate gradient

In cases where the Newtonian segment of the curve was not reached in the experiment, ηn was found by the method of extrapolation of the dependence $lg\ \eta$ – $lg\ \tau$ at $lg\ \tau \rightarrow 0$, as described in [146].

Generalization is possible provided that the relaxation spectra of polymer systems are similar at different temperatures and concentrations. It is known that for many binary mixtures of polymers there are quite wide regions where the dependence of the viscosity on the shear rate in the reduced coordinates is invariant with respect to the composition [72,147]. At the same time, the superposition always takes place for that dispersion medium, the melt of which is characterized by a greater anomaly of viscosity and elasticity. The processing of experimental data on the viscous properties of PP/SPA mixtures indicates the absence of composition invariance (Fig. 2.1) [148]. This is in agreement with the conclusions of [147]: for the studied mixtures, the dispersion medium is SP, the flow regime and elasticity of which are significantly lower than the similar indicators for the dispersed phase (PP).
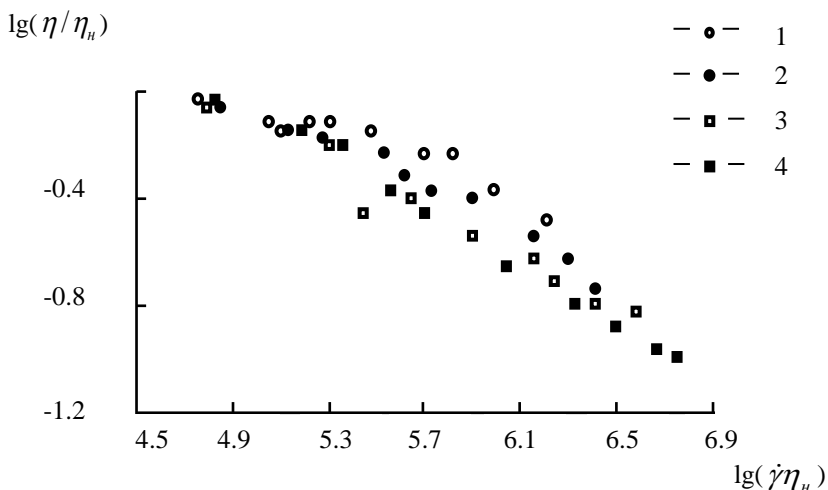
Fig. 2.1. Dependence of the melt viscosity of the PP/SPA
mixture on the shear rate in the given coordinates. Points 1 4 correspond to
the content of polypropylene, wt. %: 20; 30; 40; 50

For the visual presentation and generalization of experimental data, special software was created in the C++ language in the C++ Builder environment [149-151]. In Fig. 2.2 presents the results of the program in the absence of temperature-compositional superposition.
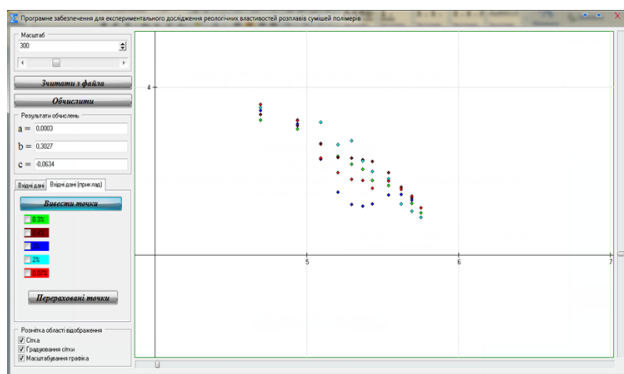

Fig. 2.2. Program representation of the dependence of the melt viscosity of
the PP/SPA mixture on the shear rate in the reduced coordinates

133

The results of summarizing the data for PP/PVA mixtures with different polypropylene content showed the invariance of the dependence of viscosity on the shear rate in the given Vinogradov-Malkin coordinates with respect to PP concentration (Fig. 2.3).
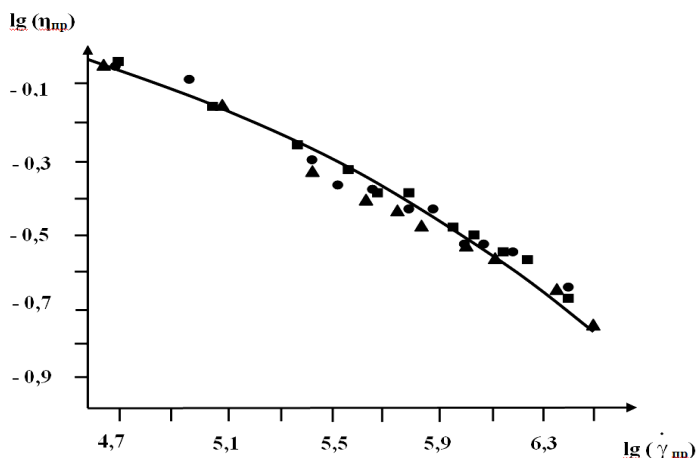

Fig. 2.3. Dependence of viscosity on shear rate in the given coordinates for melts of PP/PVA mixtures composition, mass %:
■ – 20/80; ▲ – 30/70; ● – 40/60

As can be seen from Fig. 2.3, in the coordinates $lg(\eta/\eta_{\scriptscriptstyle H}) - lg(\eta_{\scriptscriptstyle H} \cdot \dot\gamma)$ for all mixtures, the points are quite densely located near one common curve, despite the fact that the PVA melt is characterized by lower elasticity and the degree of deviation from the Newtonian flow regime. This indicates that the influence of the composition of the mixture on the effective viscosity is manifested only through the highest Newtonian viscosity.

Regarding the possibility of concentration superposition in multicomponent compositions, information is

limited. Thus, the authors [136] showed the absence of invariance for PP/SPA mixtures compatibilized with sodium oleate at different salt contents. This is explained by the changes in the relaxation spectrum of the melts of the modified mixtures due to the surface activity and plasticizing action of the compatibilizer. At the same time, the invariance of viscosity with respect to the concentration of siloxane liquid additives (PES-5) and binary compositions of compatibilizers PES-5/ copolymer ethylene with vinyl acetate was established for PP/SPA mixtures [137].

Study of the properties of the PP/SPA mixture with a composition of 30/70 wt. %, filled with carbon nanotubes (CNTs), showed [131] that they are invariant with respect to the additive content (Fig. 2.4).
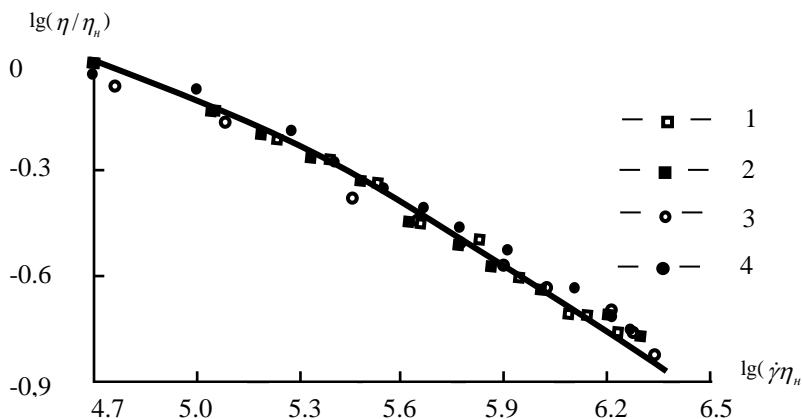

Fig. 2.4. Dependence of melt viscosity on shear rate in the reduced coordinates for PP/SPA/BNT mixtures. Points 1 – 4 correspond to the content of CNT, wt. %: 0; 0.1; 0.5; 1.0

This indicates that in the investigated nanofilled mixtures the influence of the composition on the effective viscosity of the

melt is fully manifested through the highest Newtonian viscosity, and the possibility of concentration superposition in the melts is determined by the difference in the sensitivity of the components to shear intensity

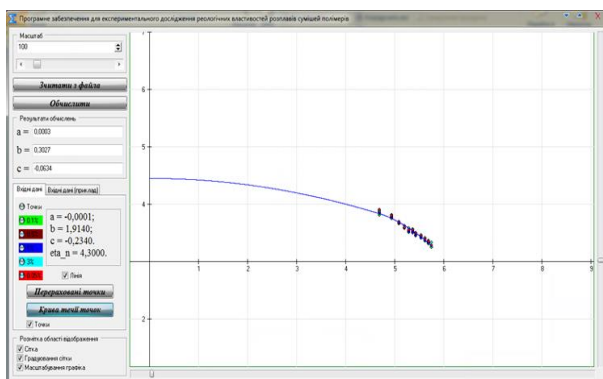The program image of the given results, as well as the flow curve, is presented in Fig. 2.5.

Fig. 2.5. Software representation of the dependence of melt viscosity on the shear rate in the reduced coordinates for PP/SPA/CNT mixtures

It is known that the dependence of the viscosity of melts and solutions of the starting polymers in the given coordinates is invariant to temperature [147]. The issue of the possibility of temperature superposition in melts of binary and modified polymer mixtures is debatable. In a number of works, it was concluded that temperature reduction for melts of polymer mixtures is, as a rule, possible. Thus, temperature-invariant curves were obtained in the given coordinates for melts of PP/SPA mixtures with additions of sodium oleate as a compatibilizer [136].

Generalization of viscous properties for PP/SPA compositions containing 0.5 wt. % of CNTs at different temperatures shows that temperature invariance is fulfilled for the initial and modified mixtures at all investigated concentrations of carbon nanotubes (Fig. 2.6) [131].
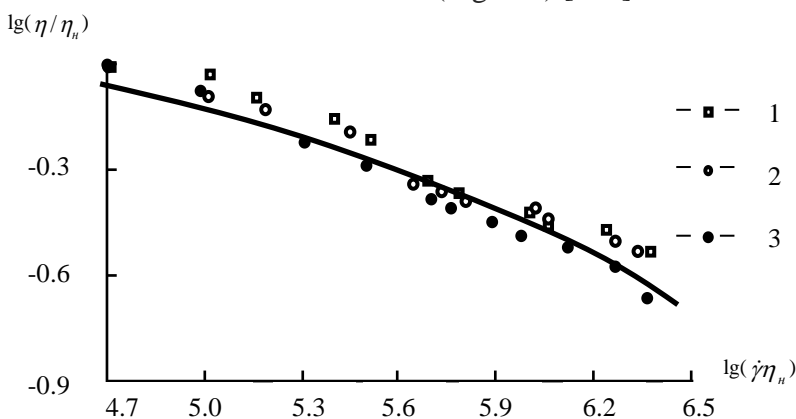

Fig. 2.6. Temperature-invariant dependence of the melt viscosity of the PP/SPA/BNT mixture on the shear rate in the given coordinates. Points 1-3 correspond to temperatures, 0C: 190 (1); 210(2); 220(3)

Thus, it was confirmed that carbon nanotubes do not change the character of the relaxation spectrum of the melt of the original mixture, and the effect of temperature on the effective viscosity of the melts of three-component systems, as for the original polymers, is manifested through $\eta_{\text{н}}$.

The existence of a universal dependence of η in the given coordinates proves that the relaxation spectra of the melts of the investigated mixtures are similar and are described by the same functional dependence, i.e., the logarithmic form of the relaxation spectrum is the same for the melts of the mixture in the entire range of concentrations. Thus, for the

melts of nano-filled compositions, the same regularities of their rheological behavior are manifested, as for the melt of the original mixture.

In practical terms, the use of the method of constructing a temperature- or concentration-invariant viscosity characteristic makes it possible, knowing the temperature (concentration) dependence of $\eta_{\text{н}}$ and the dependence of the effective viscosity on the shear rate for one composition or the temperature of the mixture, to determine the values of η for all shear stress values for other concentrations and temperatures.

2.1.2. Software for determining the rheological characteristics of polymer melts and their mixtures. A feature of the processing of polymers into products is the need to convert them into a viscous-liquid state in order to give them the required shape. It is known that classical hydromechanics is based on Newton's model of a viscous fluid, according to which the shear stress (τ) is directly proportional to the strain rate (γ): $\tau = \eta\gamma$, where the proportionality coefficient η is called viscosity. Melts of high molecular compounds are characterized by the so-called viscosity anomaly, i.e. deviation from the specified Newton's law, which is associated with the internal structure of polymer melts. The nature of the flow of such systems is subject to the power law:

$$\tau = \eta\gamma^{n} \qquad (2.2)$$

where: η – degree of deviation from Newtonian flow

In view of this, it is advisable to study the rheological behavior of the original, modified melts of polymers and their mixtures

in order to establish the main patterns of flow as a factor affecting the formation of the morphology of composites and the technological parameters of processing. Among the various properties of polymer systems in the viscous-fluid state, effective viscosity is important in practical terms. Capillary viscometers of constant pressure are used to study the rheological characteristics of polymer melts, since the flow in them occurs by a shear mechanism, as in technological equipment for their processing [152]. Calculating the flow parameters of polymer melts and presenting the obtained results graphically is quite time-consuming and requires considerable time, which led to the creation of special software (listing - see the appendix) [153], which was developed in the Delphi environment in the Object Pascal language [154] . To conduct experimental studies, the original polypropylene and silver/aluminum oxide (Ag/Al$_2$O$_3$) modified with a nano additive were used, which was introduced in the amount of (0.1÷3.0) wt. %. The rheological characteristics of the studied melts of polymer systems were studied using a capillary viscometer brand MV-2. The flow of melt through the capillary occurs due to the pressure difference between its ends:

$$\Delta P = P\!\big/\!F \qquad\qquad (2.3)$$

where: P – the mass of the piston, frame and loading discs and the force of the indicator spring; F – piston area Processing of experimental results was carried out using generally accepted methods for non-Newtonian systems. The

shear stress on the capillary wall was determined by the equation:

$$\tau = \frac{\Delta P \cdot r}{2L}$$

$$\tau = \frac{4r \cdot P}{\pi \cdot d_n^2 \cdot 2L} = K_1 \cdot P \qquad (2.4)$$

where: r, L – radius and length of the capillary, respectively;

d_n – piston diameter;

K_1 – constant value for a given capillary, which depends on its diameter and length
To simplify calculations, equation (2.4) was converted into a logarithmic system:

$$\lg \tau = \lg K_1 + \lg P \qquad (2.5)$$

The shear rate depends on the volume flow rate of the melt from the capillary (Q) and is calculated by the formula:

$$D = \frac{Q}{\pi r^3} \qquad (2.6)$$

$$Q = \frac{S \cdot \pi \cdot d_n^2}{4t} \qquad (2.7)$$

where S – displacement of the piston under the influence of a pressure drop, measured on the indicator;

t – time during which the piston is moved.

In the logarithmic system, equation (2.7) will have the form:

$$\lg D = \lg K_2 + \lg\left(\frac{S}{t}\right) \qquad (2.8)$$

where K_2 – constant value for this capillary

The value of the shear rate, determined according to equation (2.8), is approximate, because it does not take into account the input phenomena that take place during the transition from the wide reservoir of the viscometer to the narrow capillary, therefore, at the entrance to it, due to the flow of the polymer melt, a pressure drop occurs that is much larger, than for Newtonian fluids [152,153]. Pressure losses at the inlet to the capillary are caused by the pressure drop resulting from the easterly current, the restructuring of the flow velocity profile, and the ability of the polymer melt to accumulate elastic energy. These losses are taken into account by the Weisenberg-Rabinovych correction. For this purpose, a preliminary flow curve relating the voltage to the shear rate gradient on the capillary wall is constructed according to equation (2.8). From it, the flow regime is calculated as the tangent of the angle of inclination of the tangent at this point of the curve:

$$n = \frac{\Delta \lg D}{\Delta \lg \tau} \qquad (2.9)$$

The software image of the previous flow curve is shown in Fig. 2.7. This curve describes a set of stable flow regimes with different speeds and shear stresses. A typical flow curve for a non-Newtonian fluid has an S-like shape. For sufficiently low and high values of velocities and shear stresses, these values are directly proportional to each other. The average section of the flow curve of a non-Newtonian fluid is called "structural", each point of which corresponds to a state of dynamic equilibrium between the processes of destruction and restoration of the melt structure.
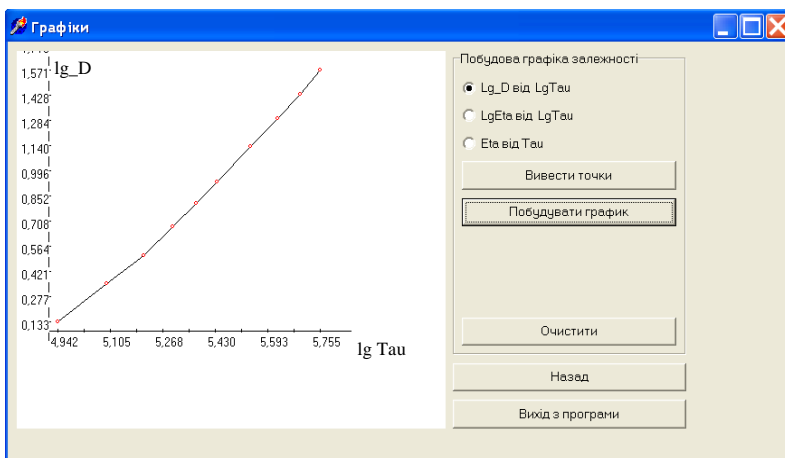
Fig. 2.7. Program image of the previous flow curve

To obtain the true flow curve and calculate the viscosity value, the previous flow curve is conditionally divided into two parts: one corresponds to the highest Newtonian viscosity, and the second to the "structural" section, and then the average value of the n_{cp} indicator is calculated for them. Taking into account the Weissenberg-Rabinovych correction, the shear rate is determined by the formula:

$$\gamma = \frac{(n_{cp.} + 3)\cdot Q}{\pi \cdot r^3} \quad \text{або} \quad \gamma = (n_{cp.} + 3)\cdot D \qquad (2.10)$$

In the logarithmic system, equation (2.10) will have the form

$$\lg \gamma = \lg(n + 3) + \lg D \qquad (2.11)$$

The viscosity value is calculated from the expression:

$$\lg \eta = \lg \tau - \lg D \qquad (2.12)$$

The results of experimental data processing on the flow of polypropylene melt modified by 1.0 wt. % of Ag/Al$_2$O$_3$, using the created program are presented in Fig. 2.8.
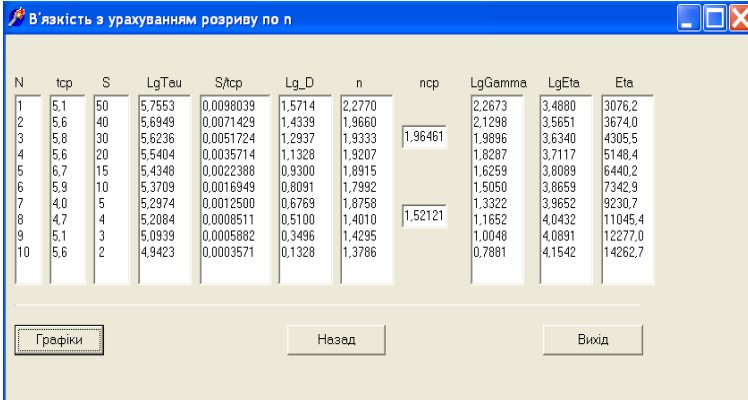
142

Fig. 2.8. Material functions of the modified polypropylene melt flow proces

The developed software allows you to graphically present the true current curve $\lg \gamma = f(\lg \tau)$, as well as the dependence of η on shear stress and shear rate. In Fig. 2.9 is shows the function $\lg \eta = f(\lg \tau)$ for a polypropylene melt filled with 1.0 wt. % of Ag/Al_2O_3.
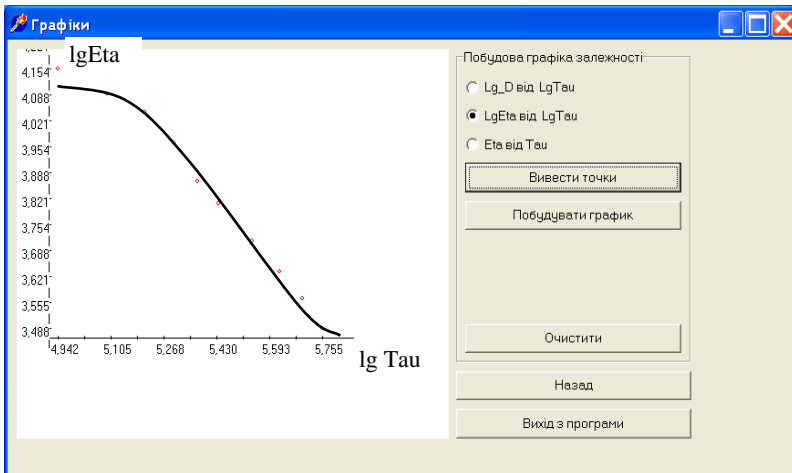

Fig. 2.9. Program image of dependency $\lg \eta = f(\lg \tau)$

143

The influence of the silver/aluminum oxide nanoadditive content on the polypropylene melt flow pattern, calculated using the developed program, is shown in Table 2.1. The obtained results indicate that the viscosity of polypropylene melts naturally increases with the introduction of a nano-additive, i.e., the effect of filling with a solid substance is manifested. The nature of the flow of the original and modified PP melts is subject to a power law.

Table 2.1. Rheological properties of the source melts and nano-filled polypropylene

Indicators	Nanoadditive concentration, wt. %				
	0	0,1	0,5	1,0	3,0
viscosity, Pa·s	260	290	300	310	350
flow regime	2,1	2,0	2,0	1,9	1,9

At this, the degree of deviation from Newtonian flow slightly decreases with increasing filler content.

Thus, software was developed in the Delphi environment in the Object Pascal language [154] for processing the experimental results of the study of the rheological properties of polymer melts by the capillary viscometry method. The created program allows you to calculate the viscosity and flow mode of melts, as well as to present the results in the form of graphical images of the flow curve and the dependence of viscosity on stress and shear rate. The obtained data, determined at different temperatures and the composition of polymer systems, provide important information about the structure and structural transformations

144

of polymer melts. The created software allows you to significantly shorten the term and simplify the process of processing experimental results, as well as to select technological parameters of processing depending on the rheological characteristics of melts.

2.1.3. Software for calculating the parameters of the kinetics of the disintegration of liquid jets of one polymer in the matrix of another and the value of interfacial tension. As shown in sections 1.2-1.4, the properties of polymer composites are determined by the phase structure of the component of the dispersed phase in the matrix, which depends on the degree of their thermodynamic compatibility (absolutely compatible homogeneous systems, partially compatible and completely incompatible). In incompatible systems, a microfibrillar morphology often occurs, in which one component forms in the mass of another many liquid jets (microfibrils) with diameters from tens of fractions to several micrometers. Considerable interest in such structures is due to the fact that the self-reinforcement effect is achieved during the formation of composite materials, the degree of which can be adjusted by changing the value of the ratio of the length and diameter of the fibrils of the dispersed phase component [64,65,72,75]. Microfibers with a unique structure and properties and new thin-fiber materials based on them (cotton-like synthetic fibers and threads, precision filter materials, sorbents, etc.) are obtained by processing melts of polymer mixtures [40-42,68,72]. The formation of microfibrils (microfibers) is a special type of structure formation, during

which there is deformation and merging of droplets of the dispersed phase in the jet, which must maintain their stability in the channel of the forming hole and upon exiting it. The final morphology is the result of a balance between the processes of deformation and decay, on the one hand, and coalescence, on the other. Deformation, capillary instability and coalescence are effective factors in creating the desired structure of the polymer dispersion. Establishing the patterns of jet disintegration of one polymer in the matrix of another is important for controlling the processes of polymer mixing and fiber formation. Thus, the life time of the liquid jet determines the possibility of realizing the formation of microfibers of one polymer in the matrix of another, and the temperature of their disintegration determines the operating conditions.

Based on the above, one of the important microrheological processes affecting the morphology of the polymer mixture is the disintegration of deformed droplets or liquid cylinders. Breakdown will occur when the spherical droplet is elongated enough to form an ellipsoid or filamentous liquid cylinder. The variables that control the degree of deformation will also determine the critical conditions of disintegration. Such parameters are the ratio of the viscosities of the polymer of the dispersed phase and the matrix and the Weber number. A liquid polymer jet is thermodynamically unstable due to an unfavorable surface-to-volume ratio. By its nature, the destruction of a liquid cylinder is a transient phenomenon. Before disintegration, thickening and thinning are formed on the surface of the cylinder, which leads to an increase in its surface energy, and destruction is the result of

the system's desire to decrease it (Fig. 2.10). To study the regularities of the disintegration of liquid jets of one polymer in the matrix of another, a technique was developed [134,147], based on the measurement of the growth rate of capillary waves, in accordance with the classical Tomotika theory.
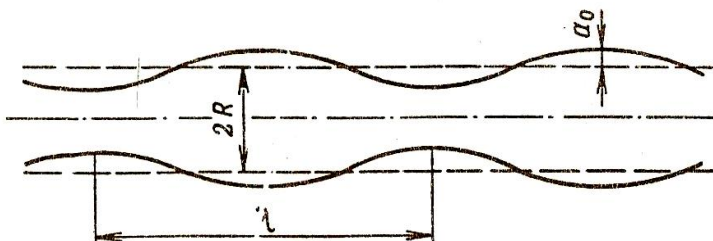

Fig. 2.10. Schematic representation of a liquid cylinder in action destructive wave

For the experiments, we used the original mixture of polypropylene/copolyamide with a composition of 30/70 by weight. % and a nanofilled composition containing 3.0 wt. % titanium oxide/silica nanoadditives. In order to evaluate the kinetics of jet decay and determine the value of the surface tension of polymer mixtures ($\gamma_{\alpha\beta}$), extrudates were previously formed from them, longitudinal sections with a thickness of (10÷20) μm were made, they were placed on a glass slide in an immersion medium and heated on the stage of an MP-6 microscope according to constant rate of temperature rise (0.6 degrees/s). After certain time intervals, different stages of jet disintegration (microfibrils) were photographed. At the appropriate temperature, the jet began to collapse in places of reduced cross-section under the action of interphase tension forces and disintegrated into a chain of droplets (see Fig. 1.15).

147

The initial jet diameter (d_0), thickness diameters (d_e), and droplet diameters (d_k), formed under the influence of temperature, and the distance between their centers (λ_m) were measured from microphotographs. For each pair of polymers, up to 100 photographs were analyzed, and since up to 10 microfibrils fell into one frame, the total number of r_k and λ_m values exceeded 1000. The time of decay was taken as the time during which the majority of them in the cross-section were destroyed. The lowest temperature at which microfibrils disintegrated was recorded. This temperature determines the scope of their operation. Calculations were performed according to the well-known algorithm [155] using specially developed software [154].

The input data for the program were the results of processing microphotographs taken at appropriate time intervals (t), on which the diameters of "varicose" thickenings (d_e) were measured and entered into the text files "*Волокна.txt*". An example of an input file is shown in Fig. 2.11.
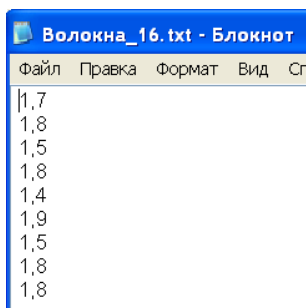

Fig. 2.11. Data input file for "varicose" cylinders

After the disintegration of the jets, the diameters of the drops (d_k) and the distance between their centers, which corresponds to the wavelength of the destructive excitation (λ_m), were determined. The data were entered into the text files "*Частки.txt*" and "*Лямбда.txt*", their appearance is similar to the file for fibers. The number of suitable input files depends on the number of photomicrographs, as well as on the presence of corresponding types of structures. In addition, the time points at which each frame was photographed were entered from a separate file ("Time.txt" file). Using the program, the average diameter of the initial microfibrils (d_0) and the average value of $d_в$ for each t were calculated.

The cause of the destruction of the liquid jet is the occurrence of wave-like disturbances on its surface, the amplitude (a) of which increases exponentially with time [156]. Jets break up under the condition that the magnitude of the perturbation amplitude becomes equal to their radius. In logarithmic coordinates, the dependence of a on t is expressed by a straight line.

$$\ln a = \ln a_0 + qt \qquad (2.13)$$

The tangent of the angle of inclination of this straight line to the abscissa axis is the coefficient of instability q.

At the same time, the value q is a complex function of the wave number and the ratio of the viscosities of the mixture components:

$$q = \frac{\gamma_{\alpha\beta}}{2\eta R} \cdot F(\chi, K) \qquad (2.14)$$

149

To determine the value of the instability coefficient, first calculated $\ln\left(\dfrac{d_{\text{в}} - d_0}{d_0}\right)$ and then determined q by the formula:

$$q = \frac{\Delta\ln\left(\dfrac{2(d_{\text{в}} - d_0)}{d_0}\right)}{\Delta t} \qquad (2.15)$$

The calculated values were tabulated. The intermediate results of the program are shown in Fig. 2.12.

ln(2a0/d)	delta(ln(2a0/d))	t	delta(t)	q= delta(ln(2a0/d)/delta(t)
-2,613	0,538	22,34	10	0,053773
-2,075	0,310	22,44	10	0,030956
-1,765	0,448	22,54	10	0,044784
-1,318	0,323	23,04	10	0,032335
-0,994	0,191	23,12	8	0,023849
-0,803	0,106	23,22	10	0,010586
-0,698	0,132	23,38	16	0,008224
-0,566	0,079	23,47	9	0,008776
-0,487	0,055	23,56	9	0,006060
-0,432	0,045	24,07	11	0,004109
-0,387	0,053	24,14	7	0,007515
-0,335	0,103	24,22	8	0,012898
-0,232	0,030	24,38	16	0,001897
-0,201	0,068	24,46	8	0,008533

Fig. 2.12. Intermediate results of the program

To estimate the value of the surface tension at the separation boundary of the components of the mixture, the dependence was used [158]:

$$\gamma_{\alpha\beta} = \frac{q \cdot \mu \cdot d_0}{\Omega(\chi, K)} \qquad (2.16)$$

where μ – matrix polymer melt viscosity;

χ – the wave number of the destructive disturbance;

Ω – a tabulated function determined from the curve of the dependence of χ on K.

The wave number of the destructive disturbance was calculated according to the formula:

$$\chi = \frac{2\pi R}{\lambda_m} \qquad (2.17)$$

where R – jet radius before breakup.

The value of R was found from the equation:

$$r_k = (3R\lambda_m / 4)^{\frac{1}{3}} \qquad (2.18)$$

In logarithmic form it has the form:

$$\lg R = \frac{3}{2}\lg r_k - \frac{1}{2}\lg \lambda_m + 0.0625 \qquad (2.19)$$

In order to determine R, the average values of the diameter (d_k), the radius of the drops (r_k), the wave magnitude of the destructive disturbance (λ_m), as well as the ratio of the viscosities of the dispersed phase component (PP) and the matrix (SPA) were calculated $K = \dfrac{\eta}{\mu}$.

Based on the found parameters of the wave number and the ratio of component viscosities, the value of the tabulated function Ω was found from the dependence graph $\chi = f(K)$. The program prompts the user to enter its value (Fig. 2.13). After that, final calculations of the surface tension at the phase separation boundary were performed with the help of the program (Fig. 2.14).

Fig. 2.13. Entering the value of the tabulated function Ω

Fig. 2.14. Calculation of surface tension

To assess the stability of liquid jets of one polymer in the matrix of another, the reduced values of the droplet radius (r_k/R) and life time ($t_{ж}/R$) were also determined.

For example, in the Table 2.2 and 2.3 show data on the influence of titanium oxide/silica nanoadditive on the patterns of disintegration of polypropylene microfibrils in the co-polyamide matrix and on the value of the interfacial tension, calculated using the developed program.

Table 2.2. The effect of nanoadditive on the parameters of PP microfibril disintegration in the CPA matrix

The name of the additive	R, µm	$r_к$, µm	λ_m, µm	$r_к/R$	$2\pi R/\lambda_m$	$t_ж$, s	$t_ж/R$, s/ µm
without additive	2,1	3,1	13,8	1,8	0,69	56	37
titanium oxide/silica	1,5	2,7	9,2	1,6	1,42	130	62

Table 2.3. The results of determining the values of the interfacial tension and the coefficient of instability according to the kinetics of the disintegration of PP microfibrils in the CPA matrix

The name of the additive	Ω	q	$\gamma_{\alpha\beta}$, mN/m
without additive	0,18	0,0618	2,60
titanium oxide/silica	0,04	0,0247	1,52

Thus, software was developed in the Delphi environment in the Object Pascal language, which allows processing the experimental results of the kinetics of disintegration of liquid jets of the dispersed phase polymer in the matrix component. Calculations in the program were carried out using the dependences obtained from the measurement of the growth rate of capillary waves in liquid jets according to the classical theory of Tomotika. The created software makes it possible to determine the main parameters of the process for binary and multicomponent mixtures of

polymers, namely: the value of interfacial tension, the life time and the coefficient of instability of liquid jets, and also allows to significantly simplify the process of processing experimental results, shorten its term and increase efficiency.

2.1.4. Software for processing the results of studies of the microstructure of extrudates of polymer mixtures. As already noted, the formation of microfibrillar morphology takes place during the flow of melts of thermodynamically incompatible mixtures of polymers. At the same time, along with microfibrils of continuous length, which are the predominant type of structure, the component of the dispersed phase can form short fibers, particles and films. For quantitative assessment of structure formation, a special technique was developed [146], which consists in the direct determination under a microscope of the geometric shape and dimensions of the elements of the dispersed phase. The obtained results were processed by the methods of mathematical statistics, as a result of which the following were determined: the total number of microfibrils (n) in the extrudate, the average diameter (d) of microfibrils and particles, the dispersion (σ^2) of the size distribution of this type of structure and the mean square deviation (σ) [157] . Their numerical and mass fate in the extrudate was also calculated and size distribution curves were constructed.

For conducting experimental studies, extrudates of the mixtures with a length of (5÷10) mm were formed and the matrix polymer was extracted from them. From the resulting bundle of microfibrils, a staple with a length of (0.2÷0.3) mm

was cut across the entire cross section of the bundle, which was placed on a glass slide and dispersed in an immersion liquid. Then, under a microscope, the types and number of formed structures were recorded and their sizes were measured. The obtained data were grouped by types of structures, and microfibrils by diameters. The total number of structures was determined and the numerical or mass percentage of each of them was calculated. For microfibrils and particles, all values of random variables obtained in the experiment were summarized in a table, which is the initial series of observation results. To carry out statistical analysis, the initial series was ordered, that is, the data were grouped and the minimum and maximum values of the options were found. The general interval, in which all the obtained data lie, was divided into classes and the frequency of options for a given class was calculated (that is, the number of values that have a value determined by the range of the class), which were summarized in a distribution table or an ordered series of the distribution of the measured value. The range of the class interval Δ was found by the equation:

$$\Delta = {R_b}\Big/{(5 \cdot \lg n)} \quad \text{або} \quad \Delta = {(R_{\max} - R_{\min})}\Big/{(1 + 3.2 \cdot \lg n)} \quad (2.20)$$

where R_b – the difference between the maximum and minimum values of R

At the same time, the interval must exceed the margin of error, but cannot be smaller than it. The classes were placed in ascending order and the number of variants (Z_i) within each class was found.

Initial and central moments were used to calculate

155

numerical characteristics. The initial moments were determined by the formulas:

$$m_1 = \frac{\sum \chi_i Z_i}{n} \ , \qquad m_2 = \frac{\sum \chi_i^2 Z_i}{n}$$

$$m_3 = \frac{\sum \chi_i^3 Z_i}{n} \ , \qquad m_4 = \frac{\sum \chi_i^4 Z_i}{n} \qquad (2.21)$$

where χ_i – the middle of the class, Z_i – the frequency of the corresponding class

The central moments were calculated based on the initial ones:

$$M_1 = 0, \qquad M_2 = m_2 - m_1^2$$

$$M_3 = m_4 - 4 m_1 m_3 + 6 m_1^2 m_2 - 3 m_1^4 \qquad (2.22)$$

To simplify the calculations, instead of the actual values of the midpoints of the classes $K_{н.ср.}$ used values a (so-called conditional options), which were determined by the formula:

$$a = \frac{(K_{н.ср.} - K_{н.о})}{\Delta} \qquad (2.23)$$

where $K_{н.о}$ – the middle of the class, occupying a central position in the row

Then, conditional initial moments were calculated:

$$m_1^1 = \frac{\sum Z_i a}{n} \ , \qquad m_2^1 = \frac{\sum Z_i a^2}{n}$$

$$m_3^1 = \frac{\sum Z_i a^3}{n} \ , \qquad m_4^1 = \frac{\sum Z_i a^4}{n} \qquad (2.24)$$

Next, the arithmetic mean of the distribution was determined.

$$đ = m_1^1 \Delta + K_{н.о.} \qquad (2.25)$$

Through the second conditional central moment M_2^1, the variance of the distribution series was found:

$$M_2^1 = m_2^1 - (m_1^1)^2 \qquad (2.26)$$

In fact, the second central moment is equal to the variance of the distribution σ^2:

$$M_2 = M_2^1 \Delta^2 = \sigma^2 \qquad (2.27)$$

where: σ – root mean square deviation of the arithmetic mean or standard deviation, which has the dimension of a random variable

If it is necessary to compare the dispersion of random variables with different measurement units, the coefficient of variation was used c:

$$c = \left(\sigma / n^{0.5} \right) \cdot 100\% \qquad (2.28)$$

The third and fourth initial moments were used to calculate the third and fourth central moments, which are necessary to quantify the asymmetry and compactness of the actual distributions, that is, their approximation to the normal distribution. For this purpose, asymmetry (*as*) and kurtosis (*ex*) were determined:

$$as = \frac{M_3}{\sigma^3} \quad ; \qquad ex = \frac{M_4}{\sigma^4}$$

Since asymmetry and kurtosis are dimensionless quantities, they can be calculated directly through conditional moments without going to the actual:

$$as = \frac{M_3^1}{\left(M_2^1 \cdot \left(M_2^1 \right)^{0.5} \right)} \quad ; \qquad ex = \frac{M_4^1}{\left(M_2^1 \right)^{0.5}} - 3 \qquad (2.29)$$

where: $M_3^1 = m_3^1 - 3m_2^1 m_1^1 + 2(m_1^1)^3$;

$$M_4^1 = m_4^1 - 4m_1^1 m_3^1 + 6m_1^1 m_2^1 - 3m_1^4$$

Provided that *as* < 0.1, the actual distribution is

considered to be practically symmetrical; if $as \sim 0.25$ – the distribution is weakly asymmetric, in the case when $as > 0.5$ – the distribution is asymmetric.

Kurtosis is an indicator of the deviation of the actual series of the distribution from the normal one in terms of the concentration of individual values around the center of the distribution. It indicates how much the curve obtained in the experiment will be more flat and stretched or, on the contrary, compressed (convex) in the center, compared to the curve of the normal distribution, for which $ex = 0$. If the value of the kurtosis is greater than zero, the actual curve is compressed around the center and pointed. Provided that $ex < 0$, the curve is flattened and stretched, compared to the normal distribution curve.

To process the experimental results of studies on the determination of the dimensional characteristics of the types of dispersed phase structures (particles, continuous and short microfibrils) and the homogeneity of their diameter distribution, software (listing - see the appendix) was developed in the Delphi environment in the Object Pascal language [154]. In Fig. 2.15 and 2.16 show the results of statistical processing of experimental data for the study of the microstructure of the extrudate of the mixture of polypropylene/copolyamide with a composition of 30/70 wt. % performed using the created program.

From fig. 2.16 shows that the distribution curve of PP microfibrils in terms of diameters is asymmetric, that is, it cannot be described by both normal and log-normal distribution laws, which are often found in other types of

158

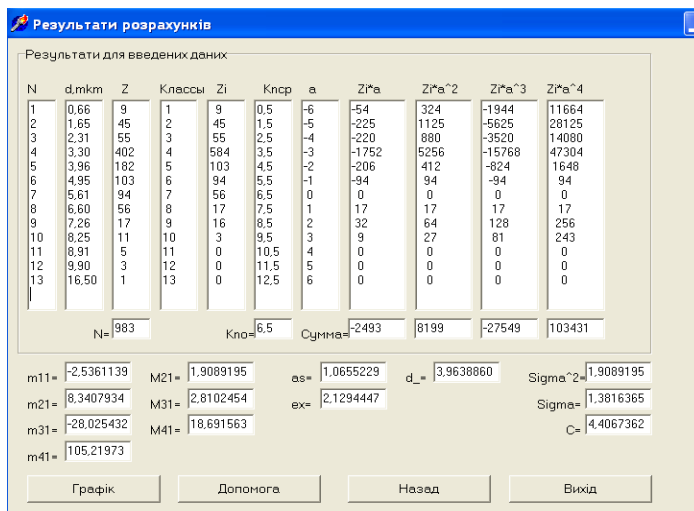dispersed systems. Similar results were obtained when studying the microstructure of many polymer mixtures [72].

Результати розрахунків

Результати для введених даних

N	d,mkm	Z	Классы	Zi	Кпср	a	Zi*a	Zi*a^2	Zi*a^3	Zi*a^4
1	0,66	9	1	9	0,5	-6	-54	324	-1944	11664
2	1,65	45	2	45	1,5	-5	-225	1125	-5625	28125
3	2,31	55	3	55	2,5	-4	-220	880	-3520	14080
4	3,30	402	4	584	3,5	-3	-1752	5256	-15768	47304
5	3,96	182	5	103	4,5	-2	-206	412	-824	1648
6	4,95	103	6	94	5,5	-1	-94	94	-94	94
7	5,61	94	7	56	6,5	0	0	0	0	0
8	6,60	56	8	17	7,5	1	17	17	17	17
9	7,26	17	9	16	8,5	2	32	64	128	256
10	8,25	11	10	3	9,5	3	9	27	81	243
11	8,91	5	11	0	10,5	4	0	0	0	0
12	9,90	3	12	0	11,5	5	0	0	0	0
13	16,50	1	13	0	12,5	6	0	0	0	0

N= 983   Кпо= 6,5   Сумма= -2493   8199   -27549   103431

m11= -2,5361139   M21= 1,9089195   as= 1,0655229 $d_=$ 3,9638860   Sigma^2= 1,9089195
m21= 8,3407934   M31= 2,8102454   ex= 2,1294447   Sigma= 1,3816365
m31= -28,025432   M41= 18,691563   C= 4,4067362
m41= 105,21973

Графік   Допомога   Назад   Вихід

Fig. 2.15. Results of statistical processing experimental data

Графіки

Побудова графіка залежності процентного вмісту від діаметра

Вивести точки

Побудувати графік

Апроксимувати

Залежність
Pr=   D^2+   D+

Очистити

Назад

Вихід з програми

(Y-axis: 40,895 36,816 32,737 28,657 24,578 20,498 16,419 12,340 8,260 4,181 0,102)
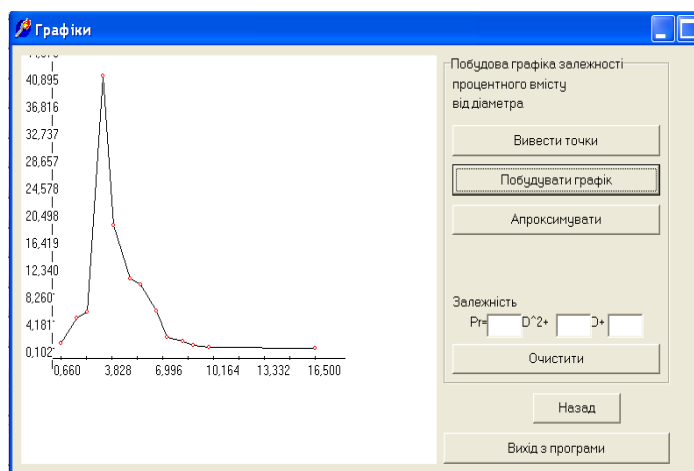(X-axis: 0,660 3,828 6,996 10,164 13,332 16,500)

Fig. 2.16. Distribution curve of PP microfibrils by diameters

159

With the use of the created software, the influence of different grades of organosilicon substances on the processes of structure formation during the melt flow of a polypropylene/co-polyamide mixture was investigated. It was shown that organosilicon substances act as effective compatibilizers and significantly change the morphology of the system [141]. Detailed quantitative microscopic studies show that the introduction into the mixture of PP/SPA composition 30/70 wt. % siloxane liquid of the PES-5 brand contributes to the improvement of the microfibrillar structure: the average diameter of microfibrils decreases, the homogeneity of their diameter distribution increases (Fig. 2.17).
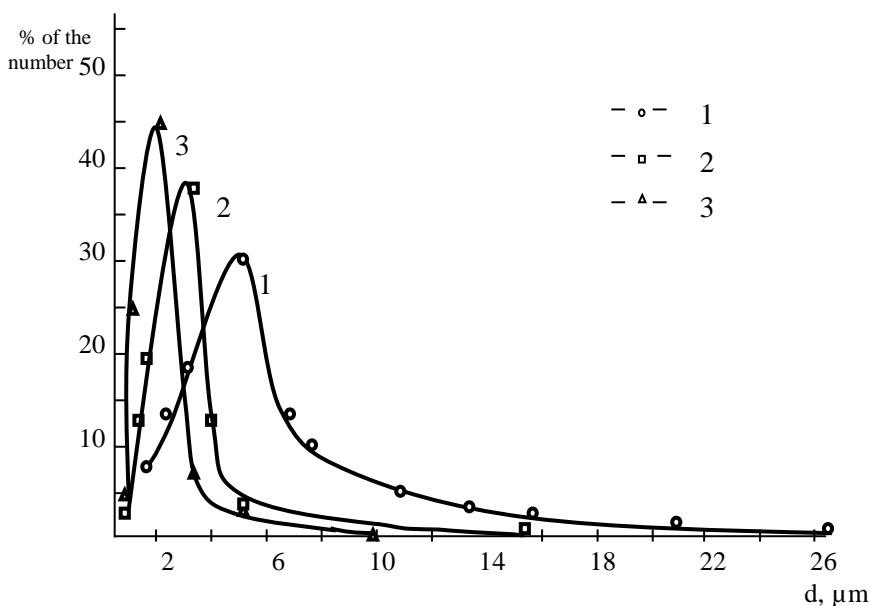
Fig. 2.17. Experimental curves of distribution of PP microfibrils by diameters in extrudates of mixtures containing the additive in quantity, wt. %: 0.0 (1); 0.1(2); 0.5(3)

Processing of the results by methods of mathematical statistics [157] showed that the experimental curves of the distribution of continuous microfibrils by diameters for the modified, as well as the original, mixtures are not described by normal, as well as logarithmically normal distribution laws, judging by the agreement criteria of Pearson and Kolmogorov.

It should be noted that at the content of the modifier (0.1-1.0) wt. % polypropylene microfibrils are formed even in PP/SPA mixtures with a ratio of components that belong to the phase change region (40/60 and 50/50 wt. %). In the absence of modifying additives for PP/SPA mixtures of the indicated compositions, the microfibrillar structure is not formed (Table 2.4).

Table 2.4. The effect of the content of organosilicon liquid PES-5 on the microstructure of extrudates of PP/SPA mixtures with a composition of 50/50 wt. %

Additive content wt.%	Continuous fibrils			Short fibrils		Particles		Films % of the number
	d^*, μm	% of the number	δ^2	d^*, μm	% of the number	d^*, μm	% of the number	
0	Microfibrils are not formed							
0,1	5,6	80,2	19,3	5,4	5,4	6,3	5,8	8,6
0,3	3,8	89,4	3,2	3,2	4,2	3,7	3,3	3,1
0,5	4,1	72,0	5,0	4,3	12,6	4,5	9,3	6,1
1,0	6,3	73,0	32,0	6,0	14,9	7,1	7,6	4,5

*d – average diameter of fibers and particles

At the same time, the compatibilizer concentration affects the dimensional characteristics of microfibrils and the ratio between different types of structures.

The simultaneous use of two compatibilizers is more effective: the average diameter of microfibrils decreases by almost three times, their number increases and homogeneity improves [158]. The curve of the distribution of microfibrils by diameters in the presence of a binary additive is narrower, there are no coarse fibers (Fig. 2.18).
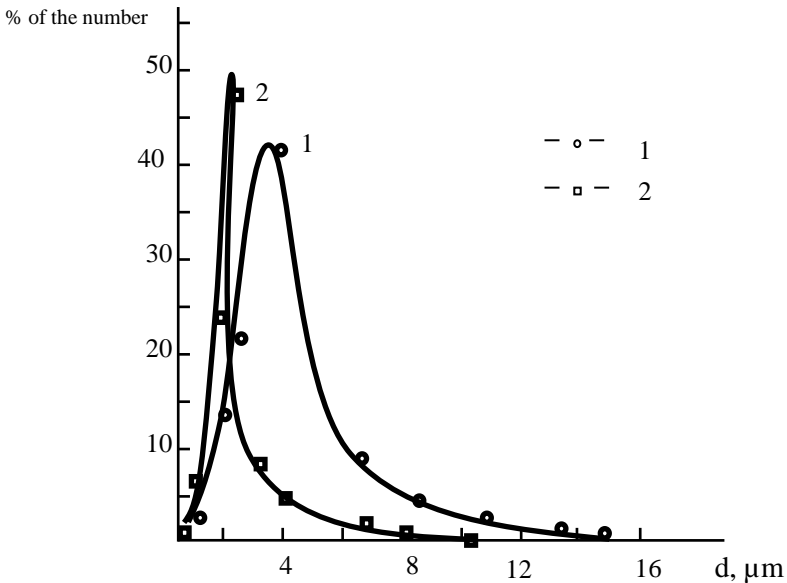

Fig. 2.18. Experimental distribution curves of PP microfibrils by diameters in extrudates of mixtures with binary additives PES-5/SEVA in quantity, wt.%: 0/0 (1); 0.5/5.0 (2)

It should be especially noted that the diameters of fibrils formed from modified mixtures of composition 50/50 wt. %, are smaller than when using binary PP/SPA systems of

composition 20/80; 30/70 wt. %. Established regularities regarding the effect of organosilicon liquids on the processes of structure formation in the PP/SPA mixture allow to increase the content of the dispersed phase component up to 50 wt. %, which in turn will ensure an increase in the production productivity of products based on PP microfibrils and simplify the processes of matrix polymer extraction and SPA and solvent regeneration.

Quantitative assessment of the dimensional characteristics of microfibrils and the ratio between different types of structures is of practical importance, as it allows to improve the microfibrillar structure of composites and obtain new polymer materials with improved operational characteristics based on them.

2.2. Mathematical modeling of rheological processes during the flow of melts of polymer mixtures using structural-continuum approach

Mixing polymers is one of the effective ways to create materials with a given set of properties. Many phenomena and processes that take place during the processing of polymer mixtures are based on the well-known principles of colloidal chemistry. Melts of polymer mixtures are dispersed systems that have a number of special properties [69,127]. However, theoretical studies in the mechanics of dispersed systems show that the same approaches of classical mechanics and structural models that are used in modeling systems such as suspensions, emulsions, and colloidal solutions can be chosen to describe

the rheological behavior of melts of polymer mixtures [130-132].

2.2.1. Mathematical methods of modeling the rheological behavior of dispersed systems. Much attention is paid to the study of the flow characteristics of dispersed systems, as it contributes to a better understanding of the technological processes that take place during their processing. To date, a large amount of experimental data has been accumulated, on the basis of which a number of empirical dependencies have been formulated. The latter make it possible to characterize with sufficient accuracy some important features of the rheological behavior of dispersed systems. Theoretical models are also proposed. However, in general, in the mechanics of dispersed systems, there is a noticeable lag between theoretical research and experimental research.

Any theoretical research on the creation of mathematical models begins with the establishment of rheological equations of state, which connect the stress tensor in the suspension with the kinematic characteristics of the flow and make it possible to close the system of equations of motion obtained on the basis of the general laws of mechanics. Two approaches are used to construct the rheological equations of state of dispersed systems: phenomenological (macroscopic), structural (microscopic), and in recent years, their unification – structural-phenomenological. The phenomenological approach is based on the assumption that the environment is continuous and homogeneous. The equations of state with this approach are created on the basis of the general laws of classical mechanics and phenomenological thermodynamics under

certain assumptions regarding the properties of the environment (instability, isotropicity, elasticity, etc.). The use of modern methods of mathematics - tensor analysis, group theory, functional analysis allows obtaining the dependence of the stress tensor on kinematic parameters and other characteristics that determine the nature of the flow in a fairly general form, which is undoubtedly a strong point of the phenomenological approach [146,147]. The structural approach describes the rheological properties of systems based on the study of the flow behavior of their constituent elements. At the same time, the macroscopic characteristics of dispersed systems are expressed by averaging the parameters of the microstructure and dispersion medium. The first work in which a structural approach was used to study the behavior of dilute suspensions was a study by Einstein. He proposed an equation for determining the effective viscosity (μef) of the suspension:

$$\mu_{e\phi} = \mu \left(1 + 2{,}5\ \varPhi\right)$$

where Φ - is the volume concentration of suspended particles

Einstein's energy approach was widely used by other authors to determine the μ_{ef} of dilute suspensions with particles of different geometric shapes [127,128]. The disadvantage of this method is that, by determining the scalar function - viscosity in one or another flow, it is impossible to answer the main question - what is the form of the rheological equation of the suspension state. The dynamic method of Landau [128] is also used to study the behavior of dispersed systems from the standpoint of a structural approach, in which velocity and pressure disturbances introduced into the flow of a dispersed

medium by a suspended particle are used to find the stress tensor caused by these disturbances. With the use of the specified method, the rheological equations of state of diluted suspensions of hard spherical particles [146] and concentrated dispersed systems with hard and deformable particles [146,147] were obtained. The most widespread hydrodynamic models of the microstructure of suspensions of rigid particles are spheres, one-dimensional "dumbbells", cylindrical sticks, ellipsoids, disks, and for deformable suspended particles - elastic and viscoelastic spheres and ellipsoids [146,147]. The strength of the structural approach is that, with the selected particle model, all quantities included in the rheological equation of state are determined theoretically as functions of the parameters characterizing the microstructure and dispersion medium. But the structural approach has its weaknesses: Einstein's energy method allows you to find only the effective viscosity of a dispersed system in the simplest flow; the dynamic Landau approach leads to rather cumbersome equations and calculations, which makes it ineffective when constructing the equations of state of systems that have a complex microstructure.

The strengths of the considered methods complement each other, which indicates the expediency of combining them when creating rheological equations of state of complex environments [20,67,68]. The structural-continuum approach is based on the use of phenomenological models of the structural continuum, which contain the necessary number of internal parameters to describe the behavior of the microstructure of the dispersed system. The structural continuum is a model of a

continuous medium, in which, under the basic assumptions of continuum mechanics (continuity, inseparability of functions characterizing the movement and state of the medium), the peculiarities of changes in the microstructure of the dispersed phase and their influence on the rheological properties of the dispersion are taken into account. If in classical mechanics each point of the continuum is characterized by density, speed and pressure, then in the structural continuum, along with the listed indicators, there are also so-called internal parameters. Thus, unlike the continuum of classical mechanics, the structural continuum has additional degrees of freedom, which are used to take into account the peculiarities of the behavior of the dispersion microstructure. Internal parameters can be: scalars, vectors, tensors; their number and type are determined by the nature of the microstructure of the dispersed phase. Thus, when constructing phenomenological models of the structural continuum for suspensions of rigid and deformable particles, the choice of internal parameters is determined by the need to introduce the influence of the orientation of suspended particles, their hydrodynamic interaction and deformation into the rheological equations. In the case of dilute suspensions, the orientation and deformation of particles that have symmetry relative to an axis and a plane perpendicular to it are modeled by only one internal parameter, a vector [159]. The position of the vector in space will characterize the dependence of the rheological properties of the medium on the direction (anisotropy), and the modulus of the vector - the deformation of particles in the flow. A deformable ellipsoid of rotation, which has internal viscosity and elasticity, was considered as a

model of a suspended particle. At the same time, it was assumed that in the process of interaction with the dispersion medium, the particle changes its size, but its shape remains an ellipsoid of rotation, which retains its volume. Conducted studies of the behavior of a deformable ellipsoidal particle in an inhomogeneous flow of a Newtonian fluid showed that the deformability of a suspended particle complicates the rheological equations of state of diluted suspensions. Although the form of the equations is similar to the rheological equations of state of rigid particles, they differ significantly in content. Instead of rheological constants, these equations contain rheological functions that are included in the quantities to be averaged.

A dilute suspension of ellipsoidal particles is the most common hydrodynamic model of deformable asymmetrically elongated particles in a Newtonian fluid. Under the condition of a non-Newtonian dispersion medium and a different (more complex) geometric shape of a dispersed particle, the possibility of obtaining rheological equations of state of such dispersions is complicated due to the complexity of the analytical solution of the problem of hydrodynamic interaction of the particle with the environment. Therefore, the authors of [160] proposed to use a deformable triaxial dumbbell as a hydrodynamic model of the particle. Such models are three-dimensional and do not have the disadvantages of classical models. When using the specified models, rheological equations of state of diluted suspensions of deformable particles were obtained, which can be generalized to dispersed systems with particles of more complex geometry. Thus, the

structural-phenomenological approach makes it possible to describe the rheological properties of polymer dispersions in a fairly general way, taking into account their microrheological characteristics.

The analysis of the literature shows that compatibilization is widely used to modify the properties of melts of polymer mixtures and products made from them. Research in recent years has shown that the introduction of compatibilizers also contributes to the improvement of specific fiber formation. However, these data are very limited. One of the most researched are mixtures based on PP, due to the complex of its valuable properties. On the other hand, since PP is thermodynamically incompatible with most polymers, compatibilizers are introduced into its mixture to ensure high homogeneity of dispersions, their stability, and to improve adhesion at the boundary of phase separation. Polypropylene fibers formed according to traditional technology are characterized by low density, high specific volume and area, the highest speed of moisture transport due to a special capillary structure, high heat and sound insulation characteristics, dirt and dust repellency. All properties are enhanced in PP microfibers due to the unique structure of their surface. The use of organosilicon liquids as compatibilizers is interesting from a scientific and practical point of view, since they are physically and chemically inert substances that are resistant to high temperatures even in oxidizing environments. Siloxane liquids do not mix with most organic substances and, provided they are introduced in an amount of $\approx$ 10-4%, are displaced onto the surface of the phase separation and, due to

their low surface tension, are well distributed over the entire surface. There is no information in the literature about the use of siloxanes for the compatibilization of polymer mixtures and the improvement of specific fiber formation. To date, numerical data on research and processing technology of polymer mixtures have been accumulated, but most of them can be characterized as empirical. There is a gap between theoretical research and experimental research. It is expedient to create models to describe the characteristics of the behavior of polymer dispersions using the structural-continuum approach.

Proceeding from the above, the tasks of implementing specific fiber formation in polypropylene/co-polyamide mixtures of composition 40/60 are set in the work; 50/50 wt.%, further reduction of the diameter of PP microfibers, creation of mathematical models to describe the behavior of polymer dispersions, and development of thin-fiber materials with a complex of new characteristics are relevant, and their solution has scientific and practical significance. The problems can be solved by influencing the interfacial region in the direction of reducing surface tension and improving interfacial adhesion. The use of compatibilizers and their binary mixtures is a real way to achieve the goal.

*2.2.2. A **mathematical model for determining the effective melt viscosity of a polymer mixture in a simple shear flow.*** Among the various properties of melts of polymer mixtures, the most important in practical terms is the effective viscosity of the melt, so the task of the work was to create a mathematical model for determining the effective viscosity of

melts of polymer mixtures in a simple shear flow, using the structural-continuum approach.

We have made the assumption that the dispersion medium is a Newtonian liquid, and the volume concentration of suspended particles (droplets) is so small that their hydrodynamic interaction can be ignored. A drop of a polymer of the dispersed phase was modeled by a deformable ellipsoid of rotation, since this model is relatively simple and allows solving the hydrodynamic problem of the flow around such a particle by an inhomogeneous flow of a Newtonian fluid. The rheological state of the investigated dispersion was described by an equation derived from the structural-continuum approach for dilute suspensions with ellipsoidal deformable particles. The rheological equation has the form:

$$T_{ij} = -p\delta_{ij} + 2\langle \psi_0 d_{ij} + \psi_1 n_i n_j \rangle + \langle \psi_2 n_k n_m n_i n_j \rangle d_{km} + 2\langle \psi_3 (d_{ik} n_k n_j + d_{jk} n_k n_i \rangle$$

(2.30)

where T_{ij} – stress tensor;

p – isothermal pressure;

δ_{ij} – the Kronecker symbol;

$$\psi_0 = \mu(1 + \frac{\Phi}{ab''\alpha_0^I});$$

$$\psi_1 = \frac{4G\Phi(q/q_0)^{2/3}(1 - q_0/q)}{a(2 + 3ab^2\beta_0''\eta/\mu)};$$

$$\psi_2 = \frac{2\mu\Phi}{a^5 b^2}(\frac{\alpha_0'' + \beta_0''}{b^2\alpha_0^I\beta_0''} - \frac{4}{(a^2 + b^2)\beta_0^I} - \frac{2}{\beta_0''(2 + 3ab^2\beta_0''\eta/\mu)})$$
;

$$\psi_3 = \frac{\mu\Phi}{a^3 b^4}\left(\frac{2b^2}{(a^2+b^2)\beta_0{}^I} - \frac{1}{\alpha_0{}^I}\right);$$

$d_{km}, d_{ij}, d_{ik}, d_{jk}$ – strain rate tensors;

n_i – vector $\vec{n}_i$ coordinates ;

a, b, a_0, b_0 – semi-axes of the ellipsoid in the deformed and undeformed state;

G – modulus of elasticity of the dispersed phase;

μ – viscosity of dispersion medium;

η – viscosity of the dispersed phase;

$$q = \frac{a}{b}; \quad q_0 = \frac{a_0}{b_0};$$

Φ – volume concentration of the dispersed phase;

‹...› – means averaging using the distribution function (F) over the angular positions and lengths of the semi-axis of rotation of the weighted particle and satisfies the equation:

$$\frac{dF}{dt} + \frac{d(F\dot{n}_i)}{dn_i} = 0$$

where the dot means time differentiation.

The values $\alpha 0,\ \beta 0,\ ,\ \acute{\beta} 0',\ \alpha o'',\ \beta o''$- are defined in [161]. In equation (2.30), repeating indices mean summation from 1 to 3 by this index.

This equation has one internal parameter - the vector $\vec{n}_i$, which is related to the element of the microstructure - the weighted deformable particle. The vector depends on the nature of the medium flow and can change in space and time. The direction of the vector coincides with the direction of the

axis of symmetry of the ellipsoid, and its modulus is with the length of the semi-axis of rotation (a), i.e. $|\vec{n}_i| = a$.

Consider the behavior of a suspended particle under the condition of a simple shear flow of a diluted suspension. Let no forces act on the particle except hydrodynamic forces. In the case when the suspended particles have relatively large sizes, the influence of Brownian forces on the behavior of the microstructure can be neglected. At the same time, the rheological properties of diluted suspensions are completely determined by the nature of the microstructure. To characterize the microproperties of the dispersion, it is necessary to know the distribution of suspended particles by angular position and the length of the semi-axis of rotation of the suspended particle. The equations of motion and deformation of the semi-axis of rotation of a suspended particle in a simple shear flow are given by the authors [162-165]:

$$(q^2 + 1)\frac{d\theta}{dt} = \dot{\gamma}\frac{q^2 - 1}{4}\sin 2\varphi \sin 2\theta$$

$$(q^2 + 1) = \frac{d\varphi}{dt} = \dot{\gamma}(q^2\cos^2\varphi + \sin^2\varphi) \qquad (2.31)$$

$$\frac{dq}{dt} = -\frac{3Gab^2\beta_0^{''}q(q/q_0)^{2/3}(1 - q_0/q)}{\mu(2 + 3ab^2\beta_0^{''}\eta/\mu)} + \dot{\gamma}\frac{3q\sin 2\varphi \sin^2\theta}{2(2 + 3ab^2\beta_0^{''}\eta/\mu)}$$

where: θ and φ – angles of the cylindrical coordinate system; φ – the angle between the Ox axis and the projection of the axis of rotation of the ellipsoidal particle onto the xOy

plane; θ – the angle between the Oz axis and the axis of rotation of the particle; $\dot{\gamma}$ – shear rate.

Using the above developments, we will proceed to the creation of a model for determining the effective viscosity of melts of polymer mixtures in a simple shear flow. Let an ellipsoidal particle pass through its undeformed state at some point in time $t = 0$ in the process of movement, i.e.:

$$q = q_0, \quad \varphi = \varphi_0, \quad \theta = \theta_0 \text{ at } t = 0,$$

where: φ_0, θ_0 – unknown angles that characterize the angular position of the particle at time $t=0$ at $q=q_0$.

In order to simplify the solution of the system of equations (2.31), we will convert them into a dimensionless form, for this we will choose $1/\dot{\gamma}$ as the time scale. Then the system of equations of motion and deformation of the suspended particle will have the form:

$$(q^2 + 1)\frac{d\theta}{dt^I} = \frac{q^2 - 1}{4} \sin 2\varphi \sin 2\theta$$

$$(q^2 + 1) = \frac{d\varphi}{dt^I} = q^2 \cos^2 \varphi + \sin^2 \varphi \qquad (2.32)$$

$$\varepsilon \frac{dq}{dt^I} = -\frac{3ab^2 \beta_0^{II} q(q/q_0)^{2/3}(1 - q_0/q)}{2 + 3ab^2 \beta_0^{II} \eta / \mu} + \varepsilon \frac{3q \sin 2\varphi \sin^2 \theta}{2(2 + 3ab^2 \beta_0^{II} \eta / \mu)}$$

where: ε is the dimensionless shear rate; $\varepsilon = \dot{\gamma} \, \mu / G$

$t^I = t * \dot{\gamma}$ - dimensionless time;

The parameter ε characterizes the ratio of hydrodynamic forces to the forces of internal elasticity of the particle. The system of equations (2.32), which describe the

orientation and deformation of suspended drops, under the condition $\varepsilon = 0$, has a periodic solution over t^I:

$$q^{(0)} = q_0, \quad tg\varphi^{(0)} = q_0 tg(t^I q_0 /(q_0^{\,2} + 1))$$

$$tg\theta^{(0)} = cq_0 /(q_0^{\,2} \cos^2 \varphi^{(0)} + \sin^2 \varphi^{(0)})^{1/2}$$

where: c is the "orbit constant" that determines the location of the plane in which the rigid particle rotates; $c = tg\theta_0$; the index in parentheses above means the approximation number.

The authors of [vjz engl] established that if the system of equations of type (2.32) has a periodic solution at $\varepsilon = 0$, then the general solution of equations of this type can be represented in the form of asymptotic series in powers of ε. Based on this, to find $q, \varphi, \theta,$ in accordance with [166,167], we obtain:

$$q = \sum_{m=0}^{\infty} \varepsilon^m q^{(m)} \; ; \; \theta = \sum_{m=0}^{\infty} \varepsilon^m \theta^{(m)} \; ;$$

$$\varphi = \varphi_0 + \sum_{m=0}^{\infty} \varepsilon^m \varphi^{(m)} \qquad (2.33)$$

$$\varphi_0 = \sum_{m=0}^{\infty} \varepsilon^m \varphi_0^{\,(m)}$$

By substituting (2.33) into (2.32) and performing simple transformations, we obtained a system of three equations for finding $q^{(m)}, \varphi^{(m)}, \theta^{(m)}$.

$$(q^{(0)2} + 1)\frac{d\theta^{(0)}}{dt^I} = \frac{q^{(0)2} - 1}{4}\sin 2\varphi^{(0)} \sin 2\theta^{(0)} \; ;$$

$$(q^{(0)2} + 1)\frac{d\varphi^{(0)}}{dt^I} = q^{(0)2} \cos^2 \varphi^{(0)} + \sin^2 \varphi^{(0)} \; ; \quad (2.34)$$

175

$$\frac{3ab^2\beta_0^{\,II}q^{(0)}(q^{(0)}/q_0)^{2/3}(1-q_0/q^{(0)})}{2+3ab^2\beta_0^{\,II}\eta/\mu}=0$$

with initial conditions: $q^{(0)}=q_0;\varphi_0=0;\theta^{(0)}=\theta_0$ at $t^I=0$

The system of equations (2.34) is a mathematical model describing the behavior of a dispersed system in a simple shear flow. Moreover, the equations for determining $\varphi^{(m)}$, $\theta^{(m)}$ are differential, and those for $q^{(m)}$ are algebraic. We write the initial conditions for these systems of equations in the form:

$$q^{(m)}=0, \qquad \theta^{(m)}=0, \qquad \varphi^{(m)}=\varphi_0^{(m)}, \qquad \text{при } m\geq 1,$$
$$q^{(0)}=q_0, \qquad \theta^{(0)}=\theta_0 \qquad \varphi^{(0)}=0, \qquad \text{при } m=0.$$

The values of the unknown angles $\varphi_0^{(m)}$ were determined in such a way as to satisfy the initial conditions of $q^{(m)}$.

In the case when the suspended particle in the undeformed state had a spherical shape, i.e. $q_0=1$, we have:

$$q^{(1)}=\frac{15}{8}\frac{c^2}{c^2+1}\sin 2\varphi^{(0)}$$

$$\varphi^{(1)}=\frac{15}{32}\frac{c^2}{c^2+1}\sin 2\varphi^{(0)} \qquad (2.35)$$

$$\theta^{(1)}=\frac{15}{16}\frac{c^3}{(c^2+1)^2}(\varphi^{(0)}-\frac{1}{4}\sin 4\varphi^{(0)})$$

$$\varphi_0^{(1)}=\frac{5}{4}+\frac{1}{2}\eta/\mu$$

The higher-order approximation of ε in expansions (2.34) can be determined similarly. In the general case, the findings $q;\varphi;\theta$ from the system of equations (2.32) describing the behavior of a suspended particle in the shear flow of a

dispersion will depend on the parameters $t^{I}; c$ that characterize the properties of the polymer of the dispersed phase in the flow conditions.

Determining the distribution function of the "orbital constant" s with the assumption that Brownian motion can be neglected, similarly to works [162-165], we finally have an expression for determining the effective viscosity of the dispersion μ_{ef}:

$$\mu_{эф} = \langle \psi_0 \rangle + \frac{1}{4} \langle \psi_2 n^4 \sin^2 2\varphi \sin^4 \theta \rangle + \langle \psi_3 n^2 \sin^2 \theta \rangle + \frac{1}{2\dot{\gamma}} \langle \psi_1 n^2 \sin 2\varphi \sin^2 \theta \rangle$$

(2.36)

where $n = r_0 q^{2/3} (r_0^3 = ab^2); \; q, \varphi, \theta$ are calculated from equations (2.33) ; $\langle \; \rangle$ - means the averaging of values using the distribution function 'orbital constant'.

In order to simplify expression (2.36), let's decompose it into a Taylor series by degrees of volume concentration. Keeping only the first two terms of the Taylor series, we obtain the following equation:

$$\mu_{еф} = \mu + v\mu\Phi + ...$$ (2.37)

The coefficient (v) near μ in the linear term of the series is called the viscosity increment. Due to the fact that the theory was developed for dilute suspensions, a correction factor k was introduced, based on the reasoning that the viscosity increment of the polymer mixture melt coincides with ν of the dispersion medium at zero shear rate. The viscosity increment was determined from the expression:

$$v = k(\mu_{еф} - \mu)/\mu \; \Phi$$

177

In order to check the adequacy of the obtained mathematical model for determining the effective melt viscosity of polymer mixtures, the theoretical dependence of the viscosity increment (v) on the dimensionless shear rate (ε) was constructed and compared with the experimental dependences. For the calculations, data on the effective viscosity of melts of polyoxymethylene/polycaproamide (POM/PCA) mixtures and POM/copolyamide (SPA) were used for the calculations. The choice of these mixtures is due to the fact that the nature of the flow of the PKA melt (dispersion medium) is close to Newtonian. SPA in the viscous-fluid state also has a slight deviation from the flow of a Newtonian fluid. Figure 2.19 shows the theoretical curve $v = f(\varepsilon)$, obtained on the basis of relations (2.33), (2.35), (2.36) under the condition $q_0 = 1$ and $\eta/\mu = 1$, as well as experimental results.
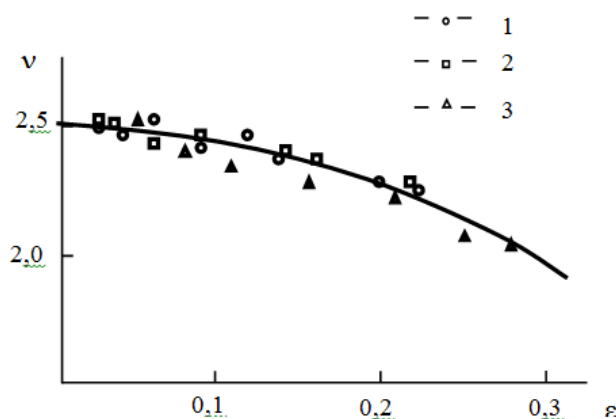
Fig. 2.19. Dependence of the viscosity increment on the dimensionless shear rate: the curve is the theoretical dependence at $q=1$; $\eta/\mu = 1$; points 1-3 correspond to POM/PKA mixtures of composition 4/96; 8/92 and POM/SPA – 16/84% vol.

178

It can be seen from Fig. 2.19 that for POM/PKA mixtures with volume concentrations of the dispersed phase (POM) of 4 and 8%, the theoretical and experimental dependences agree well with each other. At the same time, the correction coefficients are insignificant (1.04 and 1.98, respectively). For a POM/SPA mixture of 16/84% vol. the nature of the dependence remains, however, the correction factor increases to 8.93, there is a slight deviation from the theoretical dependence. This is related both to the hydrodynamic interaction between the droplets of the dispersed phase, which manifests itself when the concentration of the dispersed phase increases, and to the more non-Newtonian flow regime of the SPA. The obtained results testify to the correctness of the selected approaches and the obtained mathematical model.

Thus, for the first time, a mathematical model was created for determining the effective viscosity of melts of polymer mixtures from the standpoint of the structural-continuum approach, which adequately describes the processes in real polymer mixtures.

Using the structural-continuum approach, a mathematical model of the deformation of a polymer droplet of the dispersed phase during the flow of the melt mixture in the entrance zone of the forming hole was developed. The resulting system of differential equations satisfactorily describes the processes of deformation of droplets (q) of the dispersed phase: the quantity q is a function of the absolute values of the viscosities of the initial components and their ratio, the volume concentration of the polymer of the dispersed phase, and the value of the interfacial tension. Through the modulus of

elasticity, the effect of elasticity on the quantity q is taken into account. Comparison of the values of droplet deformation calculated using the created model with experimental data confirmed the adequacy of the model.

A mathematical model was created to determine the effective melt viscosity of a mixture of polymers in a simple shear flow. The model takes into account the influence of the viscosity of the initial components and their ratio, the elasticity and volume concentration of the polymer of the dispersed phase, the deformation of the droplets and their coordinates in the flow on the value of the effective viscosity. The adequacy of the developed model is confirmed by the satisfactory ratio of calculated and experimental data on the viscosity of melts of polymer mixtures.

REFERENCES

1. Hassan T., Salam A., . Khan A. Functional nanocomposites and their potential applications: a review. Springer Science and Business Media. 2021.

2. M. S. Saharudin, S. Hasbi, M. N. A. Nazri, F. Inam. A review of recent developments in mechanical properties of polymer–clay nanocomposites – Springer Science and Business Media Deutschland GmbH, 2020.

3. Muzata T. S. Nanoparticles influence miscibility in lcst polymer blends: from fundamental perspective to current applications / T. S. Muzata, P. L. Jagadeshvaran, S. Bose. – Royal Society of Chemistry, 2020.

4. Utraki L.A., Wilkie Ch.A. Polymer blends handbook.: monograph. London: Springer New York Heidelberg Dordrecht, 2014. 2373 p.

5. W. Khan, R. Sharma, P. Saini. Carbon Nanotube-Based Polymer Cjmposites: Synthesis, Properties and Applications, 2016.
DOI: 10.5772/62497

6. Biopolymer-clay nanocomposites as novel and ecofriendly adsorbents for environmental remediation /Orta M.M. et al; by edit. M.M. Orta. Elsevier Ltd, 2020.

7. Biomedical Applications of Polymeric Nanofibers // by editors R. Jayakumar, Shantikumar V.Nair. – New York: Springer. – 2012. – 283 p.

8. Kausar A. Flame retardant potential of clay nanoparticles. In book: Clay Nanoparticles: Properties and Applications, Chapter: 7. Elsevier Ltd, 2020.
DOI:10.1016/B978-0-12-816783-0.00007-4

9. N. Chandran, C. Sarathchandran, S. Thomas. Rheology of Polymer Blends and Nanocomposites: Theory, Modelling and Applications. — Elsevier, 2019.

10. Agrawal P. Rheological and mechanical properties of poly(lactic acid)/bio-based polyethylene/clay biocomposites containing montmorillonite and vermiculite clays / P. Agrawal, A. P. M. Araujo, G. F. Brito[et al.] // Journal of Polymers and the Environment. — 2021. — P. 1–12.

11. Ahn J. H. Synergistic toughening effect of hybrid clay particles on poly(lactic acid)/natural rubber blend / J. H. Ahn, J. S. Hong, K. H. Ahn // Polymer Composites. — 2020. — P. pc.25883.

12. Silva G. E. H. da Effect of adding modified clays on the mechanical behavior of pc/abs polymer blend / G. E. H. da Silva, J. E. Granada, C. C. N. Melo[et al.] // Macromolecular Symposia. — 2020. — Vol. 394, No. 1. — P. 2000145.

13. Dhanumalayan E. Enhanced structure, dielectric, and thermal properties of attapulgite clay and hexagonal boron nitride admixture loaded polymer blends / E. Dhanumalayan, S. Kaleemulla // Journal of Materials Science: Materials in Electronics. — 2020. — Vol. 31, No. 20. — P. 17828–17842.

14. Mooninta S. Packaging film of pp/ldpe/pla/clay composite: physical, barrier and degradable properties / S. Mooninta, S. Poompradub, P. Prasassarakich // Journal of Polymers and the Environment. — 2020. — Vol. 28, No. 12. — P. 3116–3128.

15. Achutha U. Kini, Manjunath Shettar. A technical review on epoxy-nanoclay nanocomposites: Mechanical, hygrothermal and wear properties // Cogent Engineering, 10(2), 2257949 - September 2023
https://doi.org/10.1080/23311916.2023.2257949

16**.** Christopher Igwe Idumah. Recent advancements in fire retardant mechanisms of carbon nanotubes, graphene, and fullerene polymeric nanoarchitectures **//** Journal of Analytical and Applied PyrolysisVolume 174, September 2023, 106113
https://doi.org/10.1016/j.jaap.2023.106113

17. Multilayered Composites with Carbon Nanotubes for Electromagnetic Shielding Application // Polymers 2023, *15*(4), 1053;
https://doi.org/10.3390/polym15041053

18. Waseem Khan, Rahul Sharma, Parveen Saini. Carbon Nanotube-Based Polymer Cjmposites: Synthesis, Properties snd Applications. // Materials Science,Engineering, Chemistry. - 2016
 DOI: 10.5772/62497

19. Wu M.L., Chen Yu., Zhang L., Zhan H., Qiang L., Wang J.N. High-Performance Carbon Nanotube/Polymer Composite Fiber from Layer-by-Layer Deposition. *ACS Appl. Mater. Interfaces*. 2016. Vol.8, №12. P.8137-8144.

https://doi.org/10.1021/acsami.6b01130

20. Rezanova N.M., Meĺnik I.A., Tsebrenko M.V., Korshun A.V. Preparation of Nano-Filled Polypropylene Microfibers // Fibre Chemistry. – 2014. – V.46. – P. 21-27.

21. Резанова Н.М., Савченко Б.М., Плаван В.П., Булах В.Ю., Сова Н.В Закономірності одержання нанонаповнених полімерних матеріалів з матрично-фібрилярною структурою // Наносистеми, наноматеріали, нанотехнології. – 2017.– Т.15, №3. – С.559-57121

22. Rezanova V.G., Rezanova N.M. CNT-filled polypropylene / plasticized polyvinyl alcohol mixtures: rheology, morphology, and properties of composite threads // Наносистеми, наноматеріали, нанотехнології. – 2023. – Т. 21, Вип. 2. – С. 349-361. https://www.imp.kiev.ua/nanosys/en/articles/2023/2/nano_vol21_iss 2_p0349p0361_2023_abstract.html

23. Oluwafemi S Obisesan, Timothy O Ajiboye , Sabelo D Mhlanga. Biomedical applications of biodegradable polycaprolactone-functionalized magnetic iron oxides nanoparticles and their polymer nanocomposites // Colloids and Surfaces B Biointerfaces, 227, 113342 - May 2023 https://doi.org/10.1016/j.colsurfb.2023.113342

24. Subashini K, Prakash S, Sujatha V Biological applications of green synthesized zinc oxide and nickel oxide nanoparticles mediated poly(glutaric acid-co-ethylene glycol-co-acrylic acid) polymer nanocomposites. Inorg Chem Commun 139:109314. 2022 https://doi.org/10.1016/j.inoche.2022.109314

25. Plavan V.P., Rezanova V.G., Budash Yu.O., Ishchenko O.V., Rezanova N.M. Influence of aluminum oxide nanperticles on formation of the structure and mechanical properties of microfibrillar composites. *Mechanics of Composite Materials*. 2020. Vol.56, № 3. P.1-14.

26. Podstawczyk D., Skrzypczak D., Połomska X., Stargała A., Witek-Krowiak A., Guiseppi-Elie A., Galewski Z. Preparation of antimicrobial 3D printing filament: In situ thermal formation of silver nanoparticles during the material extrusion. *Polym. Compos.* 2020. №41. P.4692-4705.

27. Fakoori E., Karami, H. Preparation and Characterization of ZnO-PP Nanocomposite Fibers and Non-Woven Fabrics. *J. Text. Inst.* 2018. Vol.109, №9. P.1152-1158.

28. Vandana Bhandari, Seiko Jose, Pratikhya Badanayak, Anuradha Sankaran and Vysakh Anandan Antimicrobial Finishing of Metals, Metal Oxides, and Metal Composites on Textiles: A Systematic Review. *Ind. Eng. Chem. Res.* 2022. Vol. 61, №1. P.86-101
https://doi.org/10.1021/acs.iecr.1c04203

29. Stephen Strassburg , Kai Mayer and Thomas Scheibel. Functionalization of biopolymer fibers with magnetic nanoparticles // Physical Sciences Reviews, 118, 2020
Doi.org/10.1515/psr-2019-0118

30. Perera, AS, Zhang, S, Homer-Vanniasinkam, S, Coppens, MO, Edirisinghe, M. Polymer-magnetic composite fibers for remote-controlled drug release. *ACS Appl Mater Interfaces* 2018;10:15524.
https://doi.org/10.1021/acsami.8b04774.

31. Sabiha Sultana, Mohammed A. Gondal, Amir Naveed. Copper Nanoparticles Doped on Polyvinyl Alcohol/Polymethyl Methacrylate/Montmorillonite (PVA-PMMA/MMT) as Ecofriendly Polymeric Hybrid Clay Composites: Study of their Bactericidal and Physical Properties // Arabian Journal for Science and Engineering, 1-9. August 2023
https://doi.org/10.1007/s13369-023-08164-2

32. A. Singh , S. Thakur. Recent advancements in the fabrication of transition metal dichalcogenides-polymer nanocomposites: Focused on molybdenum diselenide for various applications // Materials Today Chemistry, 30, 101562 - June 2023
https://doi.org/10.1016/j.mtchem.2023.101562

33. Rasana Nanoth, K. Jayanarayanan, P. Sarath Kumar . Static and dynamic mechanical properties of hybrid polymer composites: A comprehensive review of experimental, micromechanical and simulation approaches // Composites Part A Applied Science and Manufacturing, 174, 107741 - November 2023
https://doi.org/10.1016/j.compositesa.2023.107741

34. Kanjwal M.A., Barakat N.M., Shceikh F.A., Balk W., Khil M.S., Kim H.Y. Efect of silver Content and Morphology on the catalic Activity of Silver-grafted Titanium Oxide Nanostructure // Fibers and Polymers. – 2010. – V. 11, N5. – P. 700-709.

35. Hassan M.S. Bimetallic Zn/Ag doped polyurethane spider net composite nanofibers: a novel multipurpose electrospun mat. *Ceram Int.* 2013. Vol.39, №3, P.2503-2510.

36. Bagchi B., Kar S., Dey S. Kr. et al. *In situ* synthesis and antibacterial activity of copper nanoparticle loaded natural montmorillonite clay based on contact inhibition and ion release // Colloids Surf., B. – 2013. – V. 108. – P. 358–365.

37. *Demirci S., Ustaoğlu Z., Yılmazer G.A. et al.* Antimicrobial Properties of Zeolite-X and Zeolite-A Ion-Exchanged with Silver, Copper, and Zinc Against a Broad Range of Microorganisms // Appl. Biochem. Biotechnol. – 2014. – V. 172, N 3. – P. 1652–1662.

38. Structural, optical and catalytic properties of $ZnO-SiO_2$ colored powders with the visible light-driven activity // Journal of Photochemistry and Photobiology A: Chemistry**,** Volume 421**,** 1 December 2021, 113532 https://doi.org/10.1016/j.jphotochem.2021.113532

39. Borysenko M.V., Gun'ko V.M., Dyachenko A.G., Sulim I.Y., Leboda R., Skubiszewska-Zieba J., Ryczkowski J. CVD-zirconia on fumed silica and silica gel // Applied Surface Science - 2005. - Vol. 242. - P. 1-12.

40. Rezanova N.M., Plavan V.P., Rezanova V.G., Bohatyryov V.M. Regularities of producing of nano-filled polypropylene microfibers. // Vlakna a Textil. 2016. №2. P.3-8.

41. Rezanova N.M., Rezanova V.G., Plavan V.P., Viltsaniuk O.O. The Influence of Nano-Additives on the Formation of Matrix-Fibrillar Structure in the Polymer Mixture Melts and on the properties of Complex threads// *Vlakna a Textil*. 2017. №2. P.37-42.

42. Rezanova N.M, Rezanova V.G., Plavan V.P., Viltsaniuk O. O. Polypropylene fine-fiber filter materials modified with nano-additives. // Functional Materials. 2019. Vol.26, №2. P.389-396.

43. Дзюбенко Л.С., Сап'яненко О.О., Горбик П.П., Плаван В.П., Резанова Н.М., Лутковський Р.А., Вільцанюк О.А. Властивості шовного матеріалу з поліпропілену модифікованого частинками нанорозмірного срібла та кремнезему // Наносистеми, наноматеріали, нанотехнології. – 2018. – Т. 16, № 2, – С. 347-362.

44.Muralisrinivasan N. S. Polymer Blends and Composite //

185

Chemistry and Technology; John Wiley & Sons. – 2017.

45. Isayev A. I. Encyclopedia of Polymer Blends // John Wiley & Sons. – 2016 . – Vol.1

46. Luna M.S., Filippone G. Effects of nanoparticles on the morphology of immiscible polymer blends – Challenges and opportunities. *European Polym. J.* 2016. Vol.79. P. 198-218.

47. Reza S., Hyeong Y.S., Mingeum K., Woo J.C., Kyu H. Morphological Evaluation of PP/PS Blends Filled with Different Types of Clays by Nonlinear Rheological Analysis // Macromol. – 2016.– V. 8, №49. – P.3148-3160.

48. Nuzzo A., Coiai S., Carroccio S. C., Dintcheva N. T., Gambarotti C. Filippone G. Heat-Resistant Fully Bio-Based Nanocomposite Blends Based on Poly(lactic Acid) // Macromol. Mater. Eng. – 2014. – V. 299, № 1. – P. 31-40.

49. Anju Paul, Sreekala S. Sharma . Biopolymer-Based Nanocomposites. In: Sabu Thomas, Ajitha AR, Cintil Jose Chirayil, Bejoy Thomas (Eds.), Handbook of Biopolymers 523-550 - April 2023
https://doi.org/10.1007/978-981-19-0710-4_19

50. Magalhaes N. F., Dahmouche K., Lopes G. K., Andrade C. T. Using an Organically-Modified Montmorillonite to Compatibilize a Biodegradable Blend // Appl. Clay Sci. – 2013. – № 72. – P. 1-8.

51. Guo Yi., He Ch., Yang K., Xue Yu., Zuo X., Yu Yi., Liu Yi., Chang Ch., Rafailovich M. Enhancing the Mechanical Properties of Biodrgradable Polymer Blends Using Tubular Nanoparticle Stitching of the Interfaces // Appl. Mater. Interfaces. – 2016. – V. 8, № 27. – P. 17565-17573.

52. Budash Y., Rezanova N., Plavan V., Rezanova V. Thermally and organomodified montmorillonite as effective regulators of the structure formation process in polypropylene/polystyrene blends. *Polym. and Polym. Composites.* 2022. Vol. 30. P. 1–8

53. Elias L., Fenouillot F., Majeste J.C., Cassagnau PH. Morphology and rheology of immiscible polymer blends filled with silica nanoparticles // Proceeding of 19 Congress Francais de Mecanique. Marseille, August . – 2009.

54. Qi X., Yang J., Zhang N, Huang T., Zuo Z., Kühnert Z., Pötschke P., Wang Y. Selective localization of carbon nanotubes and

its effect on the structure and properties of polymer blends. Progress in Polymer Science, 2021, V. 123, P. 101471.

https://doi.org/10.1016/j.progpolymsci.2021.101471

55. Effect of the Selective Localization of Carbon Nanotubes in Polystyrene/Poly(vinylidene fluoride) Blends on Their Dielectric, Thermal, and Mechanical Properties // Materials and Design 56:807-815

DOI:10.1016/j.matdes.2013.11.073

56. V.G.Rezanova, V.I. Shchotkina Mathematical modeling of dispersed phase drop deformation in nano-filled polymer mixture melts // К.: Вісник КНУТД. – 2015. – № 3 (86). – С. 209-214

57. Gopal Yuvaraj, Manickam Ramesh, Lakshminarasimhan Rajeshkumar. Carbon and Cellulose-Based Nanoparticle-Reinforced Polymer Nanocomposites: A Critical Review // Nanomaterials, 13(11), 1803 - June 2023

https://doi.org/10.3390/nano13111803

58. Mehrnoosh Damircheli, AmirHossein MajidiRad. The Influence of the Dispersion Method on the Morphological, Curing, and Mechanical Properties of NR/SBR Reinforced with Nano-Calcium Carbonate // Polymers, 15(13), 2963 - July 2023

https://doi.org/10.3390/polym15132963

59. Zhang T., Chen X., Guo Z., Hongwei X., Bai Q., Zhang Z.Q. Controlling the selective distribution of hydrophilic silica nanoparticles in polylactide/ethylene-co-vinyl-acetate blends via tailoring the OH surface concentration of silica. // Composites Communications. 2021. Vol. 25.

60. Zhu B., Bai T., Wang P., Wang Y., Liu Ch., Shen Ch. Selective dispersion of carbon nanotubes and nanoclay in biodegradable poly(ε-caprolactone)/poly(lactic acid) blends with improved toughness, strength and thermal stabilityInt. // J. Biol Macromol

doi: 10.1016/j.ijbiomac.2019.10.262

61. Bahrami R., Loblingb T.I., SchmalzbH., Mullerd A., Altstadta V. Synergistic effects of Janus particles and triblock terpolymers on toughness of immiscible polymer blends // Polymer. – 2017. – №. 109. – P. 229-237.

62. Hammache Y. The effect of thermoplastic starch on the properties of polypropylene/high density polyethylene blend

reinforced by nano-clay / Y. Hammache, A. Serier, S. Chaoui // Materials Research Express. — 2020. — Vol. 7, No. 2. — P. 25308.

63. Azubuike L., Sundararaj U. Interface Strengthening of PS/aPA Polymer Blend Nanocomposites via In Situ Compatibilization: Enhancement of Electrical and Rheological Properties. Materials 2021, 14, 4813.

64. Li W., Karger-Koksis J., Schlarb A.K. Dispersion of TiO_2 Particles in $PET/PP/TiO_2$ and $PET/PP/PP$-g-MA/TiO_2 Composites Prepared with Different Blending Procedure // Macromol. Mater. Eng. – 2009. – №.294. – P. 582-589.

65. Li W., Schlarb A.K., Evstatiev M. Study of $PET/PP/TiO_2$ microfibrillar-structured composites: Part 1. Preparation, morphology and dynamic mechanical analysis of fibrillized blends // J. Appl. Polym. Sci. . – 2009. – №.113. – P. 1471-1479.

66. Vu Anh Doan, Masayuki Yamaguchi. Interphase transfer of nanofillers and functional liquid between immiscible polymer pairs // Recent Res. Devel. Mat. Sci. – 2013. – №.10. – P. 59-88.

67. Tsebrenko M.V., Rezanova V.G., Tsebrenko I.A. Polypropylene microfibers with filler in nano state // Chem. & Chem. Technol. – 2010. – V.4, №3. – P. 253-260.

68. Tsebrenko M. V., Rezanova V. G., Tsebrenko I. O. Features of obtaining of polypropylene microfibers with nanosize fillers // Journal of Materials Science and Engineering. – 2010. – V. 4, № 6. – P. 36-44.

69. Резанова Н.М., Цебренко М.В., Мельник І.А., Коршун А.В., Данилова Г.П. Закономірності течії та структуроутворення в розплавах сумішей поліпропілен/полівініловий спирт/ кремнезем // Полімерний журнал. – 2014. – №. 3. – С.183-189.

70. Beloshenko V.A., Plavan V.P., Rezanova N.M., Savchenko B.M., Vozniak I. Production of high-performance multi-layer fine-fibrous filter material by application of material extrusion-based additive manufacturing // The International Journal of Manufacturing Technology. 2019. № 101. P.2681-2688.

71. Beloshenko V., Chishko V., Plavan V., Rezanova N., Savchenko B., Sova N., Vozniak I. Production of Filter Material from Polypropylene/Copolyamide Blend by Material Extrusion-Based Additive Manufacturing: Role of Production Conditions and ZrO_2

Nanoparticles. // 3D Printing and Additive Manufacturing. 2021.Vol. 8, № 4. Р. 253–262.

72. Резанова Н.М., Будаш Ю.О., Плаван В.П. Інноваційні технології хімічних волокон. – К.: КНУТД. – 2017. – 240 с.

73. Rezanova V.G., Rezanova N. M., Viltsanyuk O.O. Software for planning and simulation in research of nano-filled three-component systems. // Nanosistemi, Nanomateriali, Nanotehnologii. 2022. Vol.20, №2. P.423-435.
 https://doi.org/10.15407/nnn.20.02.423

74. Резанова Н.М., Плаван В.П., Дзюбенко Л.С., Сап'яненко О.О., Горбик П.П., Коршун А.В. Структуроутворення у компатибілізованих нанонаповнених розтопах поліпропілен/пластифікований полівініловий спирт // Наносистеми, наноматеріали, нанотехнології. – 2018. – Т. 16, № 1, – С. 55 – 70.

75. Thomas S., Mishra R., Kalarikka N. Micro and nano fibrillar composites (mfcs and nfcs) from polymer blends. – Woodhead Publishing, 2017, 372 p.

76. Резанова В. Г. Резанова Н. М. Програмне забезпечення для дослідження полімерних систем : монографія. Київ: АртЕк, 2020. 358 с.

77. Резанова В.Г., Резанова Н.М. Програмне забезпечення для оптимізації складу багатокомпонентних сумішей. - К.:АртЕк. - 2022. 315 с.

78. Щербань В.Ю., Краснитський С.М., Резанова В.Г. Математичні моделі в САПР. Обрані розділи та приклади використання // К.: КНУТД, 2011. – 219 с.

79. Rezanova V.G., Rezanova N.M. Software for the research of microfibrillar composites. Monograph // Kyiv.:Publishing House ArtEk, 2023. – 269 p.
https://er.knutd.edu.ua/handle/123456789/25040

80. Rezanova V.G., Rezanova N.M. Mathematical Modelling and Software Development to Optimize the Composition of Four-Component Nanofilled Systems // Nanosistemi, Nanomateriali, Nanotehnologii. 2020. Vol. 18, № 4. P. 863–874.

81. Резанова В.Г., Резанова Н.М., Куценко С.І. Свідоцтво про реєстрацію авторського права на твір № 107120 - комп'ютерна програма «АІПЕСС» (Автоматизоване інтерактивне планування

експерименту для сумішевих систем), дата реєстрації 09.08.2021 р.

82. Резанова В.Г., Резанова Н.М., Куценко С.І. Свідоцтво про реєстрацію авторського права на твір № 107121 - комп'ютерна програма «АІПЕССу» (Автоматизоване інтерактивне планування експерименту для сумішевих систем - удосконалена), дата реєстрації 09.08.2021 р.

83. Резанова В.Г., Резанова Н.М. Свідоцтво № 115712 про реєстрацію авторського права на твір Комп'ютерна програма "Визначення реологічних характеристик полімерів та їх сумішей" . Дата реєстрації 12.01.2023

84. Резанова В.Г., Резанова Н.М. Свідоцтво № 116062 про реєстрацію авторського права на твір Комп'ютерна програма "Визначення параметрів формування і збереження мікрофібрилярної морфології в термодинамічно несумісних сумішах полімерів" Дата реєстрації 23.01.2023

85. Резанова В.Г., Резанова Н.М. Свідоцтво № 116063 про реєстрацію авторськог права на твір Комп'ютерна програма "Автоматизована побудова плану експерименту для дослідження чотирикомпонентних сумішей" . Дата реєстрації 23.01.2023

86. 32.Chen C. C., White J. L. Compatibilizing agents in polymer blends: interfacial tension, phase morphology, and mechanical properties. *Polym. Eng. and Sci.* 1993. № 33. P. 923-930.

87. 38. Shi D., Ke Z., Yang J., Gao Y. Wu J., Yin J. Rheology and morphology of reactively compatibilized PP/PA6 blends. *Macromolecules*. 2002. № 35. P.8005-8012.

88. Paul D. R., Bucknall C. B. Polymer blends: monograph. New York: John Wiley&Sons, 2000. 618 p.

89. Idrees Khan , Ibrahim Khan, Khalid Saeed. Polymer nanocomposites: an overview // Smart Polymer Nanocomposites 167-184. – 2023.
https://doi.org/10.1016/b978-0-323-91611-0.00017-7

90. Dimitrios N. Bikiaris. Nanocomposites with Different Types of Nanofillers and Advanced Properties for Several Applications // Appl. Nano 2022, *3*(3), 160-162
https://doi.org/10.3390/applnano3030012

91. Amanda D. de Oliveira, Cesar Augusto Gonçalves Beatrice Polymer Nanocomposites with Different Types of Nanofiller. In book: Nanocomposites - Recent Evolutions (pp.26), Edition: 1, Chapter: 6. IntechOpen. – 2019
DOI:10.5772/intechopen.81329
92. Chu C. C. Advancement in Biodegradation Study and Applications // Biodegradable Polymers. – 2015. – V.1. – P. 22-29.
93. Felton G. P. Biodegradable polymers: Processing, Degradation, and Applications // Nova Science Publishers. – 2011.
94. Guo J., Briggs N., Crossley S., Grady B. P. Morphology of Polystyrene/poly(methyl Methacrylate) Blends: Effects of Carbon Nanotubes Aspect Ratio and Surface Modification // AIChE J. . – 2015. – № 61 (10) . – P. 3500-3510.
95. Qi D., CaoZ., Ziener U. Recent Advances in the Preparation of Hybrid Nanoparticles in Miniemulsions // Adv. Colloid Interface Sci. – 2014. – №211. – P. 47-62.
96. Ba Linh N. T., Min Y. K., Lee B.-T. Hybrid Hydroxyapatite Nanoparticles-Loaded PCL/GE Blend Fibers for Bone Tissue Engineering. J. // Biomater. Sci. Polym. Ed. – 2013. – № 24 (5) . – P. 520-538.
97. Chen G., Li P., Huang Y., Kong M., Lv Y., Yang Q., Li G. Hybrid Nanoparticles with Different Surface Chemistries Show Higher Efficiency in Compatibilizing Immiscible Polymer Blends // Compos. Sci. Technol. – 2014. – №105. – P. 37-43.
98. Taguet A., Cassagnau P., Lopez-Cuesta J.-M. Structuration, Selective Dispersion and Compatibilizing Effect of (Nano)fillers in Polymer Blends // Prog. Polym. Sci. – 2014. – №39 (8) . – P. 1526-1563.
99. .Huang S., Bai L., Trifkovic M., Cheng X., Macosko C. W. Controlling the Morphology of Immiscible Cocontinuous Polymer Blends via Silica Nanoparticles Jammed at the Interface // Macromolecules. – 2016. – №49 (10) . – P. 3911-3918.
100. Bai L., He S., Fruehwirth J. W., Stein A., Macosko C. W., Cheng X. Localizing Graphene at the Interface of Cocontinuous Polymer Blends: Morphology, Rheology, and Conductivity of Cocontinuous Conductive Polymer Composites // J. Rheol. (N. Y. N. Y). – 2017. – №61 (4) . – P. 575-587.
101. Nuzzo A., Bilotti E., Peijs T., Acierno D., Filippone G.

Nanoparticle-Induced Co-Continuity in Immiscible Polymer Blends – A Comparative Study on Bio-Based PLA-PA11 Blends Filled with Organoclay, Sepiolite, and Carbon Nanotubes // Polymer (Guildf) . – 2014. – № 55 (19) . – P. 4908-4919.

102. .Mallick S., Kar P., Khatua B. B. Morphology and Properties of Nylon 6 and High Density Polyethylene Blends in Presence of Nanoclay and PE-G-MA. J. // Appl. Polym. Sci. – 2012. – № 123 (3). – P. 1801-1811.

103. Chow W.S., Mohd Ishak Z.A. Polyamide blend-based nanocomposites: A review // eXPRESS Polymer Letters. – 2015. – V. 9, № 3. – P. 21-232.

104. Ebrahim Jalali Dil, Basil D. Favis. Localization of micro and nano- silica particles in high interfacial tension poly(lactic acid)/low density polyethylene system // Polymer. – 2015. – №77. – P.156-166.

105. Fenouillot F., Cassagnau P., Majeste J.C. Uneven distribution of nanoparticles in inmiscible fluids: Morfology development in polymer blends // Polymer – 2009. – V.50, № 6. – P. 1333-1350.

106. Vandebril S., Vermant J., Moldenaers P., Lawson D. W., Leal-Calderon F., Bernreitner K., Rafailovich M. H., Brédas J. L. Efficiently Suppressing Coalescence in Polymer Blends Using Nanoparticles: Role of Interfacial Rheology // Soft Matter. – 2010. – №6 (14) . – P. 3353-3362.

107. Yu F., Huang H.-X. Simultaneously Toughening and Reinforcing Poly(lactic Acid)/thermoplastic Polyurethane Blend via Enhancing Interfacial Adhesion by Hydrophobic Silica Nanoparticles // Polym. Test . – 2015. – № 45. – P. 107-113.

108. Wang X., Feng X., Ma G., Yao L., Ge M. Amphiphilic Janus Particles Generated via a Combination of Diffusion-Induced Phase Separation and Magnetically Driven Dewetting and Their Synergistic Self-Assembly // Adv. Mater. – 2016. – № 28 (16) . – P. 3131-3137.

109. Bahrami R., Löbling T. I., Schmalz H., Müller A. H. E., Altstädt V. Synergistic Effects of Janus Particles and Triblock Terpolymers on Toughness of Immiscible Polymer Blends // Polymer (Guildf). – 2017. – № 109. – P. 229-237.

110. Gomez-Solano J. R., Blokhuis A., Bechinger C. Dynamics of Self-Propelled Janus Particles in Viscoelastic Fluids // Phys. Rev. Lett. – 2016. – № 116 (13) . – P. 138-301.

111. Zou Z.-M., Sun Z.-Y., A. L.-J. Effect of Fumed Silica Nanoparticles on the Morphology and Rheology of Immiscible Polymer Blends. // Rheol. Acta. – 2014. – №53 (1) . – P.43-53.

112. Filippone G., Acierno D. Clustering of Coated Droplets in Clay-Filled Polymer Blends. // Macromol. Mater. Eng. – 2012. – №297 (9) . – P. 923-928.

113. Chen Y., Yang Q., Huang Y., Liao X., Niu Y. Influence of Phase Coarsening and Filler Agglomeration on Electrical and Rheological Properties of MWNTs-Filled PP/PMMA Composites under Annealing. // Polymer (Guildf) . – 2015. – №79. – P. 159-170.

114. Taguet A., Cassagnau P., Lopez-Cuesta J.-M. Structuration, Selective Dispersion and Compatibilizing Effect of (Nano)fillers in Polymer Blends // Prog. Polym. Sci. – 2014. – № 39 (8) . – P. 1526-1563.

115. Huang M., Schlarb A.K. Polypropylene/poly(ethylene terephthalate) microfibrillar reinforced composites manufactured by fused filament fabricatio. *J. Appl. Polym. Sci.* 2021. e50557.

116. Shen J., Huang W., Zuo S. In-situ fiberized poly(ethylene terephthalate) as a reinforcement to poly(propylene) matrix // Macromol. Mater. and Eng. 2003. № 288. P. 658-664.

117. Jayanarayanan K., Thomas S., Joseph K. Morphology, static and dynamic mechanical properties of in situ microfibrillar composites based on polypropylene/poly(ethylene terephthalate) blends. *Composites.* Part A. 2008. № 39. P. 164-175.

118. Fuchs C., Bhattacharyya D., Fakirov S. Microfibril reinforced polymer-polymer composites: application of tsai-hill equation to PP/PET composites. *Composites Science and Technology*. 2006. № 66. P. 3161-3171.

119. Li Z. M., Li L. B., Shen K. Z., Yang W., Huang R., Yang M. B. Transcrystalline morphology of an in situ microfibrillar poly(ethylene terephthalate)/poly(propylene) blend fabricated through a slit extrusion hot stretching-quenching process. *Macromolecular Rapid Communications*. 2004. № 25. P. 553-558.

120. Li Z. M., Li L. B., Shen K. Z., Yang M. B., Huang R. In-situ microfibrillar PET/PP blend via slit die extrusion, hot stretching, and quenching: Influence of hot stretch ratio on morphology, crystallization, and crystal structure of iPP at a fixed PET concentration. *J. Polym. Sci. Part B: Polym. Phys.* 2004. № 42. P.

4095-4106.

121. Li Z. M., Yang M. B., Huang R. Poly(ethylene terephthalate)/polyethylene composite based on in-situ microfiber formation. *Polymer-Plastics Technology and Engineering*. 2002. № 41. P. 19-32.

122. Dai K., Xu X. B., Li Z. M. Electrically conductive carbon black (CB) filled in situ microfibrillar poly(ethylene terephthalate) (PET)/polyethylene (PE) composite with a selective CB distribution. *Polymer*. 2007. № 48. P. 849-859.

123. Li W., Schlarb A.K., Evstatiev M. Study of PET/PP/TiO₂ microfibrillar-structured composites: Part Morphology and mechanical properties // J. Appl. Polym. Sci. – 2009. – V.113. – P. 3300-3306.

124. Li W., Karger-Koksis J., Schlarb A.K. Dispersion of TiO₂ Particles in PET/PP/TiO₂ and PET/PP/PP-g-MA/TiO₂ Composites Prepared with Different Blending Procedure, Macromol. Mater. Eng., No.294: 582-589 (2009).

125. Nurazzi N.M., Asyraf M.R.M., Khalina A., Abdullah N., Sabaruddin F.A., Kamarudin S.H., Ahmad S., Mahat A.M., Lee Ch.L., Aisyah H.A., Norrrahim M.N.F., Ilyas R. A., Harussani M. M., Ishak M. R., Sapuan S. M. Fabrication, Functionalization, and Application of Carbon Nanotube-Reinforced Polymer Composite: An Overview. Polymer, 2021, N13, P.1047- 1091.

126. Morsi M.A., Rajeh A., Al-Muntaser A.A. Reinforcement of the optical, thermal and electrical properties of PEO based on MWCNTs/Au hybrid fillers: Nanodielectric materials for organoelectronic devices. Compos. Part B Eng. 2019, 173.

127. Цебренко М.В., Резанова В.Г., Картель М.Т., Мельник І.А., Приходько Г.П. Закономірності одержання нанонаповнених поліпропіленових мікроволокон // Збірник наукових праць «Хімія, фізика та технологія поверхні». – 2013. – Т.4, №3 . – С. 305-313.

128. Резанова Н.М., Мельник І.А., Цебренко М.В., Картель М.Т., Семенцов Ю.І., Приходько Г.П. Реологічні властивості розплавів сумішей поліпропілен/співполіамід/вуглецеві нанотрубки // Вісник КНУТД. – 2010. – №1. – С. 223-229.

129. Цебренко М.В., Резанова Н.М., Мельник І.А., Цебренко І.О., Картель М.Т., Приходько Г.П., Семенцов Ю.І. Вплив

добавок вуглецевих нанотрубок на реологічні властивості та процеси структуроутворення в розплавах сумішей поліпропілен/співполіамід // Вісник КНУТД. – 2010. – №4. – С. 220-225.

130. Резанова Н.М., Мельник І.А., Готфрід А.О., Цебренко І.О., Картель М.Т., Приходько Г.П. Закономірності одержання наповнених вуглецевими нанотрубками поліпропіленових мікроволокон // Вісник КНУТД . – 2011. – №.4 – С. 50-54.

131. Rezanova N., Kartel M., Sementsov Yu., Prikhod'ko G., Melnik I., Tsebrenko M. Rheological Properties of Molten Mixtures Polypropylene/Copolyamide/CNT // Хімія і фізика поверхні. – 2011. – Т.2, №4. – С. 451-456.

132. Резанова Н.М., Мельник І.А., Цебренко І.О., Готфрід А.О., Цебренко М.В., Картель М.Т., Приходько Г.П. Вплив добавок компатибілізаторів на мікро- і макрореологічні властивості розплавів сумішей поліпропілен/співполіамід/вуглецеві нанотрубки // Вісник КНУТД. – 2011. – №6. – С 134-139.

133. Резанова Н.М, Булах В.Ю., Савченко Б.М., Татаренко В.В. Закономірності течії та структуроутворення в компатибілізованих сумішах полімерів // Вісник КНУТД – 2017. – №4. – С.148-154.

134. Han C., D., Funatsu K. An experimental study of droplet deformation and breakup in pressure-driven flows through converging and uniform channels // J. Rheol. – 1978. – V.22, № 2. – P.113-133.

135. Han C.D. Multiphase flow in polymer processing. – New York: Academic Press. – 1981. – 459 p.

136. Tsebrenko M.V., Rezanova N.M., Nikolaeva A.P., Tsebrenko I.A., Lazaг I.A. Effect of Sodium-Oleate Additions on the Morphology of Polypropylene-Copolyamide Blends // Polym. Eng. and Sci., 1999, V. 39, №6, P.1014-1021.

137. Резанова В.Г. Композиційна суперпозиція в'язкості по швидкості зсуву у розплавах компатибілізованих сумішей поліпропілен/співполіамід // Вісник КНУТД, 2011, №1, С.74-77.

138. Chen J., Liu B., Gao X., Xu D. A review of the interfacial characteristics of polymer nanocomposites containing carbon nanotubes. RSC Adv., 2018, V. 8, P.28048-28085.

DOI: 10.1039/C8RA04205E

139. Zhu B., Bai T., Wang P., Wang Y., Liu Ch., Shen Ch. Selective dispersion of carbon nanotubes and nanoclay in biodegradable poly(ε-caprolactone)/poly(lactic acid) blends with improved toughness, strength and thermal stabilityInt. J Biol Macromol. Epub 2019 Nov 20.
 doi: 10.1016/j.ijbiomac.2019.10.262.

140. Lipatov Yu.S., Kasyanchuk L.F., Nesterov A.E. Phase separation in the blends in the linear polymers formed in situ according to different mechanisms // Polymer International. – 2002. –Vol.51, N9. – P.772-780.

141. Rezanova V.G., Tsebrenko M.V. Influence of binary additives of compatibilizers on the micro- and macrorheological properties of melts of polypropylene-copolyamide mixtures // Journal of Engineering Physics and Thermophysics. – 2009. – Vol. 81. – №4. – p.766 -773.

142. Rezanova, N.M., Budash, Yu.O., Plavan, V.P., Bessarabov, V.I. Formation of microfibrillar structure of polypropylene/copolyamide blends in the presence of nanoparticles of metal oxides. *Voprosy khimii i khimicheskoi tekhnologii*. 2021. № 1. P. 71-78.

143. Jin K., Eyer S., Dean W., Kitto D., Bates F.S., Ellison C.J. Bimodal nano- and micro-fiber nonwovens by melt blowing immiscible ternary polymer blends. // Industrial and Engineering Chemistry Research. 2019**.**

144. Sangroniz L., Palacios J. K., Fernandez M., Eguiazabal J.I., Santamaria A., Muller A.J., *European Polym. J*.,No 83: 10 (2016).

145. Starita J.M. Microstructure of melt blended polymer systems // Trans. Soc. Rheol. – 1972. **–** V.16, N 2. – P. 339–367.

146. Tsebrenko M.V., Rezanova N.M., Vinogradov G.V. Rheology of molten blends of polyoxymethylene and ethylene-vinyl acetate copolymer and the microstructure of extrudates as a function of their melt viscosities // Polym. Eng. and Sci. – 1980. – V.20, № 15. – P.1023-1028.

147. Tsebrenko M.V., Danilova G.P., Malkin A. Ya. Ultrafine Fibers in Flow of Mixtures of non-Newtonian Polymer melts // J. Non-Newtonian Fluid Mech. – 1989. – V. 31. – P.1 – 26.

148. Резанова В.Г., Цебренко М.В. Закономірності одержання поліпропіленових мікроволокон із компатибілізованих сумішей полімерів // Хімічна промисловість України. – 2003.- №2.- С.23-27.185.

149. Stroustrup B. The C++ Programming Language Fourth Edition. Addison-Wesley, 2013. – 1366 p.

150. Васильєв О. Програмування на С++ в прикладах і задачах. К.: Ліра-К, 2020. – 382 с.

151. Schildt H C++. A beginner's guide. McGraw Hill, 2003. – 576 p.

152. Chan C.D. Rheology and processing of polymeric materials // Volume 1: Polymer Rheology. – 2007. – 736 p.

153. Резанова В.Г., Резанова Н.М. Розробка програмного забезпечення для визначення реологічних характеристик розплавів полімерів // Вісник Хмельницького національного університету. - № 5, 2018. - с. 21-25

154. Marco Cantu Mastering Delphi // Sybex Inc; 1999. – 1104 p.

155. Резанова В.Г., Резанова Н.М., Коршун А.В. Дослідження морфології сумішей полімерів з використанням розробленого програмного забезпечення // Вісник КНУТД – 2017. – №2. – С.120–127.

156. Tomotika S. On the stability of a cylindrical thread of a viscous liquid surrounded by another viscous fluid // Proc. Roy. Soc. – 1935. – V. A150. – P. 322-337.

157. N. R. Draper, H. Smith Applied Regression Analysis. - John Wiley & Sons, 1998. - 736 p.

158. Mural P. K., Banerjee A., Rana M. S., Shukla A., Padmanabhan B., Bhadra S., Madras G., Bose S. Polyolefin Based Antibacterial Membranes Derived from PE/PEO Blends Compatibilized with Amine Terminated Graphene Oxide and Maleated PE // J. Mater. Chem. – 2014. – V. 2, № 41. P. 17635-17648.

159. Einstein A. Uber die von molekularkinetischen Theorie der Warme deforderte Beweggung von in ruhenden Flussigkeiten suspendierten Teilhen // Annalen der Physik. – 1906. - Vol.19 – S.298-306.

160. An Introduction to Continuum Mechanics // Edited by Morton E. Gurtin, Carnegie-Mellon University, Pittsburgh, Pennsylvania, Vol. 158, 1981. - 265 p.

161. .Jeffery G.B. The motion of ellipsoidal particles immersed in a viscous fluid // Proc. Roy. Soc. – 1922. – Vol. A102, №715. - P. 161-179.

162. Yu. V. Pridatchenko, Yu. I. Shmakov Rheological equations of state of weakly concentrated suspensions of rigid ellipsoidal particles // Journal of Applied Mechanics and Technical Physics, Vol. 14, No. 1. – 1973. – p. 118-119

163. E. Yu. Taran, Yu. V. Pridatchenko Rheological behavior of dilute suspensions of rigid axisymmetric particles // Journal of Engineering Physics and Thermophysics, Vol. 62, No. 1, 1992. – p. 44-51.

164. E. Yu. Taran, Yu. V. Pridatchenko, V. A. Gryaznova Features of the Formation of Composite Materials in Anisotropic Liquid Systems with Elongated Suspended Particles // Mechanics of Composite Materials, Vol. 37, No. 3, 2001. – p. 251-256.

165. Затонацька Т.Г., Придатченко Ю.В., Таран Є.Ю. Реологічна поведінка розбавлених суспезій деформівних частинок // Доповіді НАН України. – 1998. – №10. – С.88-93.

166. Shcherban V. Yu., Rezanova V. G., Demkivska T. I. Programming of numerical methods and examples of practical application: monography. – Kyiv: Education of Ukraine, 2021. –150 p.

167. Пасічник В.В. , Висоцька В.А. , Андруник В.А. Чисельні методи в ком'ютерних науках, Т.1, Львів: Новий світ, 2017. – 470 с.

PROGRAM LISTINGS

1. Procedures and functions for calculating and graphically displaying the rheological characteristics of a mixture of polymers

```
procedure TForm1.Button2Click(Sender: TObject);
var i:integer;
   q:string;
begin
for i:=0 to 10 do
  begin
    SdTcp[i]:=S[i]/Tcp[i]/1000;
    LgSdTcp[i]:=ln(SdTcp[i])/ln(10);
    Lg_D[i]:=LgK2+LgSdTcp[i];
  end;
  for i:=0 to 9 do
    begin
      dLg_D[i]:=Lg_D[i]-Lg_D[i+1];
      dLgT[i]:=LgT[i]-LgT[i+1];
      N[i]:=dLg_D[i]/dLgT[i];
    end;
  for i:=0 to 9 do
   begin
    LgD[i]:=ln(N[i]+3)/ln(10)+Lg_D[i];
    LgEta[i]:=LgT[i]-LgD[i];
    Eta[i]:=Power(10,LgEta[i]);
   end;
  Form2.Show;
  Form5.Hide;
   for i:=0 to 9 do
   begin
    Form2.Memo1.Lines.add(IntToStr(i+1));
    q:=format('%*.*f',[8,7,SdTcp[i]]);
    Form2.Memo5.Lines.add(q);
    q:=format('%*.*f',[5,4,Lg_D[i]]);
    Form2.Memo6.Lines.add(q);
    q:=format('%*.*f',[5,4,N[i]]);
    Form2.Memo7.Lines.add(q);
    q:=format('%*.*f',[2,1,Tcp[i]]);
    Form2.Memo2.Lines.add(q);
    q:=format('%*.*f',[2,0,S[i]]);
```

```
    Form2.Memo3.Lines.add(q);
    q:=format('%*.*f',[5,4,LgT[i]]);
    Form2.Memo4.Lines.add(q);
    q:=format('%*.*f',[5,4,LgD[i]]);
    Form2.Memo8.Lines.add(q);
    q:=format('%*.*f',[5,4,LgEta[i]]);
    Form2.Memo9.Lines.add(q);
    q:=format('%*.*f',[5,1,Eta[i]]);
    Form2.Memo10.Lines.add(q);
  end;
end;

procedure TForm1.Button3Click(Sender: TObject);
var i:integer;
   q:string;
begin
 for i:=0 to kd-1 do
  begin
    SdTcp[i]:=S[i]/Tcp[i]/1000;
    LgSdTcp[i]:=ln(SdTcp[i])/ln(10);
    Lg_D[i]:=LgK2+LgSdTcp[i];
  end;
   for i:=0 to kd-2 do
    begin
     dLg_D[i]:=Lg_D[i]-Lg_D[i+1];
     dLgT[i]:=LgT[i]-LgT[i+1];
     N[i]:=dLg_D[i]/dLgT[i];
    end;
  for i:=0 to kd-2 do
   begin
    LgD[i]:=ln(N[i]+3)/ln(10)+Lg_D[i];
    LgEta[i]:=LgT[i]-LgD[i];
    Eta[i]:=Power(10,LgEta[i]);
   end;
  Form2.Show;
  Form5.Hide;
    for i:=0 to kd-2 do
  begin
   Form2.Memo1.Lines.add(IntToStr(i+1));
   q:=format('%*.*f',[8,7,SdTcp[i]]);
   Form2.Memo5.Lines.add(q);
```

200

```
     q:=format('%*.*f',[5,4,Lg_D[i]]);
     Form2.Memo6.Lines.add(q);
     q:=format('%*.*f',[5,4,N[i]]);
     Form2.Memo7.Lines.add(q);
     q:=format('%*.*f',[2,1,Tcp[i]]);
     Form2.Memo2.Lines.add(q);
     q:=format('%*.*f',[2,0,S[i]]);
     Form2.Memo3.Lines.add(q);
     q:=format('%*.*f',[5,4,LgT[i]]);
     Form2.Memo4.Lines.add(q);
     q:=format('%*.*f',[5,4,LgD[i]]);
     Form2.Memo8.Lines.add(q);
     q:=format('%*.*f',[5,4,LgEta[i]]);
     Form2.Memo9.Lines.add(q);
     q:=format('%*.*f',[5,1,Eta[i]]);
     Form2.Memo10.Lines.add(q);
   end;
  for i:=0 to kd-2 do
   begin
     LgD2[i]:=ln(N2[i]+3)/ln(10)+Lg_D2[i];
     dLgD[i]:=LgD[i]-LgD[i+1];
     LgEta2[i]:=LgT2[i]-LgD2[i];
    Eta2[i]:=Power(10,LgEta2[i]);
   end;
    end;

procedure TForm1.Button5Click(Sender: TObject);
begin
 kd:=StrToInt(Edit34.Text);
end;

procedure vvod(c:STRING; var F_Tcp,F_S,F_LgT:TS );
var f:textfile;
i,j:integer;
begin
   assignfile(f,c);
   reset(f);
   readln(f,kd);
      for i:=0 to kd-1 do
   begin
      read(f,F_Tcp[i]);
```

```
      read(f,F_S[i]);
      read(f,F_LgT[i]);
      readln(f);
    end;
end;

procedure TForm1.Button7Click(Sender: TObject);
var f:textfile;
i,j:integer;
begin
  assignfile(f,'inp.txt');
   reset(f);
   readln(f,kd);
     for i:=0 to kd-1 do
    begin
     read(f,Tcp[i]);
     read(f,S[i]);
     read(f,LgT[i]);
         readln(f);
    end;
closefile(f);}
Form6.Show;
end;
end.


   Unit2
   Procedure vivid(C:STRING;D:TS);
   var f1:textfile;
   i,j:integer;
   begin
     assignfile(f1,C);
     append(f1);
     for i:=1 to kd-1 do
     begin
       write(f1,D[i]:0:4); //write(f1,' ');
       writeln(f1);
     end;
   close(f1);
   end;
   procedure TForm2.Button1Click(Sender: TObject);
```

```pascal
var i:integer;
   f2, f3,f4:textfile;
    q:string;
begin
 kNazhatiy:=kNazhatiy+1;
 Nr:=StrToInt(Edit21.Text);
 Form3.Show;
 Ncp1:=0;
 Ncp2:=0;
for i:=0 to Nr-1 do
 begin
   Ncp1:=Ncp1+N[i];
 end;
 Ncp1:=Ncp1/Nr;
 for i:=0 to Nr-1 do
  begin
    LgD[i]:=ln(Ncp1+3)/ln(10)+Lg_D[i];
    LgEta[i]:=LgT[i]-LgD[i];
    Eta[i]:=Power(10,LgEta[i]);
  end;
    for i:=0 to Nr-1 do
  begin
    if kNazhatiy=1 then LgEta1[i]:=LgEta[i];
    if kNazhatiy=2 then LgEta2[i]:=LgEta[i];
    if kNazhatiy=3 then LgEta3[i]:=LgEta[i];
  end;
  for i:=0 to Nr-1 do
  begin
    LgEta123[i]:=LgEta1[i];
  end;
  for i:=Nr to (Nr-1)*2 do
  begin
    LgEta123[i]:=LgEta2[i];
  end;
  for i:=(Nr-1)*2+1 to (Nr-1)*3 do
  begin
    LgEta123[i]:=LgEta3[i];
  end;
  for i:=Nr to kd-1 do
  begin
    Ncp2:=Ncp2+N[i];
```

203

```
   end;
 Ncp2:=Ncp2/(kd-1-Nr);
Form3.Edit1.Text:=FloatToStr(Ncp1);
Form3.Edit2.Text:=FloatToStr(Ncp2);
  for i:=Nr to kd-2 do
  begin
    LgD[i]:=ln(Ncp2+3)/ln(10)+Lg_D[i];
    LgEta[i]:=LgT[i]-LgD[i];
   Eta[i]:=Power(10,LgEta[i]);
   Memo1.Lines.add(FloatToStr(LgEta[i]));
   Memo2.Lines.add(FloatToStr(Eta[i]));
    end;
  for i:=0 to kd-2 do
  begin
   Form3.Memo4.Lines.add(IntToStr(i+1));
   q:=format('%*.*f',[8,7,SdTcp[i]]);
   Form3.Memo1.Lines.add(q);
   q:=format('%*.*f',[5,4,Lg_D[i]]);
   Form3.Memo2.Lines.add(q);
   q:=format('%*.*f',[5,4,N[i]]);
   Form3.Memo3.Lines.add(q);
   q:=format('%*.*f',[2,1,Tcp[i]]);
   Form3.Memo5.Lines.add(q);
   q:=format('%*.*f',[2,0,S[i]]);
   Form3.Memo6.Lines.add(q);
   q:=format('%*.*f',[5,4,LgT[i]]);
   Form3.Memo7.Lines.add(q);
   q:=format('%*.*f',[5,4,LgD[i]]);
   Form3.Memo8.Lines.add(q);
   q:=format('%*.*f',[5,4,LgEta[i]]);
   Form3.Memo9.Lines.add(q);
   q:=format('%*.*f',[5,1,Eta[i]]);
   Form3.Memo10.Lines.add(q);
  end;
 vivid ('out.txt',LgT);
 vivid ('out2.txt',LgEta);
 end;

Unit3
procedure Det3x3(Koef:MyArr; var Det:Real);
begin
```

```
  Det:=Koef[1,1]*Koef[2,2]*Koef[3,3]+
     Koef[2,1]*Koef[3,2]*Koef[1,3]+
     Koef[1,2]*Koef[2,3]*Koef[3,1]-
     Koef[1,3]*Koef[2,2]*Koef[3,1]-
     Koef[2,1]*Koef[1,2]*Koef[3,3]-
     Koef[1,1]*Koef[2,3]*Koef[3,2];
end;

procedure MinSq(X,Y:TS; Ac,Bc,Cc:real);
var i,j:integer;
   S1,S2,S3,S4,S5,S6,S7:real;
begin
for i:=0 to 9 do
 begin
  S1:=S1+power(X[i],4);
  S2:=S2+power(X[i],3);
  S3:=S3+X[i]*X[i];
  S4:=S4+X[i];
  S5:=S5+X[i]*X[i]*Y[i];
  S6:=S6+X[i]*Y[i];
  S7:=S7+Y[i];
 end;
 Koef[1,1]:=S1;
 Koef[2,1]:=S2;
 Koef[3,1]:=S3;
 Koef[1,2]:=S2;
 Koef[2,2]:=S3;
 Koef[3,2]:=S4;
 Koef[1,3]:=S3;
 Koef[2,3]:=S4;
 Koef[3,3]:=1;
 St[1]:=S5;
 St[2]:=S6;
 St[3]:=S7;
 Kramer3(Koef,St,Ac,Bc,Cc);
end;

Unit4
procedure Scale(A,B:TS;var Mx,My,KA,KB,MinA,MinB,ShA,ShB:Real);
var k:integer;
   pr,pr1,Min,Min1,Max,Max1:Real;
```

```
begin
 Min:=A[0];
 Max:=A[0];
 Min1:=B[0];
 Max1:=B[0];
  for k:=1 to kd-2 do
   begin
    if A[k]>Max then Max:=A[k];
    if A[k]<Min then Min:=A[k];
    if B[k]>Max1 then Max1:=B[k];
    if B[k]<Min1 then Min1:=B[k];
   end;
MinA:=Min;
MinB:=Min1;
 pr:=Max-Min;
 Mx:=290/pr;
 pr1:=Max1-Min1;
 My:=270/pr1;
 ShA:=pr/10;
 ShB:=pr1/10;
 KA:=0;
 KB:=0;
if Min>pr then KA:=1;
if Min1>pr1 then KB:=1;
end;

procedure OsiCoord;
var i:integer;
begin
 X0:=35;
 Y0:=300;
Form4.Image1.Canvas.MoveTo(X0,Y0+10);
Form4.Image1.Canvas.LineTo(X0,5);
Form4.Image1.Canvas.MoveTo(X0-10,Y0);
Form4.Image1.Canvas.LineTo(370,Y0);
for i:=1 to 11 do
 begin
  Form4.Image1.Canvas.MoveTo(X0+10+29*(i-1),Y0-2);
  Form4.Image1.Canvas.LineTo(X0+10+29*(i-1),Y0+2);
  Form4.Image1.Canvas.MoveTo(X0+2,Y0-10-27*(i-1));
  Form4.Image1.Canvas.LineTo(X0-2,Y0-10-27*(i-1));
```

```
 end;
end;

procedure RazmetkaOsey(A,B:TS);
var i:integer;
   q,q1:string;
   Mx,My,KA,KB,MinA,MinB,ShA,ShB:Real;
begin
Scale(A,B,Mx,My,KA,KB,MinA,MinB,ShA,ShB);
 for i:=0 to 5  do
  begin
  q:=format('%*.*f',[4,3,MinA]);
  Form4.Image1.Canvas.TextOut(X0+29*2*i+2,Y0+4,q) ;
  MinA:=MinA+2*ShA;
  end;
  for i:=0 to 11  do
  begin
  q1:=format('%*.*f',[4,3,MinB]);
  Form4.Image1.Canvas.TextOut(X0-30,Y0-14-27*i,q1) ;
  MinB:=MinB+ShB;
  end;
end;

procedure Griphic_Lg_D_LgT;
var Mx,My,KA,KB,MinA,MinB,ShA,ShB:Real;
   i:integer;
begin
RazmetkaOsey(LgT,Lg_D);
Scale(LgT,Lg_D,Mx,My,KA,KB,MinA,MinB,ShA,ShB);
Form4.Image1.Canvas.MoveTo
   (X0+round(LgT[0]*Mx-KA*MinA{4.9}*Mx+10),
   Y0-(round(Lg_D[0]*My-{KB*}{0.3}MinB*My{177.8}))-10);
for i:=1 to kd-2 do
 begin
  Form4.Image1.Canvas.LineTo
   (X0+round(LgT[i]*Mx-KA*MinA{4.9}*Mx+10{4.6*MSx{181.8-
4.6*181.8}),
    Y0-(round(Lg_D[i]*My-{KB*}MinB{0.3}*My{177.8}))-10);
 end;
for i:=0 to kd-2 do
 begin
```

```
   Form4.Image1.Canvas.Pen.Color:=clRed;
   Form4.Image1.Canvas.Ellipse(
     X0+round(LgT[i]*Mx-KA*MinA{4.9}*Mx)-2+10,
     Y0-round(Lg_D[i]*My-{KB*}{0.3}MinB*My)-2-10,
     X0+round(LgT[i]*Mx-KA*MinA{4.9}*Mx)+2+10,
     Y0-round(Lg_D[i]*My-{KB*}MinB{0.3}*My)+2-10
       );
 end;

   Form4.Image1.Canvas.Pen.Color:=clBlack;
end;

procedure Griphic_LgEta_LgT;
var Mx,My,KA,KB,MinA,MinB,ShA,ShB:Real;
   i:integer;
begin
RazmetkaOsey(LgT,LgEta);
Scale(LgT,LgEta,Mx,My,KA,KB,MinA,MinB,ShA,ShB);
Form4.Image1.Canvas.MoveTo(
        X0+round(LgT[0]*Mx-KA*MinA*Mx)+10,
        Y0-round(LgEta[0]*My-{KB*}MinB*My)-10
                  );
for i:=1 to kd-2 do
 begin
 Form4.Image1.Canvas.LineTo
   (X0+round(LgT[i]*Mx-KA*MinA*Mx)+10,
    Y0-round(LgEta[i]*My-{KB*}MinB*My)-10);
 end;
 for i:=0 to kd-2 do
 begin
 Form4.Image1.Canvas.Pen.Color:=clRed;
 Form4.Image1.Canvas.Ellipse(
   X0+round(LgT[i]*Mx-KA*MinA{4.9}*Mx)-2+10,
   Y0-round(LgEta[i]*My-{KB*}{0.3}MinB*My)-2-10,
   X0+round(LgT[i]*Mx-KA*MinA{4.9}*Mx)+2+10,
   Y0-round(LgEta[i]*My-{KB*}MinB{0.3}*My)+2-10
                    );
 end;

   Form4.Image1.Canvas.Pen.Color:=clBlack;
end;
```

```
procedure Griphic_Eta_T;
var Mx,My,KA,KB,MinA,MinB,ShA,ShB:Real ;
   i:integer;
   T:TS;
begin
for i:=0 to kd-2 do
 begin
  T[i]:=power(10,LgT[i]);
 end;
RazmetkaOsey(T,Eta);
Scale(T,Eta,Mx,My,KA,KB,MinA,MinB,ShA,ShB);
Form4.Image1.Canvas.MoveTo
   (X0+round(T[0]*Mx-KA*MinA*Mx)+10,
   Y0-round(Eta[0]*My-{KB*}MinB*My{177.8})-10);
for i:=1 to kd-2 do
 begin
  Form4.Image1.Canvas.LineTo
   (X0+round(T[i]*Mx-KA*MinA*Mx)+10,
    Y0-round(Eta[i]*My-{KB*}MinB*My)-10);
 end;

  for i:=0 to kd-2 do
 begin
  Form4.Image1.Canvas.Pen.Color:=clRed;
  Form4.Image1.Canvas.Ellipse(
    X0+round(T[i]*Mx-KA*MinA{4.9}*Mx)-2+10,
    Y0-round(Eta[i]*My-{KB*}{0.3}MinB*My)-2-10,
    X0+round(T[i]*Mx-KA*MinA{4.9}*Mx)+2+10,
    Y0-round(Eta[i]*My-{KB*}MinB{0.3}*My)+2-10
                   );
 end;
   Form4.Image1.Canvas.Pen.Color:=clBlack;
end;

procedure Points_Lg_D_LgT;
var Mx,My,KA,KB,MinA,MinB,ShA,ShB:Real;
   i:integer;
begin
RazmetkaOsey(LgT,Lg_D);
Scale(LgT,Lg_D,Mx,My,KA,KB,MinA,MinB,ShA,ShB);
```

```
for i:=0 to kd-2 do
 begin
  Form4.Image1.Canvas.Pen.Color:=clRed;
  Form4.Image1.Canvas.Ellipse(
    X0+round(LgT[i]*Mx-KA*MinA{4.9}*Mx)-2+10,
    Y0-round(Lg_D[i]*My-{KB*}{0.3}MinB*My)-2-10,
    X0+round(LgT[i]*Mx-KA*MinA{4.9}*Mx)+2+10,
    Y0-round(Lg_D[i]*My-{KB*}MinB{0.3}*My)+2-10
                   );
 end;
   Form4.Image1.Canvas.Pen.Color:=clBlack;
end;

procedure Points_LgEta_LgT;
var Mx,My,KA,KB,MinA,MinB,ShA,ShB:Real;
   i:integer;
begin
kv:=kv+1;
if kv=1 then RazmetkaOsey(LgT,LgEta);
if kv=3 then RazmetkaOsey(LgT,LgEta123);
if kv=1 then Scale(LgT,LgEta,Mx,My,KA,KB,MinA,MinB,ShA,ShB);
if kv=3 then Scale(LgT,LgEta123,Mx,My,KA,KB,MinA,MinB,ShA,ShB);
 for i:=0 to kd-2 do
 begin
  if kv=1 then Form4.Image1.Canvas.Pen.Color:=clRed;
  if kv=2 then Form4.Image1.Canvas.Pen.Color:=clGreen;
  if kv=3 then Form4.Image1.Canvas.Pen.Color:=clBlue;
  Form4.Image1.Canvas.Pen.width:=2;
  Form4.Image1.Canvas.Ellipse(
    X0+round(LgT[i]*Mx-KA*MinA{4.9}*Mx)-3+10,
    Y0-round(LgEta[i]*My-{KB*}{0.3}MinB*My)-3-10,
    X0+round(LgT[i]*Mx-KA*MinA{4.9}*Mx)+3+10,
    Y0-round(LgEta[i]*My-{KB*}MinB{0.3}*My)+3-10
                   );
 end;

   Form4.Image1.Canvas.Pen.Color:=clBlack;
end;

procedure Points_Eta_T;
var Mx,My,KA,KB,MinA,MinB,ShA,ShB:Real ;
```

```
    i:integer;
    T:TS;
begin
for i:=0 to kd-2 do
 begin
  T[i]:=power(10,LgT[i]);
 end;
RazmetkaOsey(T,Eta);
Scale(T,Eta,Mx,My,KA,KB,MinA,MinB,ShA,ShB);
  for i:=0 to kd-2 do
 begin
 Form4.Image1.Canvas.Pen.Color:=clRed;
 Form4.Image1.Canvas.Ellipse(
    X0+round(T[i]*Mx-KA*MinA{4.9}*Mx)-2+10,
    Y0-round(Eta[i]*My-{KB*}{0.3}MinB*My)-2-10,
    X0+round(T[i]*Mx-KA*MinA{4.9}*Mx)+2+10,
    Y0-round(Eta[i]*My-{KB*}MinB{0.3}*My)+2-10
                    );
 end;
  Form4.Image1.Canvas.Pen.Color:=clBlack;
end;

procedure Points_3_LgEta_LgT;
var Mx,My,KA,KB,MinA,MinB,ShA,ShB:Real;
   i:integer;
begin
RazmetkaOsey(LgT,LgEta123);
Scale(LgT,LgEta123,Mx,My,KA,KB,MinA,MinB,ShA,ShB);
 for i:=0 to kd-2 do
 begin
 Form4.Image1.Canvas.Pen.Color:=clRed;
 Form4.Image1.Canvas.Pen.width:=2;
 Form4.Image1.Canvas.Ellipse(
    X0+round(LgT[i]*Mx-KA*MinA{4.9}*Mx)-3+10,
    Y0-round(LgEta[i]*My-{KB*}{0.3}MinB*My)-3-10,
    X0+round(LgT[i]*Mx-KA*MinA{4.9}*Mx)+3+10,
    Y0-round(LgEta[i]*My-{KB*}MinB{0.3}*My)+3-10
                    );
 end;
  Form4.Image1.Canvas.Pen.Color:=clBlack;
end;
```

```
procedure TForm4.Button1Click(Sender: TObject);
begin
OsiCoord;
if RadioButton1.Checked then Griphic_Lg_D_LgT;
if RadioButton2.Checked then Griphic_LgEta_LgT;
if RadioButton3.Checked then Griphic_Eta_T;
//RazmetkaOsey(LgT,Lg_D);
end;

procedure Approx_LgEta_LgT;
var Mx,My,KA,KB,MinA,MinB,ShA,ShB:real;
   i:integer;
   Ma,Mb,hA,hB, Ac,Bc,Cc:real;
begin
RazmetkaOsey(LgT,LgEta);
Scale(LgT,LgEta,Mx,My,KA,KB,MinA,MinB,ShA,ShB);
MinSq(LgT,LgEta, Ac,Bc,Cc);
Form4.Image1.Canvas.MoveTo(X0+10,Y0-10-round(
                (Ac*MinA*MinA+Bc*MinA+Cc)*My-MinB*My)
                      );
 Form4.Edit1.Text:=FloatToStr(Ac);
 Form4.Edit2.Text:=FloatToStr(Bc);
 Form4.Edit3.Text:=FloatToStr(Cc);
for i:=1 to 101 do
 begin
  Form4.Image1.Canvas.LineTo
   (X0+round((MinA+i*ShA/10)*Mx-MinA*Mx)+10,
    Y0-round((Ac*(MinA+i*ShA/10)*(MinA+i*ShA/10)+
                Bc*(MinA+i*ShA/10)+Cc)*My-
                MinB*My)-10);
 end;
 for i:=0 to kd-2 do
 begin
 Form4.Image1.Canvas.Pen.Color:=clRed;
 Form4.Image1.Canvas.Ellipse(
   X0+round(LgT[i]*Mx-MinA*Mx)-2+10,
   Y0-round(LgEta[i]*My-MinB*My)-2-10,
   X0+round(LgT[i]*Mx-KA*MinA*Mx)+2+10,
   Y0-round(LgEta[i]*My-MinB*My)+2-10
                  );
```

```
 end;
   Form4.Image1.Canvas.Pen.Color:=clBlack;
end;

procedure Approx4_LgEta_LgT;
var Mx,My,KA,KB,MinA,MinB,ShA,ShB:real;
   i:integer;
   Ma,Mb,hA,hB, Ac4,Bc4,Cc4,Dc4:real;
begin
RazmetkaOsey(LgT,LgEta);
Scale(LgT,LgEta,Mx,My,KA,KB,MinA,MinB,ShA,ShB);
MinSq4(LgT,LgEta, Ac4,Bc4,Cc4,Dc4);

Form4.Image1.Canvas.MoveTo(X0+10,Y0-10-round(

(Ac4*MinA*MinA*MinA+Bc4*MinA*MinA+Cc4*MinA+Dc4)*My
                        -MinB*My)
                              );
 Form4.Edit1.Text:=FloatToStr(Ac4);
 Form4.Edit2.Text:=FloatToStr(Bc4);
 Form4.Edit3.Text:=FloatToStr(Cc4);
for i:=1 to 101 do
 begin
  Form4.Image1.Canvas.LineTo
   (X0+round((MinA+i*ShA/10)*Mx-MinA*Mx)+10,
    Y0-
round((Ac4*(MinA+i*ShA/10)*(MinA+i*ShA/10)*(MinA+i*ShA/10)+
         Bc4*(MinA+i*ShA/10)*(MinA+i*ShA/10)+
         Cc4*(MinA+i*ShA/10)+Dc4)*My-
              MinB*My)-10);
 end;
 for i:=0 to kd-2 do
 begin
 Form4.Image1.Canvas.Pen.Color:=clRed;
 Form4.Image1.Canvas.Ellipse(
    X0+round(LgT[i]*Mx-MinA*Mx)-2+10,
    Y0-round(LgEta[i]*My-MinB*My)-2-10,
    X0+round(LgT[i]*Mx-KA*MinA*Mx)+2+10,
    Y0-round(LgEta[i]*My-MinB*My)+2-10
                  );
 end;
```

213

```
    Form4.Image1.Canvas.Pen.Color:=clBlack;
end;
procedure Approx_Eta_T;
var Mx,My,KA,KB,MinA,MinB,ShA,ShB:real;
   i:integer;
   Ma,Mb,hA,hB, Ac,Bc,Cc:real;
   T:TS;
begin
for i:=0 to kd-2 do
 begin
  T[i]:=power(10,LgT[i]);
 end;

RazmetkaOsey(T,Eta);
Scale(T,Eta,Mx,My,KA,KB,MinA,MinB,ShA,ShB);
MinSq(T,Eta, Ac,Bc,Cc);
Form4.Image1.Canvas.MoveTo(X0+10,Y0-10-round(
                 (Ac*MinA*MinA+Bc*MinA+Cc)*My-MinB*My)
                           );
 Form4.Edit1.Text:=FloatToStr(Ac);
 Form4.Edit2.Text:=FloatToStr(Bc);
 Form4.Edit3.Text:=FloatToStr(Cc);
 for i:=1 to 101 do
 begin
   Form4.Image1.Canvas.LineTo
    (X0+round((MinA+i*ShA/10)*Mx-MinA*Mx)+10,
     Y0-round((Ac*(MinA+i*ShA/10)*(MinA+i*ShA/10)+
                Bc*(MinA+i*ShA/10)+Cc)*My-
                MinB*My)-10);
 end;
 for i:=0 to kd-2 do
 begin
 Form4.Image1.Canvas.Pen.Color:=clRed;
 Form4.Image1.Canvas.Ellipse(
    X0+round(T[i]*Mx-MinA*Mx)-2+10,
    Y0-round(Eta[i]*My-MinB*My)-2-10,
    X0+round(T[i]*Mx-KA*MinA*Mx)+2+10,
    Y0-round(Eta[i]*My-MinB*My)+2-10
                    );
 end;
   Form4.Image1.Canvas.Pen.Color:=clBlack;
```

214

```
end;


procedure Approx_Lg_D_LgT;
var Mx,My,KA,KB,MinA,MinB,ShA,ShB:real;
   i:integer;
   Ma,Mb,hA,hB, Ac,Bc,Cc:real;
begin
RazmetkaOsey(LgT,Lg_D);
Scale(LgT,Lg_D,Mx,My,KA,KB,MinA,MinB,ShA,ShB);
Form4.Image1.Canvas.MoveTo(
        X0+round(LgT[0]*Mx-MinA*Mx)+10,
        Y0-round(Lg_D[0]*My-MinB*My)-10
                 );
MinSq(LgT,Lg_D, Ac,Bc,Cc);
 Form4.Edit1.Text:=FloatToStr(Ac);
 Form4.Edit2.Text:=FloatToStr(Bc);
 Form4.Edit3.Text:=FloatToStr(Cc);
for i:=1 to 99 do
 begin
  Form4.Image1.Canvas.LineTo
   (X0+round((MinA+i*ShA/10)*Mx-MinA*Mx)+10,
    Y0-round((Ac*(MinA+i*ShA/10)*(MinA+i*ShA/10)+
               Bc*(MinA+i*ShA/10)+Cc)*My-
               MinB*My)-10);
 end;
 for i:=0 to 9 do
 begin
 Form4.Image1.Canvas.Pen.Color:=clRed;
 Form4.Image1.Canvas.Ellipse(
    X0+round(LgT[i]*Mx-MinA*Mx)-2+10,
    Y0-round(Lg_D[i]*My-MinB*My)-2-10,
    X0+round(LgT[i]*Mx-KA*MinA*Mx)+2+10,
    Y0-round(Lg_D[i]*My-MinB*My)+2-10
                    );
 end;
  Form4.Image1.Canvas.Pen.Color:=clBlack;
end;

Unit6
procedure TForm6.FormCreate(Sender: TObject);
```

```
begin
x0:=-1000;
y0:=2200;
Mx:=300;
My:=300;
kn:=0;
end;

function xk(xmat:real):integer;
begin
 xk:=trunc(x0+xmat*Mx);
end;

function yk(ymat:real):integer;
begin
 yk:=trunc(y0-ymat*My);
end;

procedure osi;
var i:integer;
 begin
  Form6.Image1.Canvas.Pen.Width:=1;
  //ShowMessage("0");
  Form6.Image1.Canvas.Pen.Color:=clWhite;

Form6.Image1.Canvas.Rectangle(0,0,Form6.Image1.Width,Form6.Image1.
Height);
  Form6.Image1.Canvas.Pen.Color:=clMoneyGreen;
   for i:=0 to 100 do
  begin
   Form6.Image1.Canvas.MoveTo(5,y0+i*My);
   Form6.Image1.Canvas.LineTo(Form6.Image1.Width-5,y0+i*My);
   Form6.Image1.Canvas.MoveTo(5,y0-i*My);
   Form6.Image1.Canvas.LineTo(Form6.Image1.Width-5,y0-i*My);
   Form6.Image1.Canvas.MoveTo(x0+i*Mx,5);
   Form6.Image1.Canvas.LineTo(x0+i*Mx,Form6.Image1.Height);
   Form6.Image1.Canvas.MoveTo(x0-i*Mx,5);
   Form6.Image1.Canvas.LineTo(x0-i*Mx,Form6.Image1.Height);
  end;
  Form6.Image1.Canvas.Pen.Color:=clBlack;
  Form6.Image1.Canvas.MoveTo(5,y0);
```

216

```
  Form6.Image1.Canvas.LineTo(Form6.Image1.Width-5,y0);
  Form6.Image1.Canvas.MoveTo(x0,5);
  Form6.Image1.Canvas.LineTo(x0,Form6.Image1.Height);
 end;

procedure vvod(c:STRING; var F_Tcp,F_S,F_LgT:TS );
var f:textfile;
i,j:integer;
begin
     assignfile(f,c);
   reset(f);
   readln(f,kd);
   //ShowMessage(IntToStr(kd));
   for i:=0 to kd-1 do
   begin
    for j:=1 to kd do
     read(f,F_Tcp[i]);
     read(f,F_S[i]);
     read(f,F_LgT[i]);
     readln(f);
   end;
end;

procedure TForm6.Button1Click(Sender: TObject);
var i:integer;
   f:textfile;
begin
assignfile(f,'outinp.txt');
   reset(f);
    kd:=11;
     for i:=0 to kd-3 do
   begin
   for j:=1 to kd do
    readln(f,LgT[i]);
     readln(f);
    end;
   for i:=0 to kd-3 do
   begin
    read(f,LgEta1[i]);
   readln(f);
    end;
```

217

```
    for i:=0 to kd-3 do
   begin
    read(f,LgEta2[i]);
    readln(f);
    end;
    for i:=0 to kd-2 do
   begin
    read(f,LgEta3[i]);
    readln(f);
    end;
kn:=kn+1;
    osi;
    Form6.Image1.Canvas.Pen.width:=2;
 Form6.Image1.Canvas.Pen.Color:=clRed;
 for i:=0 to kd-3 do
   begin
   Form6.Image1.Canvas.Ellipse(xk(LgT[i])-3,yk(LgEta1[i])-
3,xk(LgT[i])+3,yk(LgEta1[i])+3);
   end;
   Form6.Image1.Canvas.Pen.Color:=clGreen;
  for i:=0 to kd-3 do
   begin
   Form6.Image1.Canvas.Ellipse(xk(LgT[i])-3,yk(LgEta2[i])-
3,xk(LgT[i])+3,yk(LgEta2[i])+3);
   end;
   Form6.Image1.Canvas.Pen.Color:=clBlue;
  for i:=0 to kd-3 do
   begin
   Form6.Image1.Canvas.Ellipse(xk(LgT[i])-3,yk(LgEta3[i])-
3,xk(LgT[i])+3,yk(LgEta3[i])+3);
   end;
end;

procedure TForm6.ScrollBar1Scroll(Sender: TObject; ScrollCode:
TScrollCode;
  var ScrollPos: Integer);
  var i:integer;
begin
 Form6.Image1.Canvas.Pen.Color:=clWhite;
 Form6.Image1.Canvas.Rectangle(0,0,Image1.Width,Image1.Height);
Mx:=ScrollPos;
```

```
My:=ScrollPos;
osi;
for i:=0 to kd-1 do
 begin
  Form6.Image1.Canvas.Pen.Color:=clRed;
  Form6.Image1.Canvas.Pen.width:=2;
  Form6.Image1.Canvas.Ellipse(xk(LgT[i])-3,yk(LgEta1[i])-
3,xk(LgT[i])+3,yk(LgEta1[i])+3);
  Form6.Image1.Canvas.Pen.Color:=clGreen;
  Form6.Image1.Canvas.Ellipse(xk(LgT[i])-3,yk(LgEta2[i])-
3,xk(LgT[i])+3,yk(LgEta2[i])+3);
  Form6.Image1.Canvas.Pen.Color:=clBlue;
  Form6.Image1.Canvas.Ellipse(xk(LgT[i])-3,yk(LgEta3[i])-
3,xk(LgT[i])+3,yk(LgEta3[i])+3);
  end;
end;
end.
```

2. Procedures and functions for graphical display of calculation results based on the mathematical model of deformation of a polymer droplet in a flow

```
Unit3
procedure TForm3.FormShow(Sender: TObject);
Var
    i:integer;
    SX,SIX,SIY:Real;
    StepX,StepY:Real;
    OldX,OldY,NewX,NewY:integer;
    MasX:array [0..50] of Real;
    MasY:array [1..4,0..50] of Real;
    BY:Real;
    SY:Real;
     MaxY:integer;
    Z:integer;
    iii:integer;
    countL:integer;
    index:integer;
begin
    for i:=1 to 50 do
    MasX[i-1]:= strtofloat(form1.Memo1.Lines.Strings[i]);
    for i:=1 to form1.Memo3.Lines.Count-1 do
    begin
        if (i<51) then MasY[1][i-1]:=
strtofloat(form1.Memo3.Lines.Strings[i]);
        if (i>=101) and (i<151) then MasY[2][i-101]:=
strtofloat(form1.Memo3.Lines.Strings[i]);
        if (i>=201) and(i<251) then MasY[3][i-201]:=
strtofloat(form1.Memo3.Lines.Strings[i]);
        if (i>=301) and (i<351) then MasY[4][i-301]:=
strtofloat(form1.Memo3.Lines.Strings[i]);
    end;
    Image1.Canvas.Pen.Color:=clBlack;
    Image1.Canvas.MoveTo(100,370);
    Image1.Canvas.LineTo(500,370);
    Image1.Canvas.MoveTo(100,370);
    Image1.Canvas.LineTo(100,0);
    Image1.Canvas.Pen.Color:=clBlack;
    SX:=MasX[49]-MasX[0];
    SY:=MasY[1][49]-MasY[1][0];
```

```
if SY<MasY[2][49]-MasY[2][0] then SY:=MasY[2][49]-MasY[2][0];
if SY<MasY[3][49]-MasY[3][0] then SY:=MasY[3][49]-MasY[3][0];
if SY<MasY[4][49]-MasY[4][0] then SY:=MasY[4][49]-MasY[4][0];
index:=1;
while index<=CountI do
for index:=1 to 4 do
begin
NewX:=round(100+MasX[0]);
NewY:=round(370-MasY[index][0]);
Image1.Canvas.Pen.Width:=2;
Image1.Canvas.MoveTo(NewX,NewY);
Image1.Canvas.Pen.Color:=clRed;
Image1.Canvas.LineTo(NewX,NewY);
Image1.Canvas.TextOut(80,NewY,floattostr(round(MasY[index][0])));
Image1.Canvas.Pen.Width:=1;
Image1.Canvas.MoveTo(80,NewY);
Image1.Canvas.LineTo(100,NewY);
Image1.Canvas.TextOut(NewX,380,floattostr((MasX[0])));
Image1.Canvas.MoveTo(NewX,370);
Image1.Canvas.LineTo(NewX,380);
Image1.Canvas.MoveTo(NewX,NewY);
Image1.Canvas.Pen.Color:=clBlack;
for i:=1 to 49 do
begin
Image1.Canvas.Pen.Width:=2;
    SIX:=MasX[i]-MasX[i-1];
    SIY:=MasY[index][i]-MasY[index][i-1];
    StepX:=(350*SIX)/SX;
    StepY:=(350*SIY)/SY;
    NewX:=Round(NewX+StepX);
    NewY:=Round(NewY-StepY);
    Image1.Canvas.LineTo(NewX,NewY);
    Image1.Canvas.Pen.Width:=5;
    Image1.Canvas.Pen.Color:=clRed;
    Image1.Canvas.LineTo(NewX,NewY);
    if i = 49 then
    begin
    Image1.Canvas.Pen.Width:=1;
    Image1.Canvas.TextOut(60,NewY-
5,floattostr(round(MasY[index][i])));
    Image1.Canvas.MoveTo(80,NewY);
```

```
        Image1.Canvas.LineTo(100,NewY);
        Z:=round(MasY[index][i]);
        if MaxY>NewY then MaxY:=NewY;
        end;
        if i mod 10 = 0 then
        begin
        Image1.Canvas.Pen.Width:=1;

Image1.Canvas.TextOut(NewX,380,floattostr(((MasX[i])*100000000)));
        Image1.Canvas.MoveTo(NewX,370);
        Image1.Canvas.LineTo(NewX,380);
        Image1.Canvas.MoveTo(NewX,NewY);
        end;
      end;
      if index=1 then
      Image1.Canvas.TextOut(NewX+10,NewY,'Teta1 = ' +form8.edit1.text);
        if index=2 then
      Image1.Canvas.TextOut(NewX+10,NewY,'Teta2 = ' +form8.edit4.text);
        if index=3 then
      Image1.Canvas.TextOut(NewX+10,NewY,'Teta3 = ' +form8.edit5.text);
        if index=4 then
      Image1.Canvas.TextOut(NewX+10,NewY,'Teta4 = ' +form8.edit6.text);
      inc(index);
      end;
      iii:=0;
        countL:=0;
      while iii<round(370-maxy) do
      begin
        iii:=iii+round((370-maxy)/20);
        Image1.Canvas.Pen.Width:=1;
        Z:=round((MaxY-iii)/MaxY);
        if countL mod 2 =0 then
        begin
        Image1.Canvas.MoveTo(90,370-iii);
        Image1.Canvas.LineTo(100,370-iii);
        end
        else
        begin
        Image1.Canvas.MoveTo(80,370-iii);
        Image1.Canvas.LineTo(100,370-iii);
```

222

```
        Image1.Canvas.TextOut(80,370-iii,floattostr(round((iii)*Z/(370-
MaxY))));
        end;
       inc(countL);
    end;
end;

procedure TForm3.Button2Click(Sender: TObject);
begin
Image1.canvas.fillrect(Image1.canvas.cliprect);
form1.Memo3.Clear;
form1.Memo3.Text:='Пусто';
Image1.canvas.fillrect(Image1.canvas.cliprect);
Label1.Visible:=false;
Label2.Visible:=false;
  form1.Fr:=0;
  form1.eta:=0;
  form1.mu:=0;
  form1.R0:=0;
  form1.R0_3:=0;
  form1.d:=0;
  form1.d_:=0;
  form1.Teta0:=0;
  form1.CurrTeta:=0;
  form1.h:=0;
  form1.Q0:=0;
  form1.CurrQ:=0;
  Sigma:=0
end;

procedure TForm3.Save1Click(Sender: TObject);
begin
    if      SaveDialog1.Execute then
    Image1.Picture.SaveToFile(SaveDialog1.FileName+'.bmp');
end;

procedure TForm3.Print1Click(Sender: TObject);
var
 X1,X2,Y1,Y2:Integer;
 PointsX,PointsY:double;
 PrintDlg:TPrintDialog;
```

223

```
begin
 PrintDlg:=TPrintDialog.Create(Owner);
 if PrintDlg.Execute then
  begin
   Printer.BeginDoc;
   Printer.Canvas.Refresh;
   Printer.Title:='Results';
   PointsX:=GetDeviceCaps(Printer.Canvas.Handle,LOGPIXELSX)/100;
   PointsY:=GetDeviceCaps(Printer.Canvas.Handle,LOGPIXELSY)/100;
   X1:=50;
   Y1:=500;
   X2:=round(X1+Image1.Picture.Bitmap.Width*PointsX);
   Y2:=round(Y1+Image1.Picture.Bitmap.Height*PointsY);

Printer.Canvas.CopyRect(Rect(X1,Y1,X2,Y2),Image1.Picture.Bitmap.Canv
as,

Rect(0,0,Image1.Picture.Bitmap.Width,Image1.Picture.Bitmap.Height));
   Printer.EndDoc;
  end;
 PrintDlg.Free;
 end;
end.

 Unit7
procedure TForm7.Button1Click(Sender: TObject);
begin
    form9.CountI:=0;
  if Edit1.Text<>'' then
  begin
   inc(form9.CountI);
   form1.Fr:=StrToFloat(form1.Edit4.Text);
   form1.eta:=StrToFloat(Edit3.Text);
   form1.mu:=StrToFloat(Edit2.Text);
   Form1.Edit9 .Text:=FloatToStr(form1.eta/form1.mu);
  V:=StrToFloat(Edit1.Text);
 R0_3:=V/((4/3)*3.1415);
R0:=power(R0_3,1/3);
form1.R0:=StrToFloat(form1.Edit12.Text);
 form1.R0_3:=form1.R0*form1.R0*form1.R0;
form1.V:=(4/3)*3.1415*form1.R0_3;
```

224

```
Form1.Edit1.Text:=FloatToStr(form1.V);
form1.d:=StrToFloat(form1.Edit10.Text);
form1.d_:=StrToFloat(form1.Edit11.Text);
form1.G:=G;
  form1.Teta0:=StrToFloat(Edit7.Text);
   form1.CurrTeta:=form1.Teta0;
   form1.h:=StrToFloat(form1.Edit8.Text);
    form1.Q0:=StrToFloat(form1.Edit5.Text);
    form1.CurrQ:=form1.Q0;
        Sigma:=StrToFloat(Edit1.text);
        K:=0.15e8;
        G:=(Sigma*K/form1.R0)*(power(form1.CurrQ,2/3)/(1-
form1.Q0/(form1.CurrQ+0.0000001)));
         form1.G:=G;
         Form7.Edit1.Text :=FloatToStr(G);
         form1.G:=StrToFloat(Edit1.Text);
form1.b0:=form1.R0*power(form1.CurrQ,(-1/3));
form1.a0:=form1.R0*power(form1.CurrQ,2/3);
A0:=StrToFloat(Edit5.Text);
CurrA:=A0;
 B0:=power(R0*R0*R0/A0,1/2);
q0:=A0/B0;}
Form1.Button5.Click;
end;
if Edit4.Text<>'' then
begin
 inc(form9.CountI);
form1.Fr:=StrToFloat(form1.Edit4.Text);
form1.eta:=StrToFloat(Edit3.Text);
form1.mu:=StrToFloat(Edit2.Text);
Form1.Edit9 .Text:=FloatToStr(form1.eta/form1.mu);
V:=StrToFloat(Edit1.Text);
R0_3:=V/((4/3)*3.1415);
R0:=power(R0_3,1/3);
form1.R0:=StrToFloat(form1.Edit12.Text);
form1.R0_3:=form1.R0*form1.R0*form1.R0;
form1.V:=(4/3)*3.1415*form1.R0_3;
Form1.Edit1.Text:=FloatToStr(form1.V);
form1.d:=StrToFloat(form1.Edit10.Text);
form1.d_:=StrToFloat(form1.Edit11.Text);
   form1.G:=G;
```

```
    form1.G:=StrToFloat(Edit4.Text);
    form1.Teta0:=StrToFloat(Edit7.Text);
    form1.CurrTeta:=form1.Teta0;
    form1.h:=StrToFloat(form1.Edit8.Text);
     form1.Q0:=StrToFloat(form1.Edit5.Text);
  form1.CurrQ:=form1.Q0;
        Sigma:=StrToFloat(edit4.text);
        K:=0.15e8;
        G:=(Sigma*K/form1.R0)*(power(form1.CurrQ,2/3)/(1-
form1.Q0/(form1.CurrQ+0.0000001)));
        form1.G:=G;
        Form7.Edit4.Text:=FloatToStr(G);
        form1.G:=StrToFloat(Edit4.Text);
    form1.b0:=form1.R0*power(form1.CurrQ,(-1/3));
    form1.a0:=form1.R0*power(form1.CurrQ,2/3);
     Form1.Button5.Click;  end;
  if Edit5.Text<>'' then
  begin
   inc(form9.CountI);
    form1.Fr:=StrToFloat(form1.Edit4.Text);
  form1.eta:=StrToFloat(Edit3.Text);
  form1.mu:=StrToFloat(Edit2.Text);
  Form1.Edit9 .Text:=FloatToStr(form1.eta/form1.mu);
 V:=StrToFloat(Edit1.Text);
 R0_3:=V/((4/3)*3.1415);
R0:=power(R0_3,1/3);
form1.R0:=StrToFloat(form1.Edit12.Text);
 form1.R0_3:=form1.R0*form1.R0*form1.R0;
form1.V:=(4/3)*3.1415*form1.R0_3;
Form1.Edit1.Text:=FloatToStr(form1.V);
form1.d:=StrToFloat(form1.Edit10.Text);
 form1.d_:=StrToFloat(form1.Edit11.Text);
   form1.G:=G;
   form1.G:=StrToFloat(Edit5.Text);
   form1.Teta0:=StrToFloat(Edit7.Text);
    form1.CurrTeta:=form1.Teta0;
    form1.h:=StrToFloat(form1.Edit8.Text);
    form1.Q0:=StrToFloat(form1.Edit5.Text);
  form1.CurrQ:=form1.Q0;
   Sigma:=StrToFloat(edit5.text);
    K:=0.15e8;
```

226

```
    G:=(Sigma*K/form1.R0)*(power(form1.CurrQ,2/3)/(1-
form1.Q0/(form1.CurrQ+0.0000001)));
        form1.G:=G;
        Form7.Edit5.Text:=FloatToStr(G);
        form1.G:=StrToFloat(Edit5.Text);
 form1.b0:=form1.R0*power(form1.CurrQ,(-1/3));
 form1.a0:=form1.R0*power(form1.CurrQ,2/3);
  A0:=StrToFloat(Edit5.Text);
 CurrA:=A0;
  B0:=power(R0*R0*R0/A0,1/2);
 q0:=A0/B0;
 Form1.Button5.Click;
 end;
 if Edit6.Text<>'' then
 begin
  inc(form9.CountI);
   form1.Fr:=StrToFloat(form1.Edit4.Text);
  form1.eta:=StrToFloat(Edit3.Text);
  form1.mu:=StrToFloat(Edit2.Text);
  Form1.Edit9 .Text:=FloatToStr(form1.eta/form1.mu);
 V:=StrToFloat(Edit1.Text);
 R0_3:=V/((4/3)*3.1415);
R0:=power(R0_3,1/3);
 form1.R0:=StrToFloat(form1.Edit12.Text);
 form1.R0_3:=form1.R0*form1.R0*form1.R0;
form1.V:=(4/3)*3.1415*form1.R0_3;
Form1.Edit1.Text:=FloatToStr(form1.V);
 form1.d:=StrToFloat(form1.Edit10.Text);
 form1.d_:=StrToFloat(form1.Edit11.Text);
    form1.G:=G;
  form1.G:=StrToFloat(Edit6.Text);
  form1.Teta0:=StrToFloat(Edit7.Text);
   form1.CurrTeta:=form1.Teta0;
  form1.h:=StrToFloat(form1.Edit8.Text);
   form1.Q0:=StrToFloat(form1.Edit5.Text);
 form1.CurrQ:=form1.Q0;
        Sigma:=StrToFloat(edit6.text);
        K:=0.15e8;
        G:=(Sigma*K/form1.R0)*(power(form1.CurrQ,2/3)/(1-
form1.Q0/(form1.CurrQ+0.0000001)));
        form1.G:=G;
```

227

```
form1.b0:=form1.R0*power(form1.CurrQ,(-1/3));
 form1.a0:=form1.R0*power(form1.CurrQ,2/3);
  Form1.Button5.Click;end;
end;


Unit8
procedure TForm8.Button1Click(Sender: TObject);
begin
 if Edit1.Text<>" then
 begin
 inc(form3.CountI);
 form1.Fr:=StrToFloat(form1.Edit4.Text);
 form1.eta:=StrToFloat(Edit3.Text);
 form1.mu:=StrToFloat(Edit2.Text);
 Form1.Edit9 .Text:=FloatToStr(form1.eta/form1.mu);
 V:=StrToFloat(Edit1.Text);
R0:=power(R0_3,1/3);
 form1.R0:=StrToFloat(form1.Edit12.Text);
 form1.R0_3:=form1.R0*form1.R0*form1.R0;
form1.V:=(4/3)*3.1415*form1.R0_3;
Form1.Edit1.Text:=FloatToStr(form1.V);
 form1.d:=StrToFloat(form1.Edit10.Text);
 form1.d_:=StrToFloat(form1.Edit11.Text);
      Sigma:=StrToFloat(edit7.text);
      K:=0.15e8;
      G:=(Sigma*K/form1.R0)*(power(form1.CurrQ,2/3)/(1-
form1.Q0/(form1.CurrQ+0.0000001)));
   form1.G:=G;
  form1.Teta0:=StrToFloat(Edit1.Text);
   form1.CurrTeta:=form1.Teta0;
   form1.h:=StrToFloat(form1.Edit8.Text);
    form1.Q0:=StrToFloat(form1.Edit5.Text);
 form1.CurrQ:=form1.Q0;
 form1.b0:=form1.R0*power(form1.CurrQ,(-1/3));
 form1.a0:=form1.R0*power(form1.CurrQ,2/3);
 Form1.Button5.Click;
 end;
 if Edit4.Text<>" then
 begin
  inc(form3.CountI);
 form1.Fr:=StrToFloat(form1.Edit4.Text);
```

```
  form1.eta:=StrToFloat(Edit3.Text);
  form1.mu:=StrToFloat(Edit2.Text);
  Form1.Edit9 .Text:=FloatToStr(form1.eta/form1.mu);
end;
end.

Unit9

procedure TForm9.Formshow(Sender: TObject);
Var
    i:integer;
    SX,SIX,SIY:Real;
    StepX,StepY:Real;
    OldX,OldY,NewX,NewY:integer;
    MasX:array [0..99] of Real;
    MasY:array [1..4,0..99] of Real;
    BY:Real;
    SY,Sigma,KG:Real;
    index:integer;
    MaxY:integer;
    Z:integer;
    iii:integer;
    countL:integer;
  begin
  for i:=1 to 100 do
    MasX[i-1]:= strtofloat(form1.Memo1.Lines.Strings[i]);
    for i:=1 to Form1.Memo3.Lines.Count-1 do
    begin
        if (i<101) then MasY[1][i-1]:=
strtofloat(form1.Memo3.Lines.Strings[i]);
        if (i>=101) and (i<201) then MasY[2][i-101]:=
strtofloat(form1.Memo3.Lines.Strings[i]);
        if (i>=201) and(i<301) then MasY[3][i-201]:=
strtofloat(form1.Memo3.Lines.Strings[i]);
        if (i>=301) and (i<401) then MasY[4][i-301]:=
strtofloat(form1.Memo3.Lines.Strings[i]);
    end;
     Image1.Canvas.MoveTo(100,370);
    Image1.Canvas.LineTo(500,370);
    Image1.Canvas.MoveTo(100,370);
    Image1.Canvas.LineTo(100,0);
```

229

```
Image1.Canvas.Pen.Color:=clBlack;
SX:=MasX[99]-MasX[0];
SY:=MasY[1][99]-MasY[1][0];
if SY<MasY[2][99]-MasY[2][0] then SY:=MasY[2][99]-MasY[2][0];
if SY<MasY[3][99]-MasY[3][0] then SY:=MasY[3][99]-MasY[3][0];
if SY<MasY[4][99]-MasY[4][0] then SY:=MasY[4][99]-MasY[4][0];
index:=1;
MaxY:=round(MasY[1][99]);
while index<=CountI do
for index:=1 to 4 do
begin
NewX:=round(100+MasX[0]);
NewY:=round(370-MasY[index][0]);
Image1.Canvas.Pen.Width:=5;
Image1.Canvas.MoveTo(NewX,NewY);
Image1.Canvas.Pen.Color:=clRed;
Image1.Canvas.LineTo(NewX,NewY);
Image1.Canvas.TextOut(80,NewY,floattostr(round(MasY[index][0])));
Image1.Canvas.Pen.Width:=1;
Image1.Canvas.MoveTo(80,NewY);
Image1.Canvas.LineTo(100,NewY);
Image1.Canvas.TextOut(NewX,380,floattostr((MasX[0])));
Image1.Canvas.MoveTo(NewX,370);
Image1.Canvas.LineTo(NewX,390);
Image1.Canvas.MoveTo(NewX,NewY);
for i:=1 to 99 do
begin
Image1.Canvas.Pen.Width:=3;
   SIX:=MasX[i]-MasX[i-1];
   SIY:=MasY[index][i]-MasY[index][i-1];
   StepX:=(350*SIX)/SX;
   StepY:=(350*SIY)/SY;
   NewX:=Round(NewX+StepX);
   NewY:=Round(NewY-StepY);
   Image1.Canvas.LineTo(NewX,NewY);
   Image1.Canvas.Pen.Width:=3;
   Image1.Canvas.Pen.Color:=clRed;
   Image1.Canvas.LineTo(NewX,NewY);
   if i = 99 then
   begin
   Image1.Canvas.Pen.Width:=1;
```

```
Image1.Canvas.TextOut(80,NewY,floattostr(round(MasY[index][i])));
      Z:=round(MasY[index][i]);
      Image1.Canvas.MoveTo(80,NewY);
      Image1.Canvas.LineTo(100,NewY);
      if MaxY>NewY then MaxY:=NewY;
      end;
      if i mod 10 = 0 then
      begin
      Image1.Canvas.Pen.Width:=1;

Image1.Canvas.TextOut(NewX,380,floattostr(((MasX[i])*100000000)));
      Image1.Canvas.MoveTo(NewX,370);
      Image1.Canvas.LineTo(NewX,380);
      Image1.Canvas.MoveTo(NewX,NewY);
      Image1.Canvas.Pen.Color:=clBlack;
      end;
   end;
   if index=1 then
   Image1.Canvas.TextOut(NewX+10,NewY,'Sigma1 = '
+form7.edit1.text);
      if index=2 then
   Image1.Canvas.TextOut(NewX+10,NewY,'Sigma2 = '
+form7.edit4.text);
      if index=3 then
   Image1.Canvas.TextOut(NewX+10,NewY,'Sigma3 = '
+form7.edit5.text);

      if index=4 then
   Image1.Canvas.TextOut(NewX+10,NewY,'Sigma4 = '
+form7.edit6.text);
   inc(index);
   end;
      iii:=0;
      countL:=0;
   while iii<round(370-maxy) do
   begin
      iii:=iii+round((370-maxy)/20);
      Image1.Canvas.Pen.Width:=1;
      Z:=round((MaxY-iii)/MaxY);
      if countL mod 2 =0 then
```

```
      begin
      Image1.Canvas.MoveTo(90,370-iii);
      Image1.Canvas.LineTo(100,370-iii);
      end
      else
      begin
      Image1.Canvas.MoveTo(80,370-iii);
      Image1.Canvas.LineTo(100,370-iii);
      Image1.Canvas.TextOut(80,370-iii,floattostr(round((iii)*Z/(370-
MaxY))));
      end;
       inc(countL);
    end;
end;

procedure TForm9.Save1Click(Sender: TObject);
begin
 if    SaveDialog1.Execute then
    Image1.Picture.SaveToFile(SaveDialog1.FileName+'.bmp');
end;

procedure TForm9.Print1Click(Sender: TObject);
var
 X1,X2,Y1,Y2:Integer;
 PointsX,PointsY:double;
 PrintDlg:TPrintDialog;
begin
 PrintDlg:=TPrintDialog.Create(Owner);
 if PrintDlg.Execute then
  begin
   Printer.BeginDoc;
   Printer.Title:='Results';
   Printer.Canvas.Refresh;
   PointsX:=GetDeviceCaps(Printer.Canvas.Handle,LOGPIXELSX)/100;
   PointsY:=GetDeviceCaps(Printer.Canvas.Handle,LOGPIXELSY)/100;
   X1:=50;
   Y1:=500;
   X2:=round(X1+Image1.Picture.Bitmap.Width*PointsX);
   Y2:=round(Y1+Image1.Picture.Bitmap.Height*PointsY);
```

```
Printer.Canvas.CopyRect(Rect(X1,Y1,X2,Y2),Image1.Picture.Bitmap.Canv
as,

Rect(0,0,Image1.Picture.Bitmap.Width,Image1.Picture.Bitmap.Height));
  Printer.EndDoc;
 end;
 PrintDlg.Free;
end;
end.
```

3. Procedures and functions for calculating the parameters of the liquid jet breakup kinetics and surface tension at the phase separation boundary

```
Unit1
Procedure vvid;
var f:textfile;
i,j:integer;
begin
   assignfile(f,'inp.txt');
   reset(f);
   readln(f,n);
   for i:=1 to n do
   begin
    for j:=1 to n+1 do
     read(f,A[i,j]);
     readln(f);
   end;
     closefile(f);
end;

Procedure vivid(C:STRING;D:mas);
var f1:textfile;
i,j:integer;
begin
   assignfile(f1,'out.txt');
   append(f1);
   writeln(f1);
    writeln(f1,C);
   for i:=1 to n do
   begin
    for j:=1 to n+1 do
     begin
      write(f1,D[i,j]:0:2);  write(f1,' ');
     end;
    writeln(f1);
   end;
close(f1);
end;

procedure TForm1.Button1Click(Sender: TObject);
```

```
var i,mlc:integer;
begin
  Memo1.Lines.SaveToFile('1.txt');
  mlc:=Memo1.Lines.Count;
  for i:=1 to mlc do
   begin
    Data[i]:=StrToFloat(Memo1.lines[i-1]);
   end;
  end;

procedure TForm1.Button2Click(Sender: TObject);
var i:integer;
begin
i:=1;
Memo2.Lines.LoadFromFile('Волокна_'+IntToStr(i)+'.txt');
end;

procedure TForm1.Button4Click(Sender: TObject);
var mlc:integer;
begin
memo2.Lines.Delete(3);
mlc:=Memo2.Lines.Count;
ShowMessage(IntToStr(mlc));
end;

procedure TForm1.Memo2MouseDown(Sender: TObject; Button:
TMouseButton;
  Shift: TShiftState; X, Y: Integer);
  var mlc:integer;
  begin
  y:=memo2.Lines.Capacity;
ShowMessage(IntToStr(y));
  memo2.Lines.Delete(y);
mlc:=Memo2.Lines.Count;
ShowMessage(IntToStr(mlc));}
end;

procedure TForm1.Memo2DblClick(Sender: TObject);
var mlc:integer;
begin
  memo2.Lines.Delete(3);
```

```
mlc:=Memo2.Lines.Count;
ShowMessage(IntToStr(mlc));
end;

procedure TForm1.Button5Click(Sender: TObject);
var LineNum,mlc:integer;
begin
LineNum := SendMessage(Memo2.Handle, EM_LINEFROMCHAR,
Memo2.SelStart,0);{посылка сообщения, возвращающая номер строки}
memo2.Lines.Delete(LineNum);
mlc:=Memo2.Lines.Count;
ShowMessage(IntToStr(mlc));
end;

procedure TForm1.Button6Click(Sender: TObject);
var i,mlc:integer;
begin
 mlc:=Memo2.Lines.Count;
 for i:=1 to mlc do
  begin
 Data1[i]:=StrToFloat(Memo2.lines[i-1]);
 ShowMessage(FloatToStr(Data1[i]));
 end;
end;
procedure TForm1.Button8Click(Sender: TObject);
var q:real;
begin
 q:=12.69567689878;
 format('%3.3f',[q]);
 FormatFloat('###,####' q);
 memo1.lines.add(Format('%3.3f',[q]));
 ShowMessage(FloatToStr(Int(113.26643)));
 ShowMessage(FloatToStr(Frac(113.26643)));
end;
end.

Unit2
procedure TForm2.Button1Click(Sender: TObject);
begin
form3.Show;
 if form2.RadioButton1.Checked then
```

```
          begin
            Form3.Caption:='Ввід даних для волокон';
        Form3.Label1.Caption:='Введіть дані по волокнах для
'+IntToStr(k_obr)+' зразка';
        Form3.Button2.Enabled:=true;
        Form3.Button2.Visible:=true;
            end;
      if form2.RadioButton2.Checked then
          begin
            Form3.Caption:='Ввід даних для часток "a"';
        Form3.Label1.Caption:='Введіть дані по частках "a" для
'+IntToStr(k_obr_ch_a)+' зразка';
            end;
if form2.RadioButton3.Checked then
          begin
            Form3.Caption:='Ввід даних для часток "лямбда"';
        Form3.Label1.Caption:='Введіть дані по частках "лямбда" для
'+IntToStr(k_obr_ch_l)+' зразка';
        Form3.Button4.Enabled:=False;
        Form3.Button5.Enabled:=true;
        Form3.Button4.Visible:=False;
        Form3.Button5.Visible:=true;
            end;
nk_obr:=StrToInt(Edit1.Text);
nk_obr_ch_a:=StrToInt(Edit2.Text);
nk_obr_ch_l:=StrToInt(Edit3.Text);
end;
end.


Unit3
procedure TForm3.Button1Click(Sender: TObject);
var i:integer;
begin
   Sumv[k_obr]:=0;
   mlc:=Memo1.Lines.Count;
   for i:=1 to mlc do
    begin
     Data[i]:=StrToFloat(Memo1.lines[i-1]);
     Sumv[k_obr]:=Sumv[k_obr]+Data[i];
     end;
```

237

```pascal
    SrAr[k_obr]:=Sumv[k_obr]/mlc;
      SrAr[k_obr]:=Int(SrAr[k_obr]*1000)/1000;
     k_obr:=k_obr+1;
    Memo1.Lines.Text:='';
end;

procedure TForm3.FormCreate(Sender: TObject);
begin
   k_obr:=1;
   k_obr_ch_a:=1;
   k_obr_ch_l:=1;
   ka:=0;
   kl:=0;
   Sum_ch_l:=0;
end;

procedure TForm3.Button3Click(Sender: TObject);
var temp:Word;
   i:integer;
begin
   Label1.Caption:='Дані успішно введено!';
      temp:=MessageBox(Handle,PChar(' Продовжити ввід
даних?'),PChar("Ввід  даних '),MB_ICONQUESTION+MB_YESNO);
case temp of
 idno: begin form3.Close; form4.show; end;
 idyes: begin
    Form3.Caption:='Ввід даних для часток';
    Label1.Caption:='Введіть дані по часткахм "a" для
'+IntToStr(k_obr_ch_a)+' зразка';
       k_obr_ch_a:=k_obr_ch_a+1;
    Memo1.Lines.Text:='';
      end;
 end;
 end;

procedure TForm3.Button6Click(Sender: TObject);
var i:integer;
begin
 Suma[k_obr_ch_a]:=0;
   mlc:=Memo1.Lines.Count;
   ka:=ka+mlc;
```

238

```
  for i:=1 to mlc do
   begin
    Data[i]:=StrToFloat(Memo1.lines[i-1]);
    Suma[k_obr_ch_a]:=Suma[k_obr_ch_a]+Data[i];
   end;
    Sum_ch_a:=Sum_ch_a+Suma[k_obr_ch_a];
     k_obr_ch_a:=k_obr_ch_a+1;
     Memo1.Lines.Text:='';
end;

procedure TForm3.Button8Click(Sender: TObject);
var i:integer;
begin
  for i:=1 to nk_obr do
   begin
     button2.Click();
     button1.Click();
   end;
end;

procedure TForm3.Button9Click(Sender: TObject);
var i:integer;
begin
   for i:=1 to nk_obr_ch_a do
   begin
   button4.Click();
     button6.Click();
   end;
end;

procedure TForm3.Button10Click(Sender: TObject);
var i:integer;
begin
for i:=1 to nk_obr_ch_l do
   begin
    button5.Click();
     button7.Click();
    end;
end;

Unit4
```

```
procedure TForm4.Button1Click(Sender: TObject);
var i:integer;
    cd,cons:real;
begin
  for i:=2 to k_obr-1 do
   begin
     LnD[i]:=Ln((SrAr[i]-SrAr[1])/SrAr[1]);
     LnD[i]:=Ln((SrAr[i]-0.9)/0.9);
   end;
  for i:=1 to k_obr-1 do
   begin
     memo1.Lines.Add(FloatToStr(Sumv[i])+'  '+FloatToStr(SrAr[i])+'
'+FloatToStr(LnD[i]));
   end;
  memo1.Lines.Add('');
  memo1.Lines.Add(FloatToStr(Sum_ch_a));
  memo1.Lines.Add(IntToStr(ka));
  memo1.Lines.Add('');
  memo1.Lines.Add(FloatToStr(Sum_ch_l));
  memo1.Lines.Add(IntToStr(kl));
cd:=StrToFloat(Edit1.Text);
cons:=StrToFloat(Edit2.Text);
a0:=Sum_ch_a/ka/2*cd;
  a0:=Sum_ch_a/ka/2*3.125;
  lambdam:=Sum_ch_l/kl*3.125;
  lgR:=(3/2)*log10(a0)-(1/2)*log10(lambdam)+cons;
  lgR:=(3/2)*log10(a0)-(1/2)*log10(lambdam)+0.0625;
  R:=power(10,lgR);
  xi:=2*Pi*R/lambdam;
  memo1.Lines.Add('');
  memo1.Lines.Add(FloatToStr(a0));
  memo1.Lines.Add('');
  memo1.Lines.Add(FloatToStr(lambdam));
  memo1.Lines.Add('');
  memo1.Lines.Add(FloatToStr(lgR));
  memo1.Lines.Add('');
  memo1.Lines.Add(FloatToStr(R));
  memo1.Lines.Add('');
  memo1.Lines.Add(FloatToStr(xi));
end;
end.
```

```
Unit5
procedure TForm5.Button1Click(Sender: TObject);
var i,mlc:integer;
   q,tf,tc,w:real;
   s:string;
begin
 Memo2.Visible:=false;
 Memo2.Lines.LoadFromFile('Время.txt');
  mlc:=Memo2.Lines.Count;
  for i:=1 to mlc do
   begin
    Time[i]:=StrToFloat(Memo2.lines[i-1]);
    rTime[i]:=Int(Time[i])*60+Frac(Time[i])*100;
   end;
  for i:=2 to mlc do
   begin
    dTime[i]:=rTime[i]-rTime[i-1];
   end;
FormatFloat('###,####' value);
s:=' '+'vcjcj'+int(3.7);
Memo1.Lines.Add('_____
_____');
 Memo1.Lines.Add(' ln(2a0/d)    delta(ln(2a0/d))    t    delta(t)    q=
delta(ln(2a0/d)/delta(t)');
  for i:=2 to mlc+1 do
   begin
    w:=LnD[i+1]-LnD[i];
    if dTime[i]<>0 then
             begin
              q:=w/dTime[i];
              d0r:=2*a0/exp(q*dTime[i]);
              qo:=qo+q;
             end;
            q1:=q;
    tc:=Int(Time[i]);
    tf:=Frac(Time[i])*100;
    s:=FloatToStr(tc)+'` '+FloatToStr(tf)+'``';
    Memo1.Lines.Add(format('   '+'%3.3f',[LnD[i]])+'
'+format('%3.3f',[w])+'             '+FloatToStr(Time[i])+'
```

241

```
'+format('%3.0f',[dTime[i]])+'                    '+format('%3.6f',[q])+'
'+format('%3.6f',[d0r]));
    end;
    qo:=qo-q;
end;

procedure TForm5.Button2Click(Sender: TObject);
begin
WordApp := CreateOLEObject('Word.Application');
  WordApp.Documents.Add();
  WordApp.Selection.TypeText(Memo1.Text);
  WordApp.Visible := true;
end;

procedure TForm5.Button3Click(Sender: TObject);
begin
 eta1:=StrToFloat(Edit1.text);
  eta2:=StrToFloat(Edit2.text);
 omega:=StrToFloat(Edit3.text);
 d0:=StrToFloat(Edit4.text);
 qo:=qo-q1;
 qo:=qo/14;
  Memo1.Lines.Add('qoe='+FloatToStr(qoe));
  Memo1.Lines.Add('qo='+FloatToStr(qo));
  Memo1.Lines.Add('eta2='+FloatToStr(eta2));
  Memo1.Lines.Add('d0='+FloatToStr(d0));
  Memo1.Lines.Add('omega='+FloatToStr(omega));
   Memo1.Lines.Add('sigma='+FloatToStr(sigma));
   Edit7.Text:=FloatToStr(sigma);
end;

procedure TForm5.Button4Click(Sender: TObject);
begin
 eta1:=StrToFloat(Edit1.Text);
 eta2:=StrToFloat(Edit2.Text);
 omega:=StrToFloat(Edit3.Text);
 d0:=StrToFloat(Edit4.Text);
  xi:=3.1415*d0/lambdam;
  Edit6.Text:=FloatToStr(xi);
end;
end.
```

4. Procedures and functions for the calculation and graphical display of statistical processing of the results of studies of the microstructure of extrudates of polymer mixtures

```
Unit1
procedure TForm1.Button2Click(Sender: TObject);
var i,i1,j,k,delt1:integer;
   delt2,delt3:real;
   q:string;
begin
N:=0;
 for i:=1 to 13 do
   begin
    N:=N+Z[i];
   end;
   for i:=1 to kd do
    begin
     Pr[i]:=(Z[i]/N)*100;
    end;
delt:=round((D[13]-D[1])/(1+3.2*(ln(N)/ln(10))))+1;
delt2:=(D[13]-D[1])/(1+3.2*(ln(N)/ln(10)));
delt1:=trunc((D[13]-D[1])/(1+3.2*(ln(N)/ln(10))));
delt3:=delt2-delt1;
if delt3>0.1 then delt:=delt1+1 else delt:=delt1;}
if RadioButton1.Checked then
              delt:=trunc((D[kd]-D[1])/(1+3.2*(ln(N)/ln(10))))+1
                else delt:=round((D[13]-D[1])/(1+3.2*(ln(N)/ln(10))));
 Form2.Edit1.Text:=FloatToStr(N);
 Form2.Edit2.Text:=FloatToStr(delt);
 for i:=1 to 13 do
  begin
    Delta[i]:=delt*i; j:=i;
    if  Delta[i]>D[13] then break;
  end;
 Form2.Edit2.Text:=FloatToStr(j);
  for i:=1 to 13 do
  begin
   Zi[i]:=0;
  end;
 k:=1;
 i1:=0;
 for i:=1 to j do
```

243

```
begin
  for i1:=k to 13 do
   begin
     if D[i1]<Delta[i] then Zi[i]:=Zi[i]+Z[i1]
                else   break;
    end;
  k:=i1;
end;
Kncp[1]:=Delta[1]/2;
for i:=2 to j do
begin
  Kncp[i]:=(Delta[i-1]+Delta[i])/2;
end;
 i:=trunc(j/2);
 if i=j/2 then Kno:=(Kncp[round(j/2)]+Kncp[round(j/2+1)])/2
        else Kno:=Kncp[trunc(j/2)+1];
for i:=1 to j do
begin
  A[i]:=(Kncp[i]-Kno)/delt;
  ZiA[i]:=Zi[i]*A[i];
  ZiA2[i]:=Zi[i]*A[i]*A[i];
  ZiA3[i]:=Zi[i]*A[i]*A[i]*A[i];
  ZiA4[i]:=Zi[i]*A[i]*A[i]*A[i]*A[i];
end;
 S1:=0;
 S2:=0;
 S3:=0;
 S4:=0;
 for i:=1 to j do
begin
  S1:=S1+Zi[i]*A[i];
  S2:=S2+Zi[i]*A[i]*A[i];
  S3:=S3+Zi[i]*A[i]*A[i]*A[i];
  S4:=S4+Zi[i]*A[i]*A[i]*A[i]*A[i];
end;
 m1_:=S1/N;
 m2_:=S2/N;
 m3_:=S3/N;
 m4_:=S4/N;
 d_:=m1_*delt+Kno;
 M11,M21,M31,M41,
```

```
M11:=;
  M21:=m2_-m1_*m1_;
  M31:=m3_{-3*m2_}-3*m2_*m1_+2*m1_*m1_*m1_;
  M41:=m4_-4*m1_*m3_+6*m1_*m1_*m2_-3*m1_*m1_*m1_*m1_;
  ass:=M31/(M21*Sqrt(M21));
  ex:=M41/(M21*M21)-3;
  Sigma2:=M21*delt*delt;
  Sigma:=Sqrt(Sigma2);
  C:=(Sigma/Sqrt(N))*100;
 Form2.Edit1.Text:=FloatToStr(Kno);
Form2.Edit1.Text:=FloatToStr(S1);
Form2.Edit2.Text:=FloatToStr(S2);
Form2.Edit3.Text:=FloatToStr(S3);
Form2.Edit4.Text:=FloatToStr(S4);
Form2.Edit5.Text:=FloatToStr(N);
Form2.Edit6.Text:=FloatToStr(Kno);
Form2.Edit7.Text:=FloatToStr(m1_);
Form2.Edit8.Text:=FloatToStr(m2_);
Form2.Edit9.Text:=FloatToStr(m3_);
Form2.Edit10.Text:=FloatToStr(m4_);
Form2.Edit11.Text:=FloatToStr(ass);
Form2.Edit12.Text:=FloatToStr(ex);
Form2.Edit13.Text:=FloatToStr(d_);
Form2.Edit14.Text:=FloatToStr(M21);
Form2.Edit15.Text:=FloatToStr(M31);
Form2.Edit16.Text:=FloatToStr(M41);
Form2.Edit17.Text:=FloatToStr(Sigma2);
Form2.Edit18.Text:=FloatToStr(Sigma);
Form2.Edit19.Text:=FloatToStr(C);
  for i:=1 to 13 do
begin
  Form2.Memo1.Lines.add(IntToStr(i));
  q:=format('%*.*f',[3,2,D[i]]);
  Form2.Memo2.Lines.add(q);
  q:=format('%*.*f',[3,0,Z[i]]);
  Form2.Memo3.Lines.add(q);
end;
   for i:=1 to j do
begin
  q:=format('%*.*f',[3,0,Zi[i]]);
  Form2.Memo5.Lines.add(q);
```

```
    q:=format('%*.*f',[3,1,Kncp[i]]);
    Form2.Memo6.Lines.add(q);
    q:=format('%*.*f',[2,0,A[i]]);
    Form2.Memo7.Lines.add(q);
    q:=format('%*.*f',[2,0,Delta[i]]);
    Form2.Memo4.Lines.add(q);
    q:=format('%*.*f',[3,0,ZiA[i]]);
    Form2.Memo8.Lines.add(q);
    q:=format('%*.*f',[4,0,ZiA2[i]]);
    Form2.Memo9.Lines.add(q);
    q:=format('%*.*f',[5,0,ZiA3[i]]);
    Form2.Memo10.Lines.add(q);
    q:=format('%*.*f',[5,0,ZiA4[i]]);
    Form2.Memo11.Lines.add(q);
  end;
end;

procedure TForm1.Button3Click(Sender: TObject);
var i,i1,j,k:integer;
   q:string;
begin
 N:=0;
 for i:=1 to kd do
  begin
   N:=N+Z[i];
  end;
   for i:=1 to kd do
   begin
   Pr[i]:=(Z[i]/N)*100;
   end;
 delt:=trunc((D[kd]-D[1])/(1+3.2*(ln(N)/ln(10))))+1;
if RadioButton1.Checked then
             delt:=trunc((D[kd]-D[1])/(1+3.2*(ln(N)/ln(10))))+1
                 else delt:=round((D[13]-D[1])/(1+3.2*(ln(N)/ln(10))));
  for i:=1 to kd do
  begin
    Delta[i]:=delt*i; j:=i;
    if  Delta[i]>D[kd] then break;
  end;
  for i:=1 to kd do
  begin
```

246

```
  Zi[i]:=0;
 end;
k:=1;
i1:=0;
for i:=1 to j do
 begin
   for i1:=k to kd do
     begin
       if D[i1]<=Delta[i] then Zi[i]:=Zi[i]+Z[i1]
                    else   break;
      end;
   k:=i1;
 end;
 Kncp[1]:=Delta[1]/2;
for i:=2 to j do
 begin
   Kncp[i]:=(Delta[i-1]+Delta[i])/2;
 end;
 i:=trunc(j/2);
  if i=j/2 then Kno:=(Kncp[round(j/2)]+Kncp[round(j/2+1)])/2
        else Kno:=Kncp[trunc(j/2)+1];
for i:=1 to j do
 begin
   A[i]:=(Kncp[i]-Kno)/delt;
   ZiA[i]:=Zi[i]*A[i];
   ZiA2[i]:=Zi[i]*A[i]*A[i];
   ZiA3[i]:=Zi[i]*A[i]*A[i]*A[i];
   ZiA4[i]:=Zi[i]*A[i]*A[i]*A[i]*A[i];
 end;
 S1:=0;
 S2:=0;
 S3:=0;
 S4:=0;
 for i:=1 to j do
 begin
  S1:=S1+Zi[i]*A[i];
  S2:=S2+Zi[i]*A[i]*A[i];
  S3:=S3+Zi[i]*A[i]*A[i]*A[i];
  S4:=S4+Zi[i]*A[i]*A[i]*A[i]*A[i];
 end;
 m1_:=S1/N;
```

247

```
  m2_:=S2/N;
  m3_:=S3/N;
  m4_:=S4/N;
  d_:=m1_*delt+Kno;
   M21:=m2_-m1_*m1_;
    M31:=m3_{-3*m2_}-3*m2_*m1_+2*m1_*m1_*m1_;
    M41:=m4_-4*m1_*m3_+6*m1_*m1_*m2_-3*m1_*m1_*m1_*m1_;
    ass:=M31/(M21*Sqrt(M21));
    ex:=M41/(M21*M21)-3;
     Sigma2:=M21*delt*delt;
    Sigma:=Sqrt(Sigma2);
    C:=(Sigma/Sqrt(N))*100;
   for i:=1 to kd do
  begin
   Form2.Memo1.Lines.add(IntToStr(i));
   q:=format('%*.*f',[3,2,D[i]]);
   Form2.Memo2.Lines.add(q);
   q:=format('%*.*f',[3,0,Z[i]]);
   Form2.Memo3.Lines.add(q);
  end;
     for i:=1 to j do
  begin
   q:=format('%*.*f',[3,0,Zi[i]]);
   Form2.Memo5.Lines.add(q);
   q:=format('%*.*f',[3,1,Kncp[i]]);
   Form2.Memo6.Lines.add(q);
   q:=format('%*.*f',[3,1,A[i]]);
   Form2.Memo7.Lines.add(q);
   q:=format('%*.*f',[2,0,Delta[i]]);
   Form2.Memo4.Lines.add(q);
   q:=format('%*.*f',[4,1,ZiA[i]]);
   Form2.Memo8.Lines.add(q);
   q:=format('%*.*f',[5,1,ZiA2[i]]);
   Form2.Memo9.Lines.add(q);
   q:=format('%*.*f',[5,1,ZiA3[i]]);
   Form2.Memo10.Lines.add(q);
   q:=format('%*.*f',[5,1,ZiA4[i]]);
   Form2.Memo11.Lines.add(q);
  end;
end;
```

end.

Unit4
```
procedure Scale(A,B:TS;var Mx,My,KA,KB,MinA,MinB,ShA,ShB:Real);
var k:integer;
    pr,pr1,Min,Min1,Max,Max1:Real;
begin
  Min:=A[1];
  Max:=A[1];
  Min1:=B[1];
  Max1:=B[1];
  for k:=2 to kd do
   begin
    if A[k]>Max then Max:=A[k];
    if A[k]<Min then Min:=A[k];
    if B[k]>Max1 then Max1:=B[k];
    if B[k]<Min1 then Min1:=B[k];
   end;
MinA:=Min;
MinB:=Min1;
 pr:=Max-Min;
 Mx:=290/pr;
 pr1:=Max1-Min1;
 My:=270/pr1;
 ShA:=pr/10;
 ShB:=pr1/10;
 KA:=0;
 KB:=0;
if Min>pr then KA:=1;
if Min1>pr1 then KB:=1;
end;

procedure OsiCoord;
var i:integer;
begin
 X0:=35;
 Y0:=300;
Form4.Image1.Canvas.MoveTo(X0,Y0+10);
Form4.Image1.Canvas.LineTo(X0,5);
Form4.Image1.Canvas.MoveTo(X0-10,Y0);
Form4.Image1.Canvas.LineTo(370,Y0);
```

249

```
for i:=1 to 11 do
 begin
  Form4.Image1.Canvas.MoveTo(X0+10+29*(i-1),Y0-2);
  Form4.Image1.Canvas.LineTo(X0+10+29*(i-1),Y0+2);
  Form4.Image1.Canvas.MoveTo(X0+2,Y0-10-27*(i-1));
  Form4.Image1.Canvas.LineTo(X0-2,Y0-10-27*(i-1));
 end;
end;

procedure RazmetkaOsey(A,B:TS);
var i:integer;
   q,q1:string;
   Mx,My,KA,KB,MinA,MinB,ShA,ShB:Real;
begin
Scale(A,B,Mx,My,KA,KB,MinA,MinB,ShA,ShB);
 for i:=0 to 5  do
  begin
  q:=format('%*.*f',[4,3,MinA]);
  Form4.Image1.Canvas.TextOut(X0+29*2*i+2,Y0+4,q) ;
  MinA:=MinA+2*ShA;
  end;
  for i:=0 to 12  do
  begin
  q1:=format('%*.*f',[4,3,MinB]);
  Form4.Image1.Canvas.TextOut(X0-30,Y0-14-27*i,q1) ;
  MinB:=MinB+ShB;
  end;
end;

procedure Griphic_Pr_D;
var Mx,My,KA,KB,MinA,MinB,ShA,ShB:Real;
   i:integer;
begin
OsiCoord;
RazmetkaOsey(D,Pr);
Scale(D,Pr,Mx,My,KA,KB,MinA,MinB,ShA,ShB);
Form4.Image1.Canvas.MoveTo
  (X0+round(D[1]*Mx-MinA*Mx+10),
   Y0-(round(Pr[1]*My-MinB*My))-10);
for i:=2 to kd do
 begin
```

```
  Form4.Image1.Canvas.LineTo
    (X0+round(D[i]*Mx-MinA*Mx+10),
     Y0-(round(Pr[i]*My-{KB*}MinB{0.3}*My{177.8}))-10);
 end;
for i:=1 to kd do
 begin
  Form4.Image1.Canvas.Pen.Color:=clRed;
  Form4.Image1.Canvas.Ellipse(
    X0+round(D[i]*Mx-MinA*Mx)-2+10,
    Y0-round(Pr[i]*My-MinB*My)-2-10,
    X0+round(D[i]*Mx-MinA*Mx)+2+10,
    Y0-round(Pr[i]*My-MinB*My)+2-10
                   );
 end;
   Form4.Image1.Canvas.Pen.Color:=clBlack;
end;

procedure Griphic_LgEta_LgT;
var Mx,My,KA,KB,MinA,MinB,ShA,ShB:Real;
   i:integer;
begin
RazmetkaOsey(LgT,LgEta);
Scale(LgT,LgEta,Mx,My,KA,KB,MinA,MinB,ShA,ShB);
Form4.Image1.Canvas.MoveTo(
        X0+round(LgT[0]*Mx-KA*MinA*Mx)+10,
        Y0-round(LgEta[0]*My-MinB*My)-10
                  );
for i:=1 to kd-2 do
 begin
  Form4.Image1.Canvas.LineTo
    (X0+round(LgT[i]*Mx-KA*MinA*Mx)+10,
     Y0-round(LgEta[i]*My-MinB*My)-10);
 end;

 for i:=0 to kd-2 do
 begin
  Form4.Image1.Canvas.Pen.Color:=clRed;
  Form4.Image1.Canvas.Ellipse(
    X0+round(LgT[i]*Mx-KA*MinA*Mx)-2+10,
    Y0-round(LgEta[i]*My-MinB*My)-2-10,
    X0+round(LgT[i]*Mx-KA*MinA*Mx)+2+10,
```

251

```
          Y0-round(LgEta[i]*My-MinB*My)+2-10
                        );
 end;
   Form4.Image1.Canvas.Pen.Color:=clBlack;
end;

procedure Griphic_Eta_T;
var Mx,My,KA,KB,MinA,MinB,ShA,ShB:Real ;
   i:integer;
   T:TS;
begin
for i:=0 to kd-2 do
 begin
  T[i]:=power(10,LgT[i]);
 end;
RazmetkaOsey(T,Eta);
Scale(T,Eta,Mx,My,KA,KB,MinA,MinB,ShA,ShB);
Form4.Image1.Canvas.MoveTo
    (X0+round(T[0]*Mx-KA*MinA*Mx)+10,
    Y0-round(Eta[0]*My-MinB*My)-10);
for i:=1 to kd-2 do
 begin
  Form4.Image1.Canvas.LineTo
    (X0+round(T[i]*Mx-KA*MinA*Mx)+10,
    Y0-round(Eta[i]*My-MinB*My)-10);
 end;
  for i:=0 to kd-2 do
 begin
  Form4.Image1.Canvas.Pen.Color:=clRed;
  Form4.Image1.Canvas.Ellipse(
    X0+round(T[i]*Mx-KA*MinA*Mx)-2+10,
    Y0-round(Eta[i]*My-MinB*My)-2-10,
    X0+round(T[i]*Mx-KA*MinA*Mx)+2+10,
    Y0-round(Eta[i]*My-MinB*My)+2-10
                        );
 end;
   Form4.Image1.Canvas.Pen.Color:=clBlack;
end;

procedure Points_Lg_D_LgT;
var Mx,My,KA,KB,MinA,MinB,ShA,ShB:Real;
```

```
    i:integer;
begin
RazmetkaOsey(LgT,Lg_D);
Scale(LgT,Lg_D,Mx,My,KA,KB,MinA,MinB,ShA,ShB);
for i:=0 to kd-2 do
 begin
  Form4.Image1.Canvas.Pen.Color:=clRed;
  Form4.Image1.Canvas.Ellipse(
    X0+round(LgT[i]*Mx-KA*MinA*Mx)-2+10,
    Y0-round(Lg_D[i]*My-MinB*My)-2-10,
    X0+round(LgT[i]*Mx-KA*MinA*Mx)+2+10,
    Y0-round(Lg_D[i]*My-MinB*My)+2-10
                   );
 end;
  Form4.Image1.Canvas.Pen.Color:=clBlack;
end;

procedure Points_LgEta_LgT;
var Mx,My,KA,KB,MinA,MinB,ShA,ShB:Real;
   i:integer;
begin
RazmetkaOsey(LgT,LgEta);
Scale(LgT,LgEta,Mx,My,KA,KB,MinA,MinB,ShA,ShB);
 for i:=0 to kd-2 do
 begin
  Form4.Image1.Canvas.Pen.Color:=clRed;
  Form4.Image1.Canvas.Ellipse(
    X0+round(LgT[i]*Mx-KA*MinA*Mx)-2+10,
    Y0-round(LgEta[i]*My-MinB*My)-2-10,
    X0+round(LgT[i]*Mx-KA*MinA*Mx)+2+10,
    Y0-round(LgEta[i]*My-MinB*My)+2-10
                   );
 end;
  Form4.Image1.Canvas.Pen.Color:=clBlack;
end;

procedure TForm4.Button1Click(Sender: TObject);
begin
OsiCoord;
if RadioButton1.Checked then Griphic_Lg_D_LgT;
if RadioButton2.Checked then Griphic_LgEta_LgT;
```

```
if RadioButton3.Checked then Griphic_Eta_T;
RazmetkaOsey(LgT,Lg_D);
end;

procedure MinSq(X,Y:TS; var Ac,Bc,Cc:real);
var i:integer;
   S1,S2,S3,S4,S5,S6,S7:real;
   Koef:MyArr;
   St:MySt;
begin
S1:=0;
S2:=0;
S3:=0;
S4:=0;
S5:=0;
S6:=0;
S7:=0;
for i:=1 to kd do
 begin
  S1:=S1+power(X[i],4);
  S2:=S2+power(X[i],3);
  S3:=S3+X[i]*X[i];
  S4:=S4+X[i];
  S5:=S5+X[i]*X[i]*Y[i];
  S6:=S6+X[i]*Y[i];
  S7:=S7+Y[i];
 end;
 Koef[1,1]:=S1;
 Koef[2,1]:=S2;
 Koef[3,1]:=S3;
Koef[1,2]:=S2;
 Koef[2,2]:=S3;
 Koef[3,2]:=S4;
 Koef[1,3]:=S3;
 Koef[2,3]:=S4;
 Koef[3,3]:=1;
 St[1]:=S5;
 St[2]:=S6;
 St[3]:=S7;
 Kramer3(Koef,St,Ac,Bc,Cc);
end;
```

```
procedure MinSq4(X,Y:TS; var Ac4,Bc4,Cc4,Dc4:real);
var i:integer;
    S1,S2,S3,S4,S5,S6,S7,S8,S9,S10:real;
    Koef4:MyArr4;
    St4:MySt4;
begin
S1:=0;
S2:=0;
S3:=0;
S4:=0;
S5:=0;
S6:=0;
S7:=0;
S8:=0;
S9:=0;
S10:=0;
for i:=1 to kd do
 begin
  S1:=S1+power(X[i],4);
  S2:=S2+power(X[i],3);
  S3:=S3+X[i]*X[i];
  S4:=S4+X[i];
  S5:=S5+X[i]*X[i]*Y[i];
  S6:=S6+X[i]*Y[i];
  S7:=S7+Y[i];
  S8:=S8+power(X[i],6);
  S9:=S9+power(X[i],5);
  S10:=S10+X[i]*X[i]*X[i]*Y[i];
 end;
 Koef4[1,1]:=S8;
 Koef4[2,1]:=S9;
 Koef4[3,1]:=S1;
 Koef4[4,1]:=S2;
 Koef4[1,2]:=S9;
 Koef4[2,2]:=S1;
 Koef4[3,2]:=S2;
 Koef4[4,2]:=S3;
 Koef4[1,3]:=S1;
 Koef4[2,3]:=S2;
 Koef4[3,3]:=S3;
```

```
  Koef4[4,3]:=S4;
  Koef4[1,4]:=S2;
  Koef4[2,4]:=S3;
  Koef4[3,4]:=S4;
  Koef4[4,4]:=1;
  St4[1]:=S10;
  St4[2]:=S5;
  St4[3]:=S6;
  St4[4]:=S7;
  Kramer4(Koef4,St4,Ac4,Bc4,Cc4,Dc4);
end;

procedure Approx_Pr_D;
var Mx,My,KA,KB,MinA,MinB,ShA,ShB:real;
   i:integer;
   Ma,Mb,hA,hB, Ac,Bc,Cc:real;
begin
OsiCoord;
RazmetkaOsey(D,Pr);
Scale(D,Pr,Mx,My,KA,KB,MinA,MinB,ShA,ShB);
MinSq(D,Pr, Ac,Bc,Cc);
Form4.Image1.Canvas.MoveTo(X0+10,Y0-10-round(
                (Ac*MinA*MinA+Bc*MinA+Cc)*My-MinB*My)
                        );
Form4.Image1.Canvas.MoveTo(
        X0+round(D[1]*Mx-MinA*Mx)+10,
        Y0-round(Pr[1]*My-MinB*My)-10);
 Form4.Edit1.Text:=FloatToStr(Ac);
 Form4.Edit2.Text:=FloatToStr(Bc);
 Form4.Edit3.Text:=FloatToStr(Cc);
for i:=1 to 101 do
 begin
  Form4.Image1.Canvas.LineTo
   (X0+round((MinA+i*ShA/10)*Mx-MinA*Mx)+10,
    Y0-10-round(
        (Ac*(MinA+i*ShA/10)*(MinA+i*ShA/10)+
        Bc*(MinA+i*ShA/10)+Cc
         )*My-MinB*My)
                    );
 end;
 for i:=1 to kd do
```

```
 begin
 Form4.Image1.Canvas.Pen.Color:=clRed;
 Form4.Image1.Canvas.Ellipse(
    X0+round(D[i]*Mx-MinA*Mx)-2+10,
    Y0-round(Pr[i]*My-MinB*My)-2-10,
    X0+round(D[i]*Mx-MinA*Mx)+2+10,
    Y0-round(Pr[i]*My-MinB*My)+2-10
               );
 Form4.Image1.Canvas.Ellipse(
    X0+round(D[i]*Mx-MinA*Mx)-2+10,
    Y0-round(Pr[i]*My-MinB*My)-2-10,
    X0+round(D[i]*Mx-MinA*Mx)+2+10,
    Y0-round(Pr[i]*My-MinB*My)+2-10
                    );
 end;
   Form4.Image1.Canvas.Pen.Color:=clBlack;
end;


procedure Approx4_Pr_D;
var Mx,My,KA,KB,MinA,MinB,ShA,ShB:real;
   i:integer;
   Ma,Mb,hA,hB, Ac4,Bc4,Cc4,Dc4:real;
begin
RazmetkaOsey(D,Pr);
Scale(D,Pr,Mx,My,KA,KB,MinA,MinB,ShA,ShB);
MinSq4(D,Pr, Ac4,Bc4,Cc4,Dc4);
Form4.Image1.Canvas.MoveTo(X0+10,Y0-10-round(

(Ac4*MinA*MinA*MinA+Bc4*MinA*MinA+Cc4*MinA+Dc4)*My
                      -MinB*My)
                        );
 Form4.Edit1.Text:=FloatToStr(Ac4);
 Form4.Edit2.Text:=FloatToStr(Bc4);
 Form4.Edit3.Text:=FloatToStr(Cc4);
for i:=1 to 101 do
 begin
  Form4.Image1.Canvas.LineTo
   (X0+round((MinA+i*ShA/10)*Mx-MinA*Mx)+10,
    Y0-
round((Ac4*(MinA+i*ShA/10)*(MinA+i*ShA/10)*(MinA+i*ShA/10)+
       Bc4*(MinA+i*ShA/10)*(MinA+i*ShA/10)+
```

```
                Cc4*(MinA+i*ShA/10)+Dc4)*My-
                     MinB*My)-10);
     end;
     for i:=1 to kd do
     begin
      Form4.Image1.Canvas.Pen.Color:=clRed;
      Form4.Image1.Canvas.Ellipse(
         X0+round(D[i]*Mx-MinA*Mx)-2+10,
         Y0-round(Pr[i]*My-MinB*My)-2-10,
         X0+round(D[i]*Mx-KA*MinA*Mx)+2+10,
         Y0-round(Pr[i]*My-MinB*My)+2-10
                        );
        Form4.Image1.Canvas.Ellipse(
         X0+round(D[i]*Mx-MinA*Mx)-2+10,
         Y0-round(Pr[i]*My-MinB*My)-2-10,
         X0+round(D[i]*Mx-MinA*Mx)+2+10,
         Y0-round(Pr[i]*My-MinB*My)+2-10
                        );
     end;
       Form4.Image1.Canvas.Pen.Color:=clBlack;
     end;
     RazmetkaOsey(T,Eta);
     Scale(T,Eta,Mx,My,KA,KB,MinA,MinB,ShA,ShB);
     MinSq(T,Eta, Ac,Bc,Cc);

     Form4.Image1.Canvas.MoveTo(X0+10,Y0-10-round(
                     (Ac*MinA*MinA+Bc*MinA+Cc)*My-MinB*My)
                           );
      Form4.Edit1.Text:=FloatToStr(Ac);
      Form4.Edit2.Text:=FloatToStr(Bc);
      Form4.Edit3.Text:=FloatToStr(Cc);
     for i:=1 to 101 do
      begin
       Form4.Image1.Canvas.LineTo
        (X0+round((MinA+i*ShA/10)*Mx-MinA*Mx)+10,
         Y0-round((Ac*(MinA+i*ShA/10)*(MinA+i*ShA/10)+
                  Bc*(MinA+i*ShA/10)+Cc)*My-
                  MinB*My)-10);
      end;
      for i:=0 to kd-2 do
      begin
```

```
  Form4.Image1.Canvas.Pen.Color:=clRed;
  Form4.Image1.Canvas.Ellipse(
     X0+round(T[i]*Mx-MinA*Mx)-2+10,
     Y0-round(Eta[i]*My-MinB*My)-2-10,
     X0+round(T[i]*Mx-KA*MinA*Mx)+2+10,
     Y0-round(Eta[i]*My-MinB*My)+2-10
                    );
 end;
  Form4.Image1.Canvas.Pen.Color:=clBlack;
end;
end.
```

CONTENTS

Резанова Вікторія Георгіївна,
Резанова Наталія Михайлівна

SOFTWARE FOR THE RESEARCH
OF NANOFILLED POLYMER SYSTEMS

Редактор Резанова В.Г.
Дизайн та верстка авторські